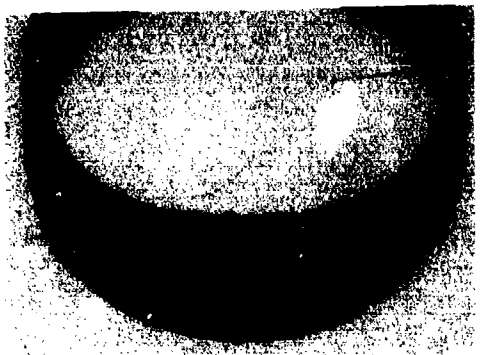

DSTO-TR-0034

Acoustic Propagation by Bottom Bounce Mode to the North East of Australia (U)

M.W. Lawrence, M.J. Bell and S. Prenc

DEPARTMENT OF DEFENCE
DEFENCE SCIENCE AND TECHNOLOGY ORGANISATION

Copy No. 26 of 45

Acoustic Propagation by Bottom Bounce Mode to the North East of Australia (U)

M.W. Lawrence, M.J. Bell and S. Prenc

Aeronautical and Maritime Research Laboratory

ABSTRACT

Technical Report

(U) Underwater acoustic propagation measurements have been made to the north east of Australia, primarily in the Coral and Solomon Seas. A few measurements were made in the Tasman Sea. The resulting data set has been analysed to provide acoustic bottom loss as a function of frequency and grazing angle for a range of sites. The experiments and the analysis are described, together with the results. The variability from site to site is considerable, sometimes even in areas which are geologically of the same province.

RELEASE LIMITATION

Distribution additional to the initial list is limited to qualified officers of the Defence Department and the Defence Force of Australia and their equivalent in US, UK, Canada and NZ. Other requests should be referred to Chief, Maritime Operations Division AMRL.

DOD ONLY

Embassy of Australia
Attn: Joan Bliss
Head. Pub. Sec.-Def/Sci.
1601 Massachusetts Ave., NW
Washington, DC 20036

DSTO-TR-0034

DEPARTMENT OF DEFENCE

DEFENCE SCIENCE AND TECHNOLOGY ORGANISATION

Published by

Aeronautical and Maritime Research Laboratory
GPO Box 4331
Melbourne Victoria 3001 Australia

Telephone: (03) 626 7000
Fax: (03) 626 7999

AR-008-549
JULY 1994

Conditions of Release and Disposal

1. *This document is the property of the Australian Government; the information it contains is released for defence purposes only and must not be disseminated beyond the stated distribution without prior approval.*

2. *The document and the information it contains must be handled in accordance with security regulations applying in the country of lodgement, downgrading instructions must be observed and delimitation is only with the specific approval of the Releasing Authority as given in the Secondary Distribution statement.*

3. *This information may be subject to privately owned rights.*

4. *The officer in possession of this document is responsible for its safe custody. When no longer required this document should be destroyed and the notification sent to: Senior Librarian, Aeronautical and Maritime Research Laboratory.*

Acoustic Propagation by Bottom Bounce Mode to the North East of Australia (U)

EXECUTIVE SUMMARY

(U) Understanding the effectiveness of sonar systems is essential for assessing their operation in pro- or anti- submarine warfare. Sonar performance varies from one ocean environment to another, with large variations in detection range resulting from differences in acoustic propagation conditions. In most instances the factor which has the largest effect on long-range propagation is the sea floor. This factor also has the largest variability from one location to another. Understanding and prediction of the interaction of acoustic energy with the sea floor is complicated by the penetration of the energy into the sediments and rocks that make up the sea floor.

(U) This report describes a series of measurements of the effect of the sea floor on acoustic propagation. These measurements have been performed to characterise the acoustic sea floor interaction as an acoustic bottom loss (that is the energy loss on a single interaction). The bottom loss (expressed in decibels) is measured for acoustic energy at each of a range of angles of incidence with the sea floor. Other properties of the sea floor at the measurement sites are also obtained, both by measurement and from published results. These other properties are useful in establishing relationships between the acoustic results and the nature of the sea floor.

(U) This report covers measurements of acoustic bottom loss to the north-east of Australia, primarily in the Coral and Solomon Seas. Earlier reports covered the regions to the east of Australia and a subsequent report will cover the north-west of Australia.

(U) Each set of acoustic propagation measurements reported here was made from a ship (H.M.A.S. Cook) which dropped a sonobuoy, and whilst steaming away, dropped explosive charges at regular intervals. The acoustic signal received by the sonobuoy was recorded and relevant sections were analysed. Bottom loss values have been calculated from these measured acoustic signals.

(U) The work reported here considerably extends the existing data set on bottom loss in this region, both in quantity of sites and frequency range of measurement. There are considerably more sites in this report than in all of the previous bottom loss investigations of this region. In conjunction with the acoustic results, there is also an accurate set of relevant environmental data at each site, which is useful for further analysis of the results. The significant variability of bottom loss results, even for the same geoacoustic province, is once again demonstrated.

(U) The purpose of the measurements of bottom loss reported here is to help characterise the effect of the sea floor on acoustic propagation in areas of direct military interest to Australia. The sea floor frequently plays a very significant role in determining the sonar effectiveness for pro- or anti-submarine warfare. Better characterisation of the sea floor allows improved sonar modelling and detection-range prediction.

Authors

M.W. Lawrence

Maritime Operations Division

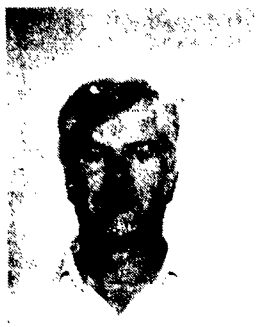

Dr Lawrence is a Principal Research Scientist in the Maritime Operations Division at AMRL Sydney. He joined DSTO (in Sydney) in 1978 after working at the AWA Research Laboratory in the field of surface acoustic waves. At DSTO he has worked on underwater acoustic propagation, with activities in both experimental measurements and computer modelling. He has worked in physical oceanography and is now working on the performance of side scan sonar systems and acoustic backscatter from the sea bed.

M.J. Bell

Maritime Operations Division

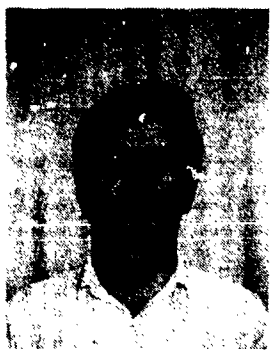

Professional Officer Class B in the Maritime Operations Division at AMRL Sydney. He has about 12 years experience in professional support of customer-problem-solving tasks with sonars of various types, together with technology-base tasks in descriptive acoustical oceanography. He is the co-author of a previous report on acoustic volume backscattering strengths measured for the SEAMAP task.

S. Prenc

Maritime Operations Division

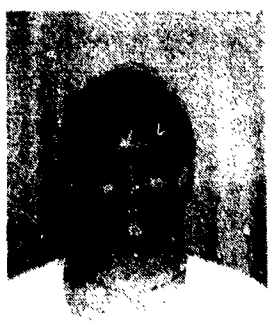

Ms Prenc is a Professional Officer Grade 2 in the Maritime Operations Division at AMRL Sydney. She has worked here since graduating from the University of Sydney at the end of 1988. At DSTO she has been working in underwater acoustics, with emphasis on the effect of the environment on acoustic propagation and also on computer modelling of acoustic propagation.

Contents

1 Introduction

(U) In May 1989 a research cruise, designated MSD 15/89, was conducted from H.M.A.S. Cook along mercantile routes to the north and east of Australia. Measurements were carried out in the Coral, Solomon and Tasman Seas. These seas comprise a portion of Australia's area of direct military interest, as defined by the Defence White Paper [Beazley, 1987, page 2]. This document contains discussion of experiments and results involving measurement of underwater acoustic propagation, particularly in relation to the effect of the sea bed. Supporting measurements were also performed on the physical properties of the water column, as well as sampling sea-floor sediments and determining swathe-mapped bathymetry. The locations of the measurement sites are shown in Figure 1.

(U) In the years 1984 to 1987 measurements of acoustic bottom reflectivity were undertaken as part of the SEAMAP program. These measurements, in regions to the east of Australia, have been described by Lawrence, Valentine and Prenc [1993a and 1993b] and by Valentine and Lawrence [1992]. The measurement technique used in the current study was an improved version of that used on the SEAMAP program. This report contains details of the differences between the two techniques. The bulk of this report deals with the results themselves.

(U) All of the acoustic propagation measurements made on this cruise involved the ship dropping a sonobuoy, and whilst steaming away, dropping explosive charges at regular intervals. The acoustic signal received by the sonobuoy was recorded and relevant sections were analysed. The sections of interest contain the bottom bounce arrival. This type of propagation run is known as a Ship-Sonobuoy-Run (SSR) (distinguishing it from the aircraft-ship experiments that have been performed on other occasions).

(U) The main characteristics of such an experiment (and the subsequent analysis) are:

- use of an impulsive source, - source and receiver located relatively near the surface,
- there are many frequencies, but few separations, - the analysis product is a bottom loss level.

(U) The main disadvantages of this technique are:

- the waves are spherical (not plane), - reflections from the sea surface cause complications,

- a long water path reduces the accuracy of the measurement, - details of the complex reflection process are not explicit in the bottom loss level.

(U) Despite these disadvantages, this classical experiment provides a relatively simple and useful characterisation of the acoustic sea-floor interaction at each location.

(U) The purpose of the measurements of bottom loss reported here is to help characterise the effect of the sea floor on acoustic propagation in areas of direct military interest to Australia. The sea floor frequently plays a very significant role in determining the sonar effectiveness for pro- or anti-submarine warfare. Better characterisation of the sea floor allows improved sonar modelling and detection range prediction.

(U) Previous measurements of bottom loss (at other than normal incidence) in this region have been reported by Brown [1981] and Hall and Nicholson [1969]. These measurements used similar techniques to the work reported here, but covered far fewer sites, a smaller frequency range, and had less ancillary oceanographic and geological data than was obtained for the sites of the present measurements. The set of bottom loss measurements reported by Brown [1981] covered three sites in the Coral Sea and one in the Tasman Sea, each analysed at frequencies from 31.5 Hz to 2 kHz. The bottom loss measurements reported by Hall and Nicholson [1969] covered a single site in the Coral Sea, analysed at frequencies from 250 Hz to 4 kHz. The data set reported here covers a much larger number of sites and a wider frequency range.

(U) This report specifically examines bottom bounce propagation (both bottom loss and transmission loss) isolated from the effects of other propagation modes (e.g. surface duct). This is in contrast to many other studies of propagation which have looked at overall propagation loss, regardless of mode.

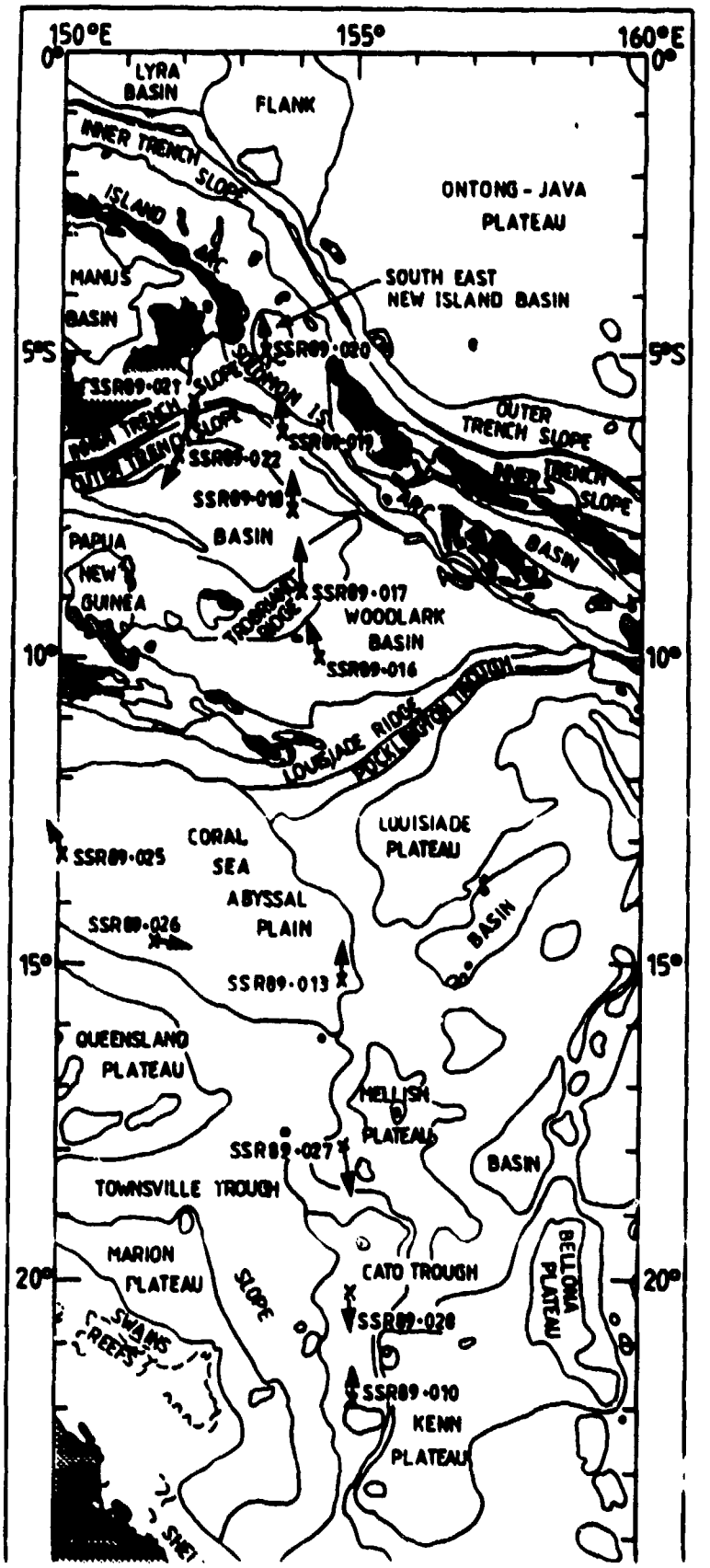
150°E
155°
160°E
0°
5°S
10°
15°
20°
LYRA BASIN
FLANK
INNER TRENCH SLOPE
ISLAND ARC
ONTONG - JAVA PLATEAU
MANUS BASIN
SOUTH EAST NEW ISLAND BASIN
SSR89-020
SSR89-021
SLOPE
EDDYSTONE IS.
OUTER TRENCH SLOPE
SSR89-022
SSR89-018
BASIN
PAPUA NEW GUINEA
TROBRIAND GROUP
SSR89-017
WOODLARK BASIN
SSR89-016
LOUISIADE RIDGE
ROCKINGHAM TROUGH
LOUISIADE PLATEAU
SSR89-025
CORAL SEA ABYSSAL PLAIN
SSR89-026
SSR89-013
QUEENSLAND PLATEAU
MELLISH PLATEAU
SSR89-027
TOWNSVILLE TROUGH
MARION PLATEAU
SWAINS REEFS
CATO TROUGH
SSR89-028
SSR89-010
KENN PLATEAU
BELLONA PLATEAU

A

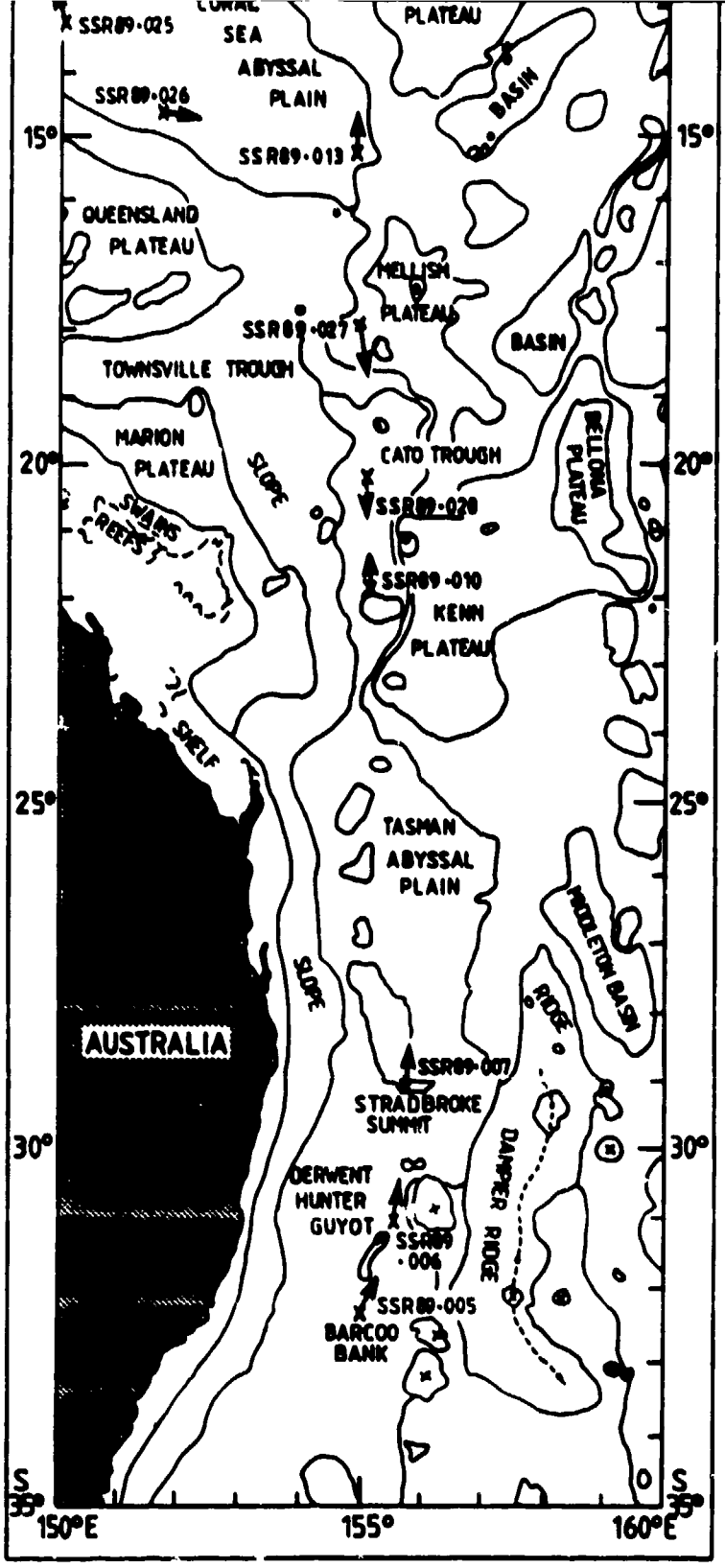

Figure 1: (U) Locations of acoustic propagation measurements. The lines delineate the geophysical regions. The sites of each sonobuoy drop is marked by an X, while the direction of travel during each propagation run is shown by an arrow.

This page intentionally left blank

2. *Nature of Received Signal*

2.1 Bottom Bounce Acoustic Propagation

(U) Consider a ray approach to acoustic propagation. Rays from an acoustic source may reach a receiver by a number of paths. The path types may be categorised into families such as: direct path (with no surface or bottom interactions), single surface reflection, single bottom reflection, double bottom reflection. Figure 2(a) illustrates these path types, based on an iso-speed water column. Refraction effects due to a varying sound speed (with depth) are discussed later. The travel time from source to receiver will in general be different for the different paths. This difference in arrival times is used to isolate in time the arrival corresponding to the relevant ray path.

(U) The path in which we are interested here is the single bottom reflection path. From measurement of the transmission loss along this path, it is possible to estimate the loss that occurred on reflection from the bottom. However, if the source and receiver depths are small relative to the ocean depth, then there are four acoustic paths that have nearly the same arrival time as the single bottom bounce path. These four paths each have one bottom bounce, but they have also either (i) no surface reflection, (ii) a surface reflection near the source, (iii) a surface reflection near the receiver, or (iv) a surface reflection near the source and another near the receiver (Figure 2(b)). At geometries that give rise to rays travelling at small grazing angles, the time separation between these four arrivals becomes less than the duration of each arrival. Thus it is not possible to isolate this quartet of arrivals from each other, under all conditions.

2.2 Source Characteristics

(U) The acoustic source used was the Mk 61 SUS (Signal Underwater Sound) charge, the same type as was used in the SEAMAP program. This is a pressure triggered charge with a charge weight of 0.82 kg. It can be set to trigger at a depth of either 244 m (800 feet) or 18 m (60 feet). Each SUS charge contains a tetryl primer of charge weight 0.031 kg to detonate the main TNT explosive. Characteristics of underwater explosives and explosions have been well described by Cole [1948], Gaspin and Shuler [1971] and Chapman [1985]. As well as the explosive shock wave, a "bubble pulse" is generated by rebound of the underwater gas bubble resulting from the explosion.

(U) For the bottom reflectivity measurements reported here, the SUS charges were set to trigger at 244 m. The source levels of Gaspin and Shuler [1971] were used for the SEAMAP analysis. A newer set of source level measurements [Chapman, 1988] indicates that the Gaspin and Shuler values underestimated

the source energy at frequencies below that of the bubble pulse (53 Hz), by approximately 2 dB at 10 Hz. For the work reported here, the Chapman source levels were used at low frequencies (up to his maximum of 630 Hz), while the Gaspin and Shuler source levels were used at higher frequencies.

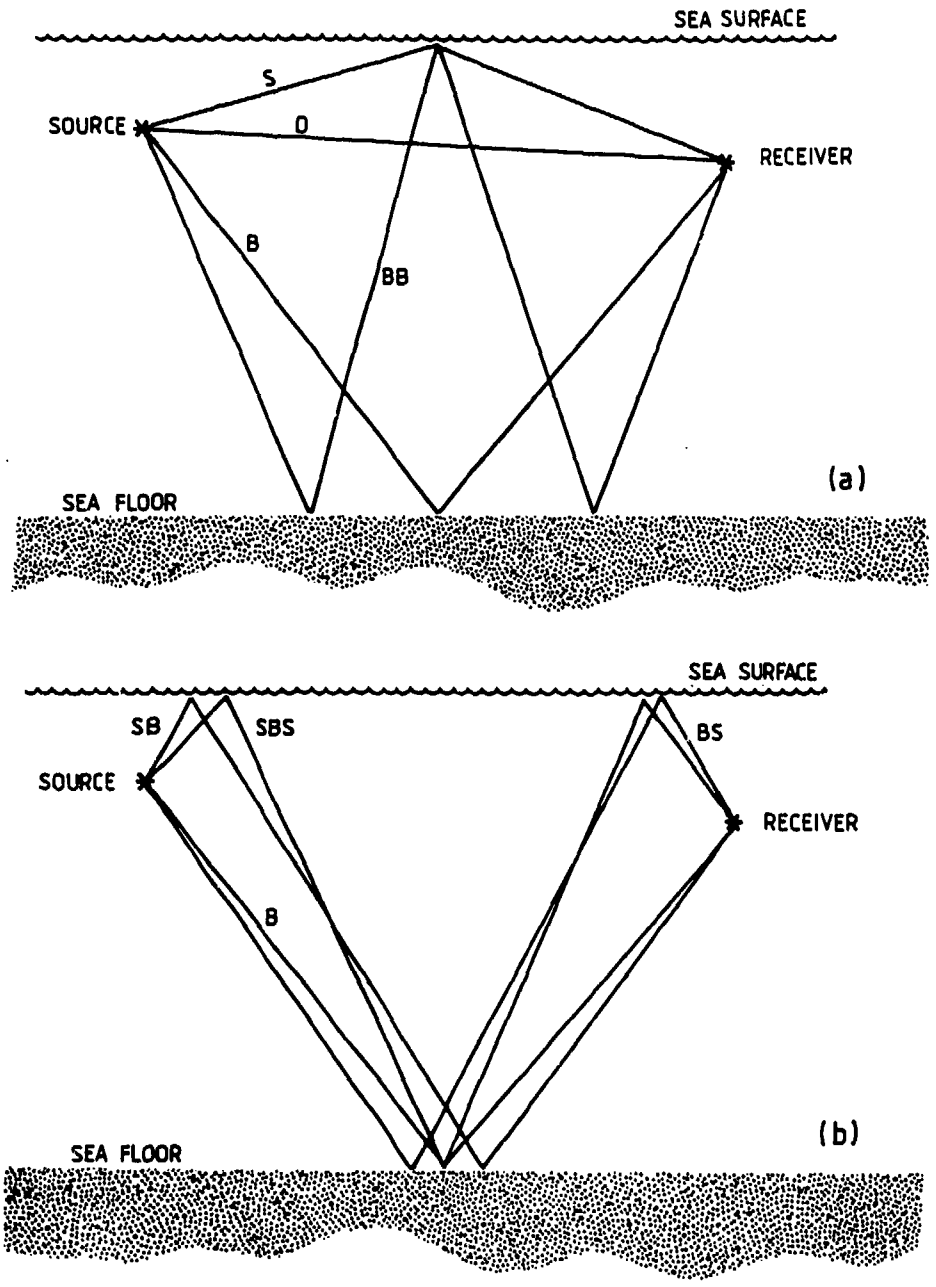

Figure 2: (U) Ray path families: (a) Major family classes: D Direct, S Surface reflected, B Single bottom bounce, BB Double bottom bounce; (b) Single-bottom-bounce families: B Bottom reflection, SB Surface then bottom reflection, BS Bottom then surface reflection, SBS Surface then bottom then surface reflection.

(U) Lawrence, Valentine and Prenc [1993a] found that the actual triggering depth of the SUS charges varied from the nominal depth by up to 17 m. Change in source depth results in a change in acoustic spectrum of the generated energy. However, for the depth variation observed, there is such a minor change to the source spectrum that it is insignificant in this analysis. Thus, the standard spectrum is used for analysing all charges, thus avoiding the extra complexity of using an individually tailored spectrum for each SUS charge.

(U) The source-level spectrum used in this report for the Mk 61 SUS charge, exploded at a depth of 244 m, is shown in Figure 3, with values given in Table 1. The spectra are given in third-octave frequency bands (the figure has tick marks on the abscissa at every third-octave centre frequency). The energy spectrum level of the source is given in the logarithm of the SI unit, i.e. dB re 1 J/sr/Hz. These energy values may be converted to the commonly used unit, dB re 1 erg/cm^2/Hz at 1 metre, by adding 30 dB to each value.

Table 1 (U): *Energy spectrum levels (in units of dB re 1 J/sr/Hz) of the acoustic source, listed with the centre frequency (in Hz) of third-octave frequency bands.*

Frequency	Energy	Frequency	Energy
10.0	7.1	250.0	17.5
12.5	9.8	315.0	17.1
16.0	12.9	400.0	16.1
20.0	15.9	500.0	15.5
25.0	19.0	630.0	14.0
31.5	21.7	800.0	13.3
40.0	24.4	1000.0	12.2
50.0	26.6	1250.0	10.9
63.0	26.2	1600.0	9.1
80.0	22.8	2000.0	7.1
100.0	23.0	2500.0	5.2
125.0	19.3	3150.0	3.6
160.0	21.6	4000.0	-0.4
200.0	19.6	5000.0	-0.4

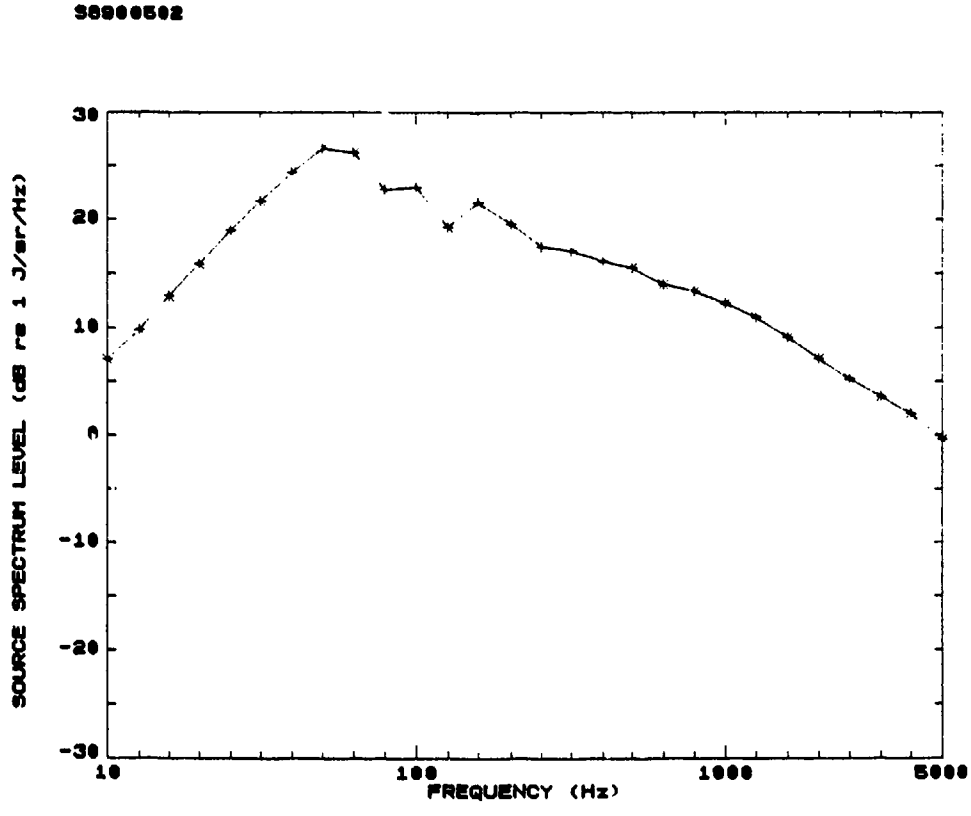

Figure 3: (U) Third-octave spectrum levels for the Mk 61 SUS charge, exploded at a depth of 244 m.

3 Experimental Method

3.1 Procedure at Sea

(U) The procedure for the SSR experiments was as follows. With the ship travelling on the required course, an expendable sonobuoy (type SSQ-41B), modified as described in Valentine and Lawrence [1992], was deployed. At regular intervals, typically one nautical mile, a Mk 61 SUS charge was detonated at a depth of 244 m and the resulting acoustic signal was transmitted by sonobuoy radio link to the ship for recording and processing. Also recorded,

from a hydrophone mounted in the hull of the ship, was the direct acoustic signal from the SUS charge for use as a trigger point in the processing. The experiment continued until the radio link became too noisy for valid data acquisition. The longest range achieved was 25 miles, in sea state 2. In sea state 2 or less a range of 20 miles was common, dropping to 18 miles in sea state 3 and 17 miles in sea state 4.

(U) As the acoustic data stream was received at the ship, it was digitised directly into the desk-top computer and stored on hard disk. Simultaneously, a long data segment was recorded digitally on magnetic tape in order to provide backup in case problems occurred with the digitising (e.g. faulty triggering). Figure 4 shows a block diagram of the shipboard electronics for signal acquisition and storage. High frequency radio transmissions from the ship's communications centre had to be suspended during each propagation run, in order to prevent contamination of the experimental results.

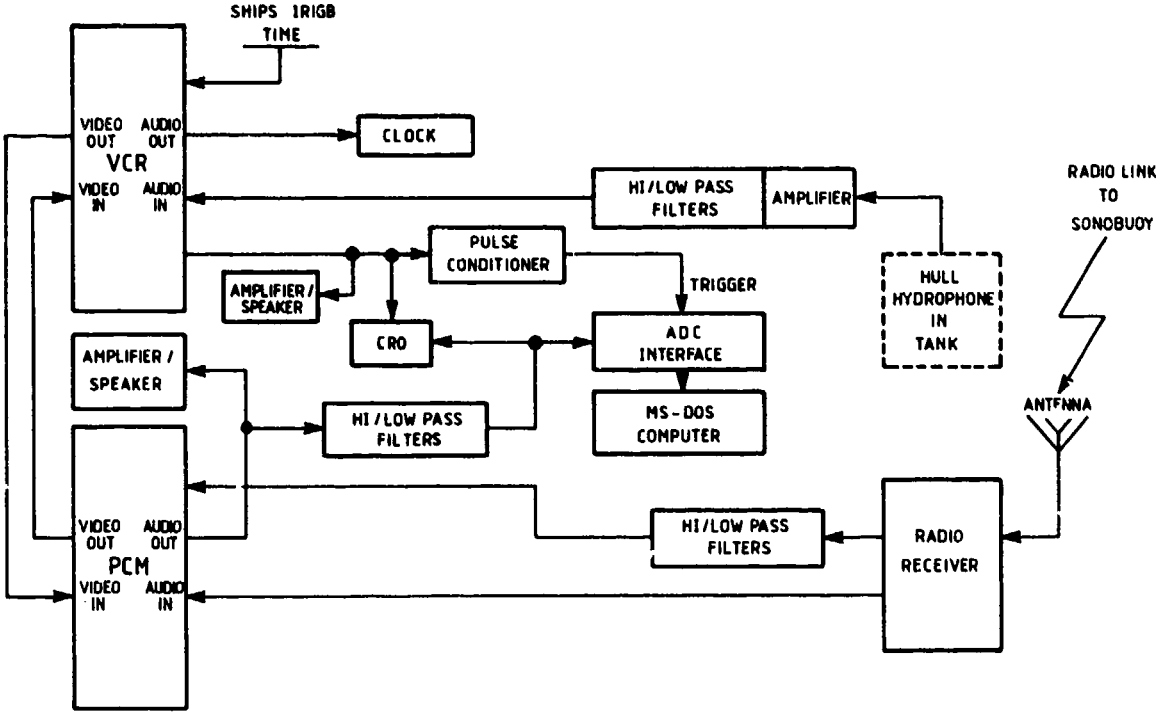

Figure 4: (U) Block diagram of the shipboard electronics for acoustic signal acquisition.

3.2 *Equipment*

(U) The major change in the measurement equipment, from that used in the SEAMAP program, was use of a different computer system for data acquisition and analysis. This change necessitated use of a new analog to digital converter (ADC), modified data storage techniques, and modified acquisition and analysis software.

(U) The computer used for data acquisition in these experiments was an NEC Powermate 386 (which has industry standard architecture based on the Intel 80386 microprocessor), running the MS-DOS operation system. The ADC used was a Data Translation DT2821F-SE plug-in card. A digitisation rate of 20480 samples per second was used (twice the rate used in SEAMAP). Combining this with the 8 second record length, plus two bytes per sample, entails an acoustic data storage requirement of 320 kbytes for each shot.

(U) To facilitate data storage and transfer, the storage media used were a LaserStor optical disk WORM drive and a Tallgrass TG-1040i internal tape storage system. The 800 Mbyte optical disks were the main storage medium. The 40 Mbyte tapes were used as independent backup storage.

(U) The data acquisition program, SONOADC, controlled all aspects of the data acquisition and disk storage of the acoustic data. It was written in (Microsoft) Fortran and is the host program for the ADC. It created a header file, one for each shot, which contained ancillary information such as gain and filter settings. Figure 5 is an example of the contents of a header file.

(U) The remaining major components of the system remained substantially the same as those used in the SEAMAP program, which are described in detail in Valentine and Lawrence [1992]. It is noteworthy here that the VCR/PCM (video cassette recorder, pulse code modulation) system records high speed digitised audio signals on the video channels of the VCR. This system is used for backup in case the direct computer acquisition of the data fails.

(U) The acoustic source and sonobuoy receiver are described above. Each sonobuoy was modified to have reduced sensitivity and a flat frequency response, and then was individually calibrated. The hydrophone depth was set to 305 m, and the sonobuoy scuttle time to 3 hours. (The sonobuoys were manufactured by Sparton, a different manufacturer to that for the SEAMAP cruises.) Further details of the measurement procedure and equipment are contained in Annex A.

```
OCEAN SCIENCE SONOBUOY DATA ACQUISITION
RUN NUMBER                          : SSR89.005
SHOT NUMBER                         :         02
TAPE NUMBER                         :      00001
TAPE COUNTER                        :      00200
RECORDING DATE                      :   09/05/89
RECORDING TIME                      :       2240
CONVERSION RATE                  Hz:   20000.00
PRE-RECORD FILTER                Hz:   12000.00
POST-REPLAY FILTER               Hz:    8000.00
SENSOR CAL          dB re 1V/uPa:    -161.70
PRE-RECORD GAIN                  dB:       0.00
TAPE INSERTION GAIN              dB:      -4.60
POST-REPLAY GAIN                 dB:       0.00
ADC GAIN          0,6,12,18 dB:      12.00
ADC CAL         dB re FTN{1}/V:      70.31
SYSTEM CAL        dB re 1V/uPa:     -83.99
ADC CHANNEL                         :         0
RECORD LENGTH             Samples:     163840
RECORD LENGTH             Seconds:       8.19
REPLAY DATE                         :   09/05/89
REPLAY TIME                         :       1101
ADC TRIGGER DELAY         Seconds:         .88
SONOBUOY NUMBER                     :      08804
                                    :
```

Figure 5: (U) Typical data header file for a single shot, produced by SONOADC.

3.3 *Calibration*

(U) In order to calibrate the measurement system, it was broken into a number of functional components. The effect of each component was individually determined, before combining to give the overall calibration. The functional components were as follows:

a) Sensitivity of each individual sonobuoy plus radio receiver (from acoustic intensity at the hydrophone to the output of the radio receiver on the ship). This sensitivity was determined at a hydrophone calibration facility located at Woronora dam, near Sydney. This procedure produces an overall sensitivity value for all but the very lowest frequencies, as well

as a low frequency roll off point. Hence the whole of the frequency response of the sonobuoy could be computed, when required.

b) Gain of programmable amplifier in the ADC unit.

c) ADC calibration (numeric output per volt at the output of ADC amplifier).

(U) The following additional calibrations were involved in those measurements which involved the VCR/PCM system:

d) Pre-record amplifier gain; between radio receiver output and VCR/PCM record input.

e) Tape insertion gain of VCR/PCM, determined as follows. Prior to commencement of the experiment an oscillator was used in place of the receiver to provide a sinusoidal reference signal, typically 1 volt rms at a frequency of 200 Hz. This level was recorded for reference, and measured at replay. The difference between the two levels was the 'Tape Insertion Gain'.

f) Post-replay amplifier gain; between VCR/PCM replay output and ADC input.

3.4 *Supporting Information*

(U) In conjunction with the acoustic data received from the sonobuoy, various types of data were obtained from the ship's on-board Hewlett-Packard data logger. At intervals of 30 seconds the latitude, longitude, ship speed, ship heading and water depth were recorded under control of the "scientist's computer". This scientist's computer was an AT compatible, which was directly connected to the on-board data logger.

(U) The ship's data logger also provided "snapshots" of the state of various parameters at the time of each sonobuoy deployment and each SUS charge drop. These snapshots contain information on the time of deployment, water depth, ship speed, ship heading, latitude and longitude. The time of deployment and SUS charge detonation were recorded by hand by the operator of the data acquisition system. A log of events was also maintained by the ship's bridge. This duplication of data recording allowed verification and reduced the likelihood of data being lost.

4 Preparation Of Acoustic Data For Analysis

4.1 Form of Data

(U) The raw acoustic data set for each shot is in the form of an 8 second record of the acoustic pressure, digitised to 12 bit accuracy at a rate of 20480 samples per second. Each sample is stored as a single 16 bit word. The acoustic data set for one shot thus occupies 320 kbytes of storage. The 12 bit accuracy corresponds to a potential signal to noise ratio of 66 dB ($\pm 2^{11}$).

4.2 Selection of Data Segment

(U) The raw acoustic data are displayed in graphical form, so that the single bottom bounce arrival can be unambiguously selected. The instant of detonation ("zero time") can be calculated from the time of arrival of the pulse at the hull-mounted hydrophone. The first few shots occur at small range between source and receiver, that is at steep ray angles with respect to the sea floor. Knowing the water depth, it is easy to identify the direct and the bottom reflected arrivals for these first shots.

(U) As the range increases, the direct path arrival reduces in amplitude until, after typically 10 km, it has virtually disappeared (the experimental geometry used usually resulted in the source and receiver being below the surface mixed layer duct). The first significant arrival at these and greater ranges is the single bottom arrival. The double bottom arrival is often also apparent.

(U) Having determined which part of the data record contained the single bottom arrival, it was necessary to delimit the region to be analysed. This was achieved by selecting the beginning of the data segment for analysis to be just before the beginning of the bottom arrival. The end of this selected segment was then set to 1.6 seconds later (32768 data points), unless it was necessary to shorten the selected segment in order to avoid unwanted signals. One cause of unwanted signals was double-bottom-bounce acoustic arrivals. Another cause was the periodic large increases in radio noise due to a wave-crest shielding of the direct radio path from sonobuoy aerial to the ship-borne antenna. This increased noise on the acoustic signal results from increasing FM modulation noise as the RF transmission signal level is reduced.

4.3 *Overload*

(U) All signals for analysis were examined for the presence of overload. Any which exceeded the criteria set in the electronic design and testing were rejected.

(U) Experience on early cruises has shown the need to modify the sonobuoys in order to consistently obtain data which were not overloaded, and could be demonstrably shown to be so. The hydrophone-preamplifier in the sonobuoy was modified both to reduce the sensitivity at this stage and to provide hard-limiting of the signal. Overloading is not a problem in the hydrophone transducer, as shown by Lawrence, Valentine and Prenc [1993a].

4.4 *Selection of Noise Data Segment*

(U) An estimate of background noise was made for each shot analysed. The background noise is due to a combination of radio transmission noise, electronic noise, recording noise and acoustic noise in the sea. The radio transmission noise normally dominated the other noise sources.

(U) The data segment for estimating the noise is chosen by selecting a segment which appears to have no acoustic signal, but does have a level of noise typical of the 8 second segment that has been digitised. As in the case of selection of the bottom bounce data segment for analysis, the segment is chosen to be 1.6 seconds in length, or less if this is not possible. There is no requirement to have the length of the noise segment the same as that of the data segment.

5 *Ancillary Information*

(U) A considerable quantity of ancillary information (ancillary to the acoustic data) was collected on the same cruise as the acoustic propagation data described herein. Some of this ancillary information is relevant to the present study because it provides valuable environmental information allowing more informed interpretation of the acoustic data. The information collected includes water property profiles, bathymetry, deep sediment properties, and surface sediment properties. Each of these properties are discussed briefly in the following paragraphs.

5.1 *Sound Speed and Absorption*

(U) The sound speed and sound absorption as a function of depth were calculated from oceanographic parameters obtained by measurements of temperature as well as climatological values of salinity and acidity (pH value), as described below.

(U) For each propagation run two XBT (expendable bathythermograph) records of water temperature versus depth were obtained; one was at the beginning of the run, the second at the end. Usually the XBT type was Sippican T5, which measures temperature to a depth of 1750 m, but occasionally it was type T4, which only measures to 450 m.

(U) Climatological salinity and temperature data used in the analysis were obtained from Levitus [1982, pp. 54 and 56], which presents annual mean values of each of these parameters, averaged over each 5-degree latitude belt in the South Pacific Ocean, at standard oceanographic depths from 0 to 5500 m. Acidity values were obtained from Gorshkov [1974].

(U) For each site, the measured values of temperature were combined with climatological values of salinity and acidity to calculate the speed of sound [Mackenzie, 1981] and the absorption [Francois and Garrison, 1982] at appropriate depths for that specific area. The computer program SOUNDP performed this operation.

(U) Usually the water depth was greater than the deepest measured temperature data. Climatological temperature values were used to extend the temperature profile to the full water depth. In a few cases, there was an unsatisfactory fit between the sound speed calculated from measured temperatures and the sound speed calculated from climatological temperatures. Manual splicing of the two segments of curve (sound speed versus depth) was used in order to produce a smooth fit.

5.2 *Bathymetry*

(U) Bathymetric information was primarily collected using the multi-beam echo-sounder SeaBeam, manufactured by General Instrument Corporation [Farr, 1980]. This device produces both a narrow beam width for the vertical beam and a swath contour map. The narrow vertical beam (2.67° width) ensures an accurate bathymetric profile along the ship's track. This is in contrast to the bathymetric record produced by conventional (wide-beam) echo-sounders which can be contaminated by artefacts resulting from nearby features, such as seamounts. The swath contour, with a width of 75% of the water depth, shows

the large scale inhomogeneity of the b. .ymetry. This is useful in interpreting the results of the acoustic experiments.

(U) For the acoustic analysis, the depths from the vertical beam are used, with depths being input at the position of sonobuoy deployment and at each SUS charge drop.

(U) In some cases, the bottom topography was rugged or exhibited a large mound or dip. For the acoustic analysis, the measured bottom profile (with range) was replaced by an approximate profile based on a small number of straight lines which served to remove these bottom roughness characteristics. This approximation was made necessary because of problems which would otherwise occur in calculating the water path transmission loss. The problem manifested itself as difficulty in finding eigenrays in the ray tracing technique which is used to calculate the water transmission loss. Ray theory cannot cope accurately with closely spaced changes of slope in the bottom profile.

5.3 Geological and Geophysical Properties

(U) The geological and geophysical properties of the sea bed may be divided into two regions for purposes of comparison with the acoustic results:

(a) properties of the top few metres of sediment (determined primarily from core and dredge samples), and

(b) properties of the deep sediments (which are determined primarily from seismic profiling).

(U) Existing knowledge of the geological and geophysical properties of the experiment sites was supplemented by data taken on MSD 15/89. In particular, core samples were obtained, using a 3 m gravity corer. These results are described and analysed (along with the SeaBeam results) by Jenkins and Pritchard [1989]. The SeaBeam results are analysed to give root-mean-square (rms) roughness values. Also in this report is a review of the existing geological and geophysical data, including seismic profiles.

6 Analysis of Acoustic Data

6.1 Time Domain Data

(U) The analysis of data is done completely digitally, following the digitisation of the 8 second segment of acoustic data containing the bottom arrival. Computer files are generated and manipulated which contain acoustic, environmental and navigational information regarding each shot and also for each entire propagation run.

(U) The selection and processing of data is performed in an interactive manner. The analysis program uses a computer screen display as shown in Figure 6, for one shot. The lower quarter of the figure shows acoustic intensity at the sonobuoy plotted against time (as the abscissa). Eight seconds of record are shown, with tick marks each second. The intensity plot is normalised and is plotted linearly. A 1.6 second length of data (32768 samples) is selected for examination, by moving the thick bar over the chosen segment. On selection, the data segment is read into the computer semiconductor memory from disk, and is displayed in the top half of the figure, as a plot of acoustic pressure against time. This pressure-time plot can be further modified by selecting a particular portion of the 1.6 second record. The final selection of the actual data for analysis is performed by delimiting using the two dashed lines, which can be moved to any desired location.

(U) The acoustic intensity display represents all points in the sampled record (by means of an averaging process). The acoustic pressure record, similarly, represents all points in the selected data segment, even though there are usually more points than there are pixels on the display device. No averaging is used on this signal, instead all points significant to the display are shown.

(U) Further details of many aspects of the analysis procedures described in section 6 can be found in Lawrence, Valentine and Prenc [1993a].

6.2 Conversion to Frequency Domain

(U) The measured data are in the form of a number of samples of the acoustic pressure at equal time intervals. These data are converted to pressure at particular frequencies by applying a fast Fourier transform and then converted to energy by squaring.

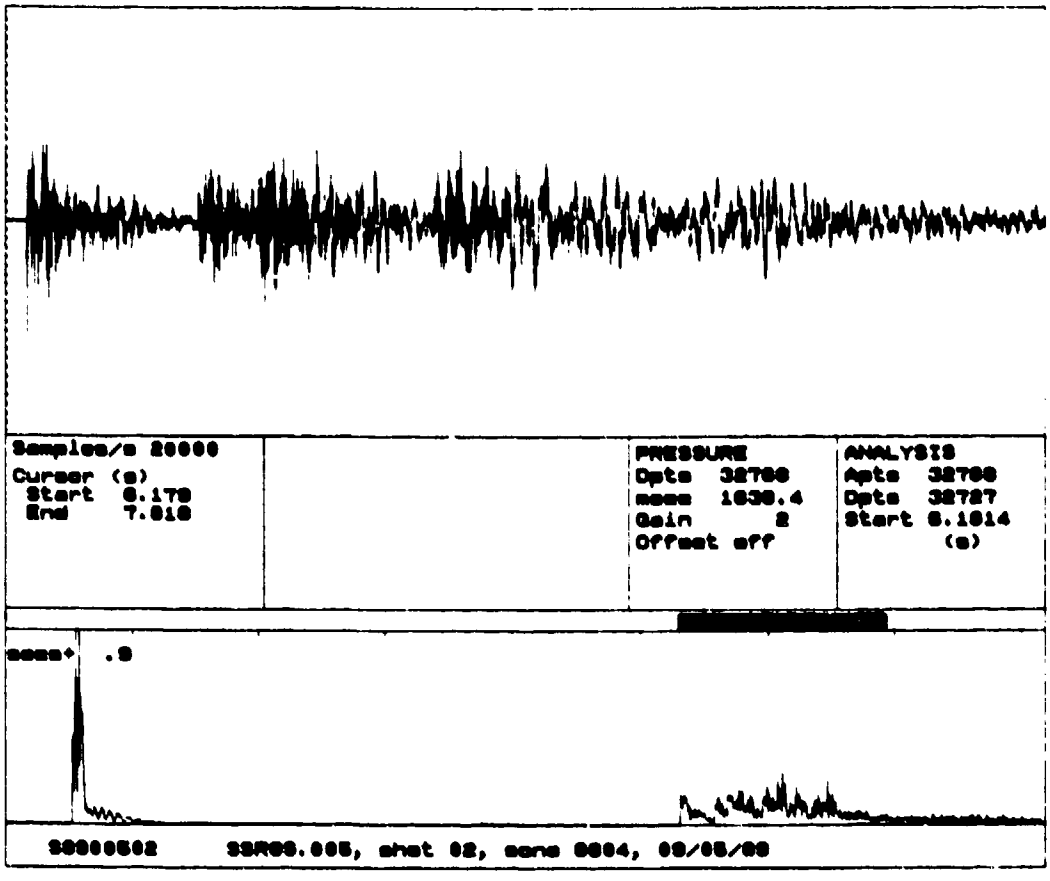

Figure 6: (U) Interactive display for analysis of a shot. The lower curve shows acoustic intensity at the sonobuoy plotted against time (8 sec length, with the left hand edge being delayed from the shot by the time indicated in the display). The upper curve shows acoustic pressure against time, for the selected 1.6 sec block..

(U) In order to determine the energy in a particular arrival, it is necessary to process the pressure signal over the total length of time of arrival of the signal. For analysis reported here, up to 1.6 seconds of acoustic signal have been processed. The single bottom bounce arrival normally is well contained within this time window. The only cases in which this was not so were short range (steep angle) shots in regions with a large amount of bottom roughness. No amplitude weighting of the time window was applied to the data, since this would be inappropriate for the transient data being examined.

(U) If the number of data points in the segment selected for processing was not a power of two, zero filling of the data array was performed before further processing. Zero filling could be performed to an array of size any power of

two, up to 32768 (2^{15}). Increasing the number of (time) data points in the Fourier transform processing results in frequency points being more closely spaced, but still having the same maximum frequency value.

6.3 *Frequency Bands*

(U) The received acoustic signal shows many rapid variations of received energy as different frequencies are examined. This results from two main causes. The first is the complexity of the detailed structure in the source spectrum. The second is the interference that occurs between the various multipath arrivals. These multipaths arise due to sea surface reflection as well as due to multi-reflection and refraction processes within the sea bed.

(U) It is desirable to have data which are not explicitly affected by the detailed nature of these fluctuations. Averaging the measured results across a frequency band causes a smoothing of the resulting spectrum. The wider the frequency band the greater the smoothing, but the more widely separated (in frequency) the spectrum points.

(U) The results of these experiments have been calculated in third-octave bands, which are easily converted to the full-octave bands in which the results are reported here. The centre frequencies of the third-octave bands ranged from 12.5 Hz to 5 kHz. This leads to centre frequencies of the full-octave bands ranging from 16 Hz to 4 kHz.

(U) After converting to third-octaves, the acoustic spectra were corrected by the measured system calibration spectrum, plus allowance for the effect of the anti-aliasing filter.

6.4 *Noise*

(U) For each shot, the noise signal in each third-octave band was compared with the received bottom signal. Processing was discontinued for any band in which the bottom bounce signal did not exceed the noise signal by a minimum of 10 dB. This signal to noise excess is larger than normally required, due to the non-stationary nature of the noise as well as the desire to exclude any doubtful results. The non-stationary noise results from intermittent shadowing of the radio transmission path due to wave and swell action on the sonobuoy.

6.5 *Separation between Source and Receiver*

(U) In order to model the acoustic propagation, and hence to determine the bottom loss, we must determine the separation between each SUS explosion and the sonobuoy. The vertical depths of the source and receiver are already known. Thus determination of the total separation will allow the horizontal separation to be readily found.

(U) In the work reported here, the total separation is determined as the time taken for the acoustic signal to propagate from the SUS explosion to the sonobuoy via the single bottom bounce path. This time is later used to determine the appropriate eigenrays in the ray theory modelling.

(U) Direct measurement is made of the time difference between the arrival of the direct path to the hull-mounted hydrophone and the arrival of the bottom bounce signal at the sonobuoy. In order to determine the desired propagation time, a correction is made to the measured time in order to allow for the (relatively small) separation between the ship and the SUS explosion. This correction time $t = r/c$ is determined from r the separation between the SUS and the hull hydrophone and c the average sound speed over the top 244 m of the ocean. The separation r is determined from the physical locations of hydrophone and SUS drop point, together with speed of advance of the ship and time from drop till explosion.

(U) At small ranges in deep water the above technique becomes inaccurate. In these circumstances, the horizontal range between acoustic source and receiver is calculated from estimates of ship speed and course.

6.6 *Water Path Transmission Loss*

(U) The transmission loss due to the water path is estimated by a ray-theory calculation of the single-bottom-bounce acoustic transmission. Each member of the bottom bounce quartet is included. The sound speed and absorption described in section 5.2 are used in the calculations. This calculation also provides the ray angles at the sea floor, which is an important parameter in presenting the results. A typical example of the results of calculating the water-path-transmission loss is shown in Figure 7. The details of this calculation are set out in Annex A of Lawrence, Valentine and Prenc [1993a].

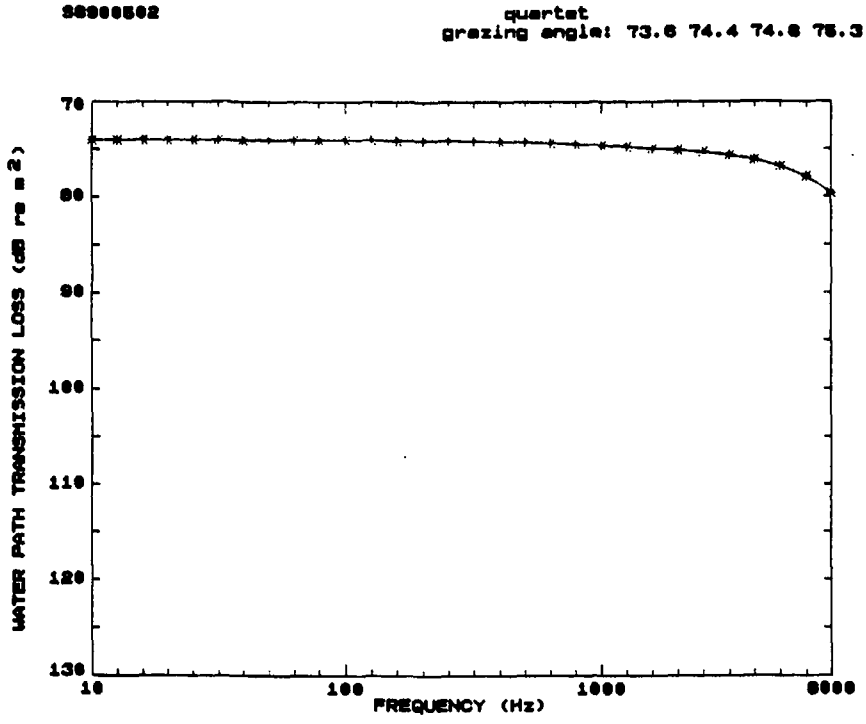

Figure 7: (U) Water path transmission loss for a typical shot.

(U) In our model the sea floor is represented as a piece-wise linear structure, from which the acoustic rays reflect. There are slope discontinuities at the ends of each linear piece of the sea floor.

6.6.1 Horizontal Sea Floor Reflection

(U) For the calculation, the rays are taken to reflect at the sea floor from a horizontal interface (rather than the experimentally estimated slope of the bottom). Despite this, the rays are taken to reflect from the range varying value of the sea-floor depth (as determined by the linear segment bathymetry). This procedure (of horizontal interface reflection) is used in order to avoid the significant errors in ray theory predictions that would otherwise occur due to the reflections from the discontinuous slope of the sea floor.

(U) An explanation of the issues involved follows. Consider rays that reflect from the sea floor in the vicinity of a discontinuity in slope of the sea floor. Consider an increase in the slope of the sea floor at this discontinuity (positive slope is downwards from the horizontal). The reflection from the sea floor at a location just before the discontinuity, will arrive at the receiver depth at a range significantly shorter than that of the ray that strikes the sea floor just after the discontinuity. That is, there will be a horizontal gap in the arrivals at the

receiver depth. If there is a receiver at a location within this range, the theory will predict no energy arriving. This result is incorrect, and is due to the limitations of ray theory in dealing with discontinuities. The problem is avoided, and a much more realistic result is achieved, by assuming that the sea floor is horizontal everywhere, but making use of the best estimate of the depth at every point.

(U) A comparison was made between modelling results with reflection angle determined by a horizontal interface and alternatively by an estimate of the bottom slope. This comparison showed that more accurate results were achieved, in general, by using the horizontal interface. For consistency, the same technique was then applied to all experiments.

(U) The angle quoted in the analysed results (Figure set B) is the grazing angle with respect to the horizontal. This is the appropriate angle for a number of reasons, including that the results of these analyses are intended to be used in circumstances where the exact slope is not known.

(U) For the case of a bathymetric profile that is approximated by a straight line of constant (non-zero) slope, a case can be made for using a reflection from this line rather than from the horizontal. However, in order to provide consistency across all the results, the reflection used in this report is with respect to the horizontal in all cases.

6.6.2 Approximate Bathymetric Profile

(U) A rugged sea floor can give rise to a further problem. Unless the bathymetry is very accurately known at closely spaced points, the ray theory will not match the focussing effects of the sea floor. However, in some sense small scale focussing effects are part of the bottom loss of the region, so it is not in fact particularly useful to avoid them by calculation. As discussed in section 5.2, for the ray theory modelling, the measured bottom profile (with range) was replaced by an approximate profile based on a small number of straight lines. This use of an approximate profile serves to remove the bottom roughness characteristics, while still incorporating the effects of major changes in the sea floor depth.

6.6.3 Interference of Bottom Bounce Quartet

(U) The four members of the bottom bounce quartet will add together to give a total signal. The signals of individual members of the quartet may overlap to some extent. Overlapping signals will, of course, add coherently to give the total signal. The frequency spectrum of the time interval containing more than one member signal will be affected by the relative phases of each member signal. This is true even for non overlapping signals.

(U) The above processes will be manifested as 'coherence' effects. The total signal may be greater or smaller than an incoherent sum depending on the relative phases of the member signals. As frequency changes, the relative phases also change giving rise to interference fluctuations (transmission anomalies). Averaging the signal across a frequency band will smooth out these interference fluctuations. The results here are all reported as full-octave band averages (the frequency at the top of the band is a factor of two times the frequency at the bottom).

(U) At higher frequencies, the averaging process across an octave band will remove interference fluctuations from the band result. However, at the lower frequencies, band averages may still have some residual effect from this interference effect. The analysis in Annex B allows estimation of the importance of this effect for any given set of experimental parameters.

(U) Examination of the experiment configurations shows that sea-surface interference should have not been a problem for any of the reported results. That is, the incoherent summation used in the water path transmission loss calculation is adequate. However, Annex B shows that this would not have been true (at the lower frequencies) for third-octave band averaging.

(U) Some further difficulties with the implementation of coherent analysis in this case are discussed in Annex B.

6.7 Bottom Loss for Single Shot

(U) The transmission loss third-octave spectrum, TL, via a single-bottom-loss path is determined from the experimental results using

$$TL = SS - ER$$

where SS is the energy source strength (section 2.2) and ER is the received energy flux density (section 6.3).

(U) The bottom loss third-octave spectrum, BL, for a single shot is determined by subtracting the water-path-transmission loss, WPL, (section 6.6) from the measured transmission loss

$$BL = TL - WPL$$

This bottom loss is in the form of a third-octave spectrum for a particular grazing angle at a particular site. An example of a bottom loss spectrum for a single shot is shown in Figure 8.

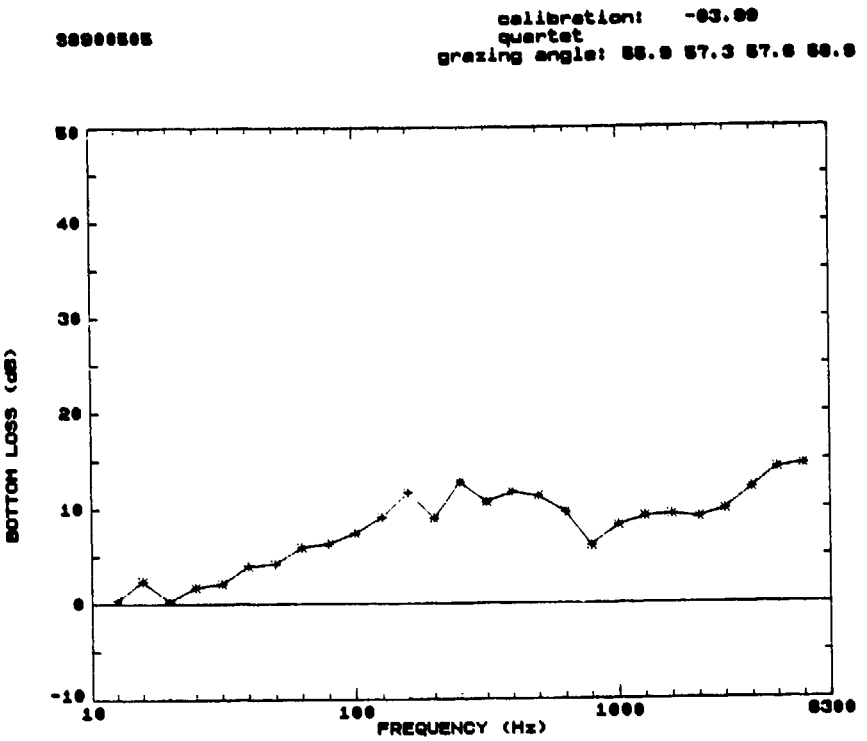

Figure 8: (U) Bottom Loss third-octave spectrum for a typical shot.

6.8 Bottom Loss for Propagation Run

(U) For any propagation run there are a number of individual shots, frequently about twenty. Combining together the bottom loss spectrum from each of these shots allows production of curves of bottom loss versus grazing angle, for the various third-octave bands. These curves can then be simplified by combining third-octave bands to produce full-octave bands. This form of result is the main product of the analysis and many examples are presented in later sections of this report.

7 Results

7.1 Locations Surveyed

(U) The successful propagation runs, performed during this cruise, covered nine different geophysical provinces, all located in the general region off north-eastern Australia. The ocean areas of the investigation are the Coral, Solomon and Tasman Seas. The positions of the propagation runs are shown on the chart of Figure 1. The physiographic province base for this chart is from Schneider [1987]. The geophysical provinces, and associated propagation runs, are described below:

* CATO TROUGH (latitudes 21-22° S)

(U) Two runs covered this region, SSR89.010 and SSR89.028. Both of these runs traversed parallel to the axis of the trough rather than the cross section. Consequently, the terrain covered was quite smooth and flat with an average depth of 3200 m. See Figures S4 and S16.

* CORAL SEA ABYSSAL PLAIN (latitudes 13-15° S)

(U) This region is a very flat smooth area with an average depth of 4600 m. Three runs were completed in this region, SSR89.013, SSR89.025 and SSR89.026. See Figures S5, S13 and S14.

* INNER TRENCH SLOPE (latitude 6° S)

(U) This region was covered by two propagation runs. SSR89.019 covered from the trench floor towards the adjacent island arc. The second run, SSR89.021 traversed the trench in the opposite fashion, that is from the island arc to the trench floor. For SSR89.019 the bathymetry indicates a rugged, steep incline from approximately 8250 m to 6450 m within 29 km. The remaining 17 km consists of a mound leading to a flat region of rough terrain, with an average depth of 6500 m. Run SSR89.021 covered a steep rugged decline, passing from a water depth of approximately 4750 m to a depth of 8250 m over a range of 40 km. See Figures S9 and S11.

* MELLISH PLATEAU (latitude 18° S)

(U) One run was completed in this area, SSR89.027. The region consisted of a small valley, leading to the gently undulating surface of the Mellish Plateau. In the vicinity of the sonobuoy the depth of water was approximately 1700 m.

Within 3 km from the sonobuoy the water depth increased to 2150 m, the bottom of the small valley. By a range of 6 km the depth had decreased to 2000 m, at which depth it remained. See Figure S15.

* OUTER TRENCH SLOPE (latitude 7° S)

(U) One propagation run, SSR89.022, covered this region of average water depth 5400 m. At 5 km away from the sonobuoy the depth began to gradually decrease. By 15 km from the sonobuoy the depth was approximately 4750 m and beginning to slowly increase. It then continued as an undulating slope, to a depth of approximately 5150 m, over a distance of 20 km. See Figure S12.

* SOUTH EAST NEW ISLAND BASIN (latitude 5° S)

(U) This region was a smooth, gently rising slope from a depth of 4550 m to 4050 m, over a distance 45 km. Only one run, SSR89.020, was completed in this region. See Figure S10.

* TASMAN ABYSSAL PLAIN (latitudes 29-32° S)

(U) This region was a very flat, smooth area with an average depth of approximately 4800 m. Three runs were completed in the region, SSR89.005, SSR89.006 and SSR89.007. See Figures S1, S2 and S3.

* TROBRIAND RIDGE (latitude 9° S)

(U) SSR89.017 was the only run that covered this sharply-jagged region. In the vicinity of the sonobuoy the depth was approximately 2000 m. Between ranges of 7 km to 20 km the depth increased from 2100 m to 3750 m. See Figure S7.

* WOODLARK BASIN (latitudes 8-10° S)

(U) Two runs were completed in this region, but the bottom profiles indicate very different sea floors. Run SSR89.016 covered a region of very rough terrain. The average depth was approximately 2550 m. The maximum depth was 2750 m, and the minimum 2100 m. See Figure S6. In comparison, run SSR89.018 covered smooth terrain with some protruding features. Toward the beginning of the run the depth was approximately 4800 m. At a range of 5 km the depth began to increase, reaching 5000 m within a distance of 2 km. Then the bottom surface became very smooth and slightly increased in depth. At 25 km from the buoy a large peak is evident, covering a range of 5 km with a height of approximately 750 m. See Figure S8.

7.2 Description of Results

7.2.1 Time Record of Acoustic Signal

(U) The acoustic signal which has undergone one bottom interaction is selected as described above. Structure is evident in this time record due to a number of effects, including bubble pulse, reflection, refraction, sediment layering and bottom roughness.

(U) The bubble signature can be observed in many of the bottom bounce records, most easily in those which exhibit little bottom scattering. The measured bubble pulse period has been used to check that the depth and magnitude of the explosion was as expected. This can be used, for example, to reject any records that might have resulted from the SUS charge having been inadvertently set to the shallow setting, or resulted from only the primer in the SUS detonating.

7.2.2 Frequency Characteristics of Acoustic Signal

(U) Three figures are presented (in Annex C) for each of the sixteen successful bottom bounce propagation runs completed during the MSD 15/89 cruise. The information includes experiment details, environmental parameters, transmission loss and finally bottom loss. Each propagation run has three pages of data associated with it.

(U) The first figure (Figure Set "S"), of each group of three, is a summary page which contains tabular information and two diagrams. The table contains details of a variety of parameters of relevance to the experiment. These are detailed below. The two diagrams on this summary page show environmental information, one being a cross section of the bathymetry and the other the vertical sound speed profile. The bathymetry figure shows two curves in cases with very rough bathymetry. The curve consisting of a few straight line segments is the bathymetry used for ray theory propagation calculations. The reason for using this is discussed in section 5.2.

(U) The second figure (Figure Set "T") shows the overall transmission loss, via the bottom bounce path, measured at the propagation site. The graph shows the transmission loss (dB) with respect to range from the sonobuoy (km), for full-octave frequency bands.

(U) The final figure (Figure Set "B") shows the overall bottom loss for the run. The graph shows bottom loss (dB) with respect to grazing angle (degrees), for full-octave frequency bands.

(U) Within Figure Sets S, B, and T, figure numbers of results are related to experiment names by the following list:

1)	SSR89.005	9)	SSR89.019
2)	SSR89.006	10)	SSR89.020
3)	SSR89.007	11)	SSR89.021
4)	SSR89.010	12)	SSR89.022
5)	SSR89.013	13)	SSR89.025
6)	SSR89.016	14)	SSR89.026
7)	SSR89.017	15)	SSR89.027
8)	SSR89.018	16)	SSR89.028

(U) The terms used in the tabular information on Figure Set "S" are elaborated here:

Shot-Run Title	Code for the experiment where: SSR indicates a Ship-Sonobuoy-Run, the next two digits are the year the measurement occurred, the final digits represent the number of the experiment.
Position of receiver	Location of the sonobuoy used in the experiment.
Time/Date	Local time, time zone and date are given first, with the Julian day and UTC time given in parentheses. The time zones are: K 10 hours ahead of UTC, L 11 hours ahead of UTC.
Heading	True direction of the propagation run in degrees.
Sound speed profile	Type of sensor used to measure the temperature profile (which was used to determine the sound speed profile).
XBT	Expendable bathythermograph.
SSP	Sound speed profile.
Position of SSP	Location where the temperature profile was measured.
Source depth	Depth at which the explosive was set to trigger.
Receiver depth	Depth of the hydrophone associated with the sonobuoy.
Sea State	Sea state described using the Beaufort Wind Scale.
Swell	Swell height, period and direction.

(U) It is noted that measurements of high bottom loss values are difficult as it requires a low level of background noise against which to accurately measure the bottom reflected signal. If the signal to noise is insufficient, then no value is recorded. Thus results will be deficient in the proportion of high bottom loss values.

7.3 Discussion of Results

(U) The results presented in Figure Set "B" may be taken directly as providing data on values of bottom reflection coefficient for various frequencies and

grazing angles, at a variety of locations in the Australian area of direct military interest.

(U) However, the results may also be examined further, in order to derive a better understanding of the mechanisms that are occurring in the bottom interaction process. The bottom loss measured is caused by a combination of bottom topography, the sediment types and the sediment layering. These aspects are briefly discussed in this section.

7.3.1 Relative Importance of Reflection and Refraction

(U) Examination of the time record (of the single bottom bounce arrival) is a useful technique in determining the nature of the processes dominating the bottom interaction. It has been found that a clean time record contains three major high frequency events in which the signal appears very spiky, and three major low frequency events, in which the signal varies much more slowly [Lawrence, Valentine and Prenc, 1993a].

(U) The time separations between the high frequency (or the low frequency) components reveal that they correspond to the four members of the bottom bounce quartet. Because the SB and BS paths arrive at nearly the same time (due to nearly equal source and receiver depths), they appear as overlapping arrivals. The B and the SBS paths are the first and last members of the sets of arrivals.

(U) By also examining the time records of the adjacent shots, it becomes evident that the high frequency arrivals are direct reflections from the water to sediment interface (the sea floor), while the low frequency arrivals are the result of refraction of the acoustic energy within the sea bed. At steeper angles of incidence, the reflected energy dominates, while at shallower angles the refracted energy dominates. The refracted arrivals have predominantly low frequency energy because the high frequencies have been absorbed on the long path though the sediment pile. The reflected arrivals, however, contain high as well as low frequencies. This results in a signal which exhibits the observed high frequency characteristics. This concept has been discussed by a number of authors, e.g. Christensen, Frank and Geddes [1975].

(U) When the sediment is very uniform there is a clear distinction between the high and low frequency arrivals. Interfaces between sediment layers cause reflections which complicate the arrival, as does rough bathymetry. These effects were observed for many of the propagation runs completed on MSD 15/89. In some runs, reflection due to rough bathymetry or nearby mounds created very complicated arrivals that could not be resolved.

(U) The bubble pulse structure of the acoustic-pressure time signal can also be used to determine details about the sediment structure. A clear, easily discerned bubble pulse structure indicates a very uniform sea bed. Sediment layers or

rough bathymetry would create multiple overlapping arrivals. The runs completed on MSD 15/89 indicate either rough bathymetry or layered bottom sediments due to their complexity. Almost all of the runs had significant complexity in the bubble pulse structure of the bottom reflected signals.

(U) It is possible to analyse the results collected in these experiments in order to obtain depth profiles of sediment properties such as sound speed. Techniques for such analysis have been explored, for example by Chapman et al [1986], Spofford [1980], and McCammon [1988], but are beyond the scope of this report.

7.3.2 *Effects of Bathymetric Blocking*

(U) In a few propagation runs, unusually high transmission loss was observed for the largest ranges. After examination of the bottom profiles, bathymetric blocking is believed to be the cause. The propagation runs showing this behaviour are SSR89.016 (see Figures S6 and T6) and SSR89.017 (see Figures S7 and T7). Propagation run SSR89.018 shows high loss at intermediate ranges (see Figures S8 and T8) and bathymetric blocking is believed to be the cause in this case also.

(U) While bathymetric blocking by a ridge or seamount is a form of bottom loss, it has deficiencies in characterising the bottom loss of regions of sea floor. This is because bathymetric blocking depends on a very specific placement of both source and receiver. If there were very large numbers of acoustic measurements available, the variability of measured bottom loss would contain the effect of bathymetric blocking that occurred in that region. However, with the small number of measurements that are available, it is more representative to characterise the bottom loss in a region by excluding such effects. By way of example, if there is only one propagation run to characterise an area, and this run shows a large peak in bottom loss at 15° grazing angle due to bathymetric blocking, it is not then sensible to assume that this is typical of the region.

(U) A ray tracing program has been used to prepare diagrams showing ray paths from rays that leave the acoustic source at equally spaced intervals of angle. In these diagrams, each ray is traced until it leaves the region of interest, or until it strikes the sea floor for a second time. These diagrams (Figures 9(a) to (c)) show bathymetric blocking, as discussed in the following paragraphs. In order to demonstrate this effect most clearly, these diagrams have been prepared using a bathymetry of complexity somewhere between the detailed measured bathymetry and the smoothed bathymetry used in the analysis.

(U) In a ray trace for propagation run SSR89.016, shown in Figure 9(a), using a modified version of the measured bathymetry, there is an obvious case of bathymetric blocking. In the results (Figure T6), high loss is observed for ranges greater than 16 km (less than 16° grazing angle). Using a ray trace diagram,

Figure 9(a), it can be seen that the seamount of height 450 m, at a range of 11 km, would be of sufficient height to cause bathymetric blocking. The energy which impinges upon this mount is directed to shorter ranges than would be expected if the sea floor was flat. The result is a dramatic decrease in energy at the longer ranges and an increase in energy at ranges around 16 km. For grazing angles less than 16° there is no single bottom bounce path between the source and receiver, so the double bottom bounce signal becomes dominant. Although measurements were made out to 25 km, the last three data points have not been included in the bottom loss results for this reason.

(U) Propagation run SSR89.017 also shows effects of bathymetric blocking. In the transmission loss results, Figure T7, there is a minimum at a range of around 10 km. Ranges greater than 16 km have significantly less single bottom bounce energy reaching them. Using a ray trace diagram, Figure 9(b), it can be seen how bathymetry is the cause. Due to a mount on the ridge, energy has been directed to shorter ranges. The steep slope falling away from the source prevents significant reflection from the sea floor, resulting in only a small percentage of the single bottom bounce energy reaching the depth of the SUS charge and sonobuoy, at those longer ranges. Transmission loss measurements were taken out to 24 km but bottom loss results are not available for ranges greater than 16 km. This bathymetric effect will differ at other positions along the ridge because the bathymetric feature, at 7 km, is a mount, as shown by the SeaBeam record [Jenkins and Pritchard, 1989], rather than a linear feature.

(U) The dips and peaks, measured in the transmission loss for propagation run SSR89.018 (Figure T8), are also believed to be caused by the bathymetry of the region. The corresponding ray trace diagram, Figure 9(c), using the measured bottom topography, demonstrates that the ridge feature at 6 km [Jenkins and Pritchard, 1989] was of sufficient height to direct energy away from the ranges around 10 km and out to the longer ranges. In the data this is matched by greater transmission loss at 9 km than at 17 km.

(U) Figure 9(c) also indicates that the ridge feature at a range of 28 km would cause focussing of the energy. Rather than the energy being refracted away from the bottom or reflected out to longer ranges it would be focussed to shorter ranges. In the measurements, there is only a small decrease in the transmission loss at this range.

(U) Accurate prediction of the bathymetric scattering is difficult because a very detailed picture of the sea floor would be required to ensure the estimated bottom slope accurately represented the actual bottom slope. Small discrepancies between the two can lead to large errors. Predictions of the scattering for propagation runs SSR89.016 and SSR89.017 cannot be performed accurately for the same reason.

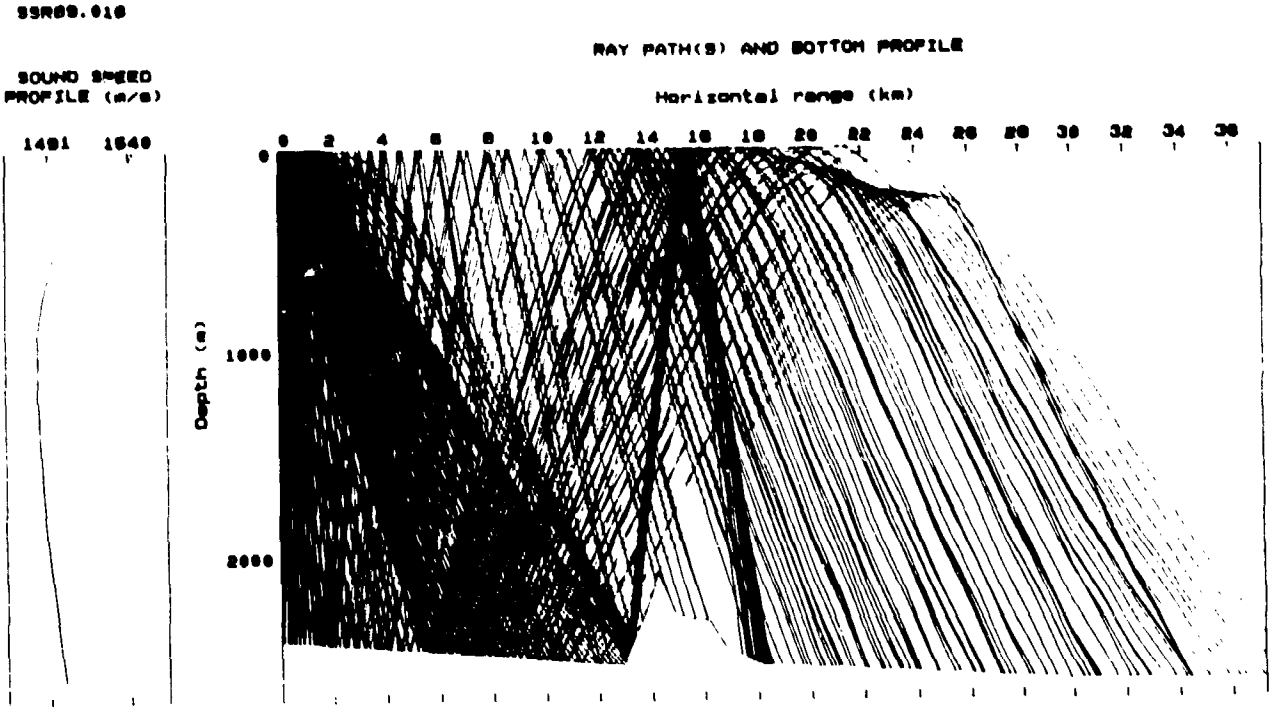

Figure 9 (a): (U) Ray paths of the bottom arrivals for the propagation run SSR89.016. Also shown is the sound speed profile and sea-floor topography.

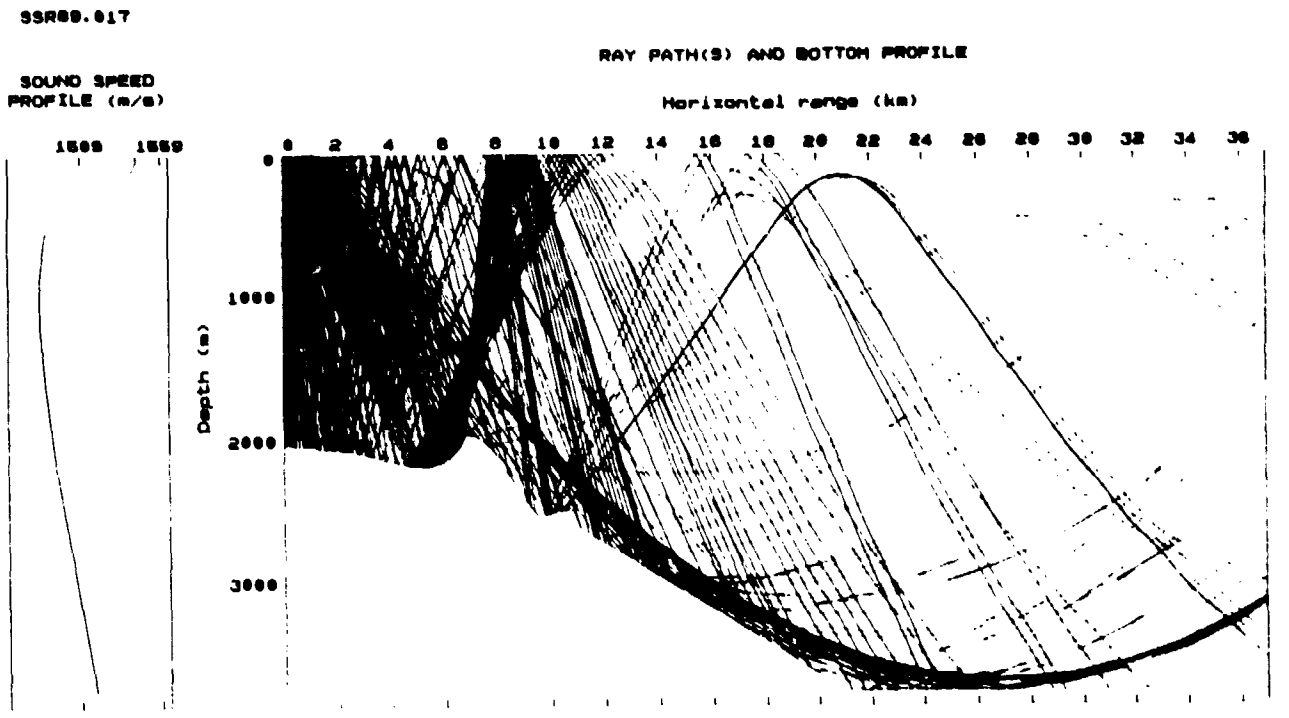

Figure 9 (b): (U) Ray paths of the bottom arrivals for the propagation run SSR89.017. Also shown is the sound speed profile and sea-floor topography.

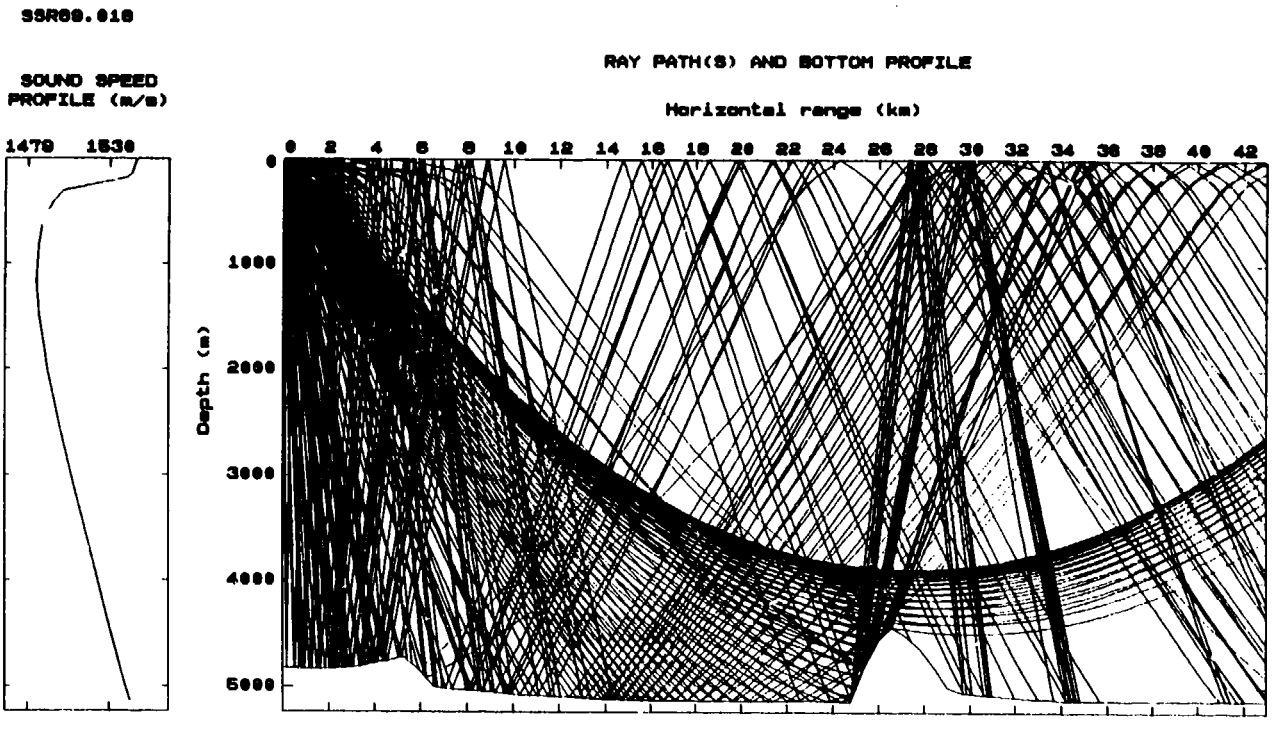

Figure 9 (c): (U) Ray paths of the bottom arrivals for the propagation run SSR89.018. Also shown is the sound speed profile and sea-floor topography.

(U) Ray traces, such as Figures 9(a), (b) and (c), can give misleading impressions of angle due to the large exaggeration of the depth scale. The depth scale covers no more than 6 km while the range scale covers, in one case, almost 43 km. This results in figures where the ray angles, at the sea floor, appear incorrect.

7.3.3 *Effects of a Constant Sea-Floor Slope*

(U) For a given horizontal range, the actual water path propagation loss of the reflection from a sloping sea floor will be somewhat different from the water path propagation loss based on a reflection from a horizontal sea floor. This an effect due to the different path lengths involved in the two cases. For the propagation run in which this effect will be largest, SSR89.021 with a slope of 5°, this effect will only cause a change in the water path propagation loss of 0.04 dB. This effect is, therefore, negligible.

7.4 Qualification of the Results

(U) The physical process whereby the acoustic energy incident on the sea bed is returned to the water column is quite complex. This complexity arises because the acoustic energy can enter the sea bed material and subsequently be returned to the water column. This can happen via reflection from layers within sea-bed material and/or from refraction of the energy. Other processes involved include generation of interface waves and shear waves. All of these processes can make the 'reflection' a complicated process. The 'bottom loss' calculated here does not reveal any more than the overall amplitude of the reflection. Phase and coherence of the reflected signal is not measured.

(U) Because the acoustic waves are generated by a point source, they are spherical, not plane, waves. The ray theory modelling provides for the refractive effects in the water column. However there is the possibility of further refraction within the sea-bed material leading to focussing of a spherical wave. The ray theory modelling does not provide for this sea-bed refraction, which results in the bottom loss reported here not explicitly revealing the presence of such effects. However, it may be argued that the use of a point source is more realistic for comparison with effects on sonar systems.

(U) In some cases, at low frequencies, focussing within the sea bed can lead to apparent gain at the bottom interaction. This phenomenon manifests itself as a negative value of bottom loss, which should not cause alarm as it is simply allowing for the focussing process. Bottom loss values will be higher at other grazing angles (for which the energy is defocussed), thus satisfying the requirement of conservation of energy.

(U) A plane wave will not be focussed by the sea bed at any range. The focussing of a spherical wave will lead to increased acoustic energy at some ranges and reduced energy at other ranges. Thus the difference between the measured spherical wave reflection and a plane wave reflection may be positive or negative, depending on the range.

(U) A significant use of bottom loss values is in propagation models. It is noteworthy that the bottom loss values reported here are very appropriate for the first bottom bounce interaction. However, they are not as appropriate for subsequent bottom bounces. For the first bottom interaction, the acoustic energy arrives from a point source near the sea surface. For subsequent bottom interactions, the acoustic energy arrives from a finite area of the sea surface (after reflection). As discussed above, focussing effects depend on 'spherical' spreading from a source. Since the geometry of the effective source for each bottom interaction is different from the first to subsequent bottom interactions, the bottom loss will also be different.

(U) This effect will be strongest when there is substantial refraction. This occurs at low frequencies and small grazing angles, and is manifested by such effects as negative bottom losses. In these circumstances, it can be expected that the bottom loss will be greater on subsequent bottom interactions. At the higher frequencies and/or higher grazing angles, the bottom loss should be essentially the same at first and subsequent bottom bounces.

(U) The accuracy of the bottom loss values is at best of order 1 or 2 dB. This is because the bottom loss (of say 10 dB) is determined by subtracting the calculated water path transmission loss (of say 70 dB) from the measured transmission loss (of say 80 dB). Inaccuracies in either TL or WPL or in the source energy spectrum can be expected to lead to errors of the above magnitude.

(U) There are fluctuations in ocean sound speed profiles with time and space as well as fluctuations in the sea-bed properties (including depth), with space. These fluctuations mean that performing the bottom loss measurements twice in substantially the same location will give some fluctuation in bottom loss results. The magnitude of this bottom loss variability will depend on the size of the fluctuations in ocean and sea-bed properties.

8 Conclusions

(U) Measurements are reported for accurate measurements of transmission loss via the bottom bounce path for sites to the north-east of Australia. Bottom loss levels have been calculated from these measured values. The existing data set on bottom loss in this region is considerably extended, both in quantity of sites and frequency range of measurement. There are considerably more sites in this report than in all of the previous bottom loss investigations of this region. The current measurements also have an accurate set of relevant environmental data at the sites, which is useful for further analysis of the results.

(C) The significant variability of bottom loss results, even for the same geoacoustic province, is once again demonstrated. Given that variability, exact correspondence between the present results and previous results can not be expected. Comparison with the bottom loss data of Brown et al. [1981] shows good agreement for the Tasman Sea site. However, the bottom loss values reported here for the Coral Sea are 4 to 5 dB higher than those of Brown et al., at all grazing angles over the frequency range reported (31.5 Hz to 2 kHz). Comparison of the present data with the bottom loss data of Hall and Nicholson [1969] shows good agreement for the one Coral Sea site reported, over the frequency range reported (250 Hz to 4 kHz).

9 Acknowledgments

(U) The authors wish to thank the officers and crew of HMAS Cook who provided extensive help in the gathering of the data on which the current report rests.

(U) Thanks are also given to Neil Tavener, for work done on the sonobuoys and Keith Levet for assistance with the analysis. Marshall Hall is thanked for helpful suggestions on the manuscript.

10 References

Beazley, K.C. (1987). *The defence of Australia 1987*. Canberra, ACT: Australian Government Publishing Service.

Brown, D.H. (Ed.) (1981). *Taniwha sea test: Final report* (Technical Report WSRL-0222-TR) (Secret). Salisbury, SA: Weapons Systems Research Laboratory.

Chapman, N.R. (1985). Measurements of the waveform parameters of shallow explosive charges, *Journal of the Acoustical Society of America*, **78**, pp. 672-681.

Chapman, N.R., Levy, S., Stinson, K., Jones, I.F., Prager, B.T. and Oldenburg, D.W. (1986). Inversion of sound-speed and density profiles in deep ocean sediments, *Journal of the Acoustical Society of America*, **79**, pp. 1441-1456.

Chapman, N.R. (1988). Source levels of shallow explosive charges, *Journal of the Acoustical Society of America*, **84**, pp. 697-702.

Christensen, R.E., Frank, J.A. and Geddes, W.H. (1975). Low-frequency propagation via shallow refracted paths through deep ocean unconsolidated sediments, *Journal of the Acoustical Society of America*, **57**, pp. 1421-1426.

Cole, R.H. (1948). *Underwater Explosions*. Princeton, NJ: Princeton University Press.

Farr, H.K. (1980). Multibeam bathymetric sonar: SeaBeam and Hydrochart, *Marine Geodesy*, **4**, pp. 77-93.

Francois, R.E. and Garrison, G.R. (1982). Sound absorption based on ocean measurements. Part II: Boric acid contribution and equation for total absorption, *Journal of the Acoustical Society of America*, **72**, pp. 1879-1890.

Gaspin, J.B. and Shuler, V.K. (1971). *Source levels of shallow underwater explosions* (NOLTR-71-160, 50p). White Oak, MD: Naval Ordnance Laboratory.

Gorshkov, S.G. (Ed.) (1974). *World Ocean Atlas, Volume 1, Pacific Ocean,* with introductory text and gazetteer translated into English. Oxford, Eng.: Pergamon Press.

Hall, M. and Nicholson, P.J. (1969). *A deep water sound propagation experiment in the Coral Sea* (Technical Note RANRL TN 2/69) (Confidential). Sydney, NSW: Royal Australian Navy Research Laboratory.

Jenkins, C.J. and Pritchard, T.R. (1989). *Geological and geophysical support of acoustic bottom-interaction experiments: HMAS Cook cruise MSD 15/89 Tasman, Coral and Solomon Seas* (Report 35, 176p). Sydney, NSW: Ocean Sciences Institute, University of Sydney.

Lawrence, M.W., Valentine Flint, S. and Prenc, S. (1993a). *Bottom bounce propagation on SEAMAP Pacific routes: measurement and analysis* (Technical Report MRL-TR-92-12). Maribyrnong, Vic.: Materials Research Laboratory.

Lawrence, M.W., Valentine Flint, S. and Prenc, S. (1993b). *Compendium of bottom bounce measurements on SEAMAP Pacific routes* (General Document MRL-GD-0039). Maribyrnong, Vic.: Materials Research Laboratory.

Levitus, S. (1982). *Climatological atlas of the world ocean,* NOAA Professional Paper 13, National Oceanic and Atmospheric Administration, Rockville, MD, 173p +17 microfiche cards.

Mackenzie, K.V. (1981). Nine-term equation for sound speed in the oceans, *Journal of the Acoustical Society of America*, **70**, pp. 807-812.

McCammon, D.F. (1988). Fundamental relationships between geoacoustic parameters and predicted bottom loss using a thin layer model, *Journal of Geophysical Research*, **93**, pp. 2363-2369.

Schneider, P.M. (1987). *Report on SP-1 maps on the sediments, morphology and acoustic properties of the south-west Pacific sea floor* (Report 23, 42p and 7 maps). Sydney, NSW: Ocean Sciences Institute, University of Sydney.

Spofford, C.W. (1980). Inference of geo-acoustic parameters from bottom-loss data, in *Bottom-Interacting Ocean Acoustics*, Ed. by W.A. Kuperman and F.B. Jensen, pp. 159-171. New York, NY: Plenum Press.

Urick, R.J. (1983). *Principles of Underwater Sound.* Third Ed. New York, NY: McGraw-Hill.

Valentine Flint, S. and Lawrence, M.W. (1992). *Bottom bounce propagation on SEAMAP Pacific routes - data acquisition and recording system* (Technical Note MRL-TN-587). Maribyrnong, Vic.: Materials Research Laboratory.

Annex A Details of the Experiment

A.1 Sonobuoy Deployment

(U) The sonobuoy was prepared for launch by noting the sonobuoy number and channel number. Also, it was ensured that the depth was set to 1000 ft and the scuttle time to 3 hours. The correct channel was then selected on the sonobuoy receiver. With the ship on the required course, the ship speed was reduced to approximately 4 knots for the sonobuoy deployment.

(U) The sonobuoy was launched by dropping the canister vertically from the quarterdeck. The top electronics module detached from the canister and floated to the surface. After a few seconds the antenna inflated and the RF signal was detected via the receiver system. Immediately after deployment the ship resumed a constant cruising speed, usually 8 to 12 knots. As the metal canister sank, the sound of the wire unwrapping was audible (this was sometimes faint depending on the sonobuoy sensitivity). The canister took approximately 140 seconds to sink to 1000 ft. At this time the canister separated from the lower part of the sonobuoy system and the clunks and bumps of the components (hydrophone/preamplifier/damping plate) exiting the canister were audible.

(U) After the sonobuoy was deployed the program SONOADC was placed in data acquisition mode.

A.2 Procedure for Analog to Digital Conversion

(U) For the SEAMAP program SBC hardware, described in Valentine .nd Lawrence [1992] was used to digitise the acoustic signal. For MSD 15/89 and subsequent cruises this was not the case.

A.2.1 Analog to Digital Conversion System

(U) The SBC hardware has been replaced. The analogue-to-digital converter (ADC) system is now based around a Data Translation DT-2821F 12 bit card installed in an AT compatible computer. Analog inputs are via a DT-707 interface connected to the DT-2821 by a 50 way cable. This interface provides 8 analog input channels, external trigger and external clock. During the conversion data are written to the lower 12 bits of the data word.

(U) ADC trigger delay is measured from the time of the Instant Of Detonation (IOD) to the commencement of the shot analogue-to-digital conversion. Trigger delay is incremented in units corresponding to integer multiples of buffer periods. As the current ADC buffer length is 16384 samples, the trigger delay is incremented in (16384/fsample) second multiples. For a sampling frequency of fsample = 20000 Hz, the trigger delay increments by 0.8192 seconds and the minimum non zero trigger delay is 0.8192 seconds. When longer delays are set, the actual value used is never greater than the set value. As an example, for an entry of 2.50 seconds a delay of 2.457 seconds is used (3 * buffer time).

(U) During the shot acquisition process digitised data and ancillary files are written to the hard disk, to a subdirectory corresponding to the Sono-SUS run number. e.g. S89021. This subdirectory must exist prior to shot digitisation.

A.2.2 Running the Data Acquisition Program

(U) The detailed procedure for running the data acquisition program is set out below:

- Run the shot digitisation program SONOADC, from the \SONO directory (assuming that SONOADC is resident in this directory).
- From the main menu presented by SONOADC, select F6 'Acquire Data'. This will present the header file entry menu. Enter data as appropriate. Default entries can be made for most inputs by keying <CR>. The exception is the shot number entry which must be entered explicitly (in order to avoid unintentionally overwriting previously digitised data).
- Maintain a listening watch on communications between the bridge and quarterdeck via the Oceanographic Intercom.
- Note the time of SUS drop.
- Set the VCR to record.
- Key <HOME> to exit the header entry routine.
- Key <F1> approximately 30 seconds after SUS launch to enter ADC on trigger.
  Note SUS detonate time (approximately 50 seconds after drop) and VCR counter.
- On reception of the IOD signal (from Z3B hydrophone in water tank), the ADC trigger count-down commences. Progress is displayed on screen as number of buffers and elapsed time.
- On expiration of delay, ADC of acoustic signal commences. Progress is displayed on screen as number of samples and seconds. Digitised data are written to a temporary *.TIM file which may reside on a RAM disk.
- Wait for ADC to complete, then stop tape.
- On completion of ADC, the data are converted from the internal ADC format (which was temporarily stored in *.TIM file), and scaled up by a factor of 16 to shift it from the bottom 12 bits of the data word to the upper 16 bits. The converted and scaled data are written to the *.ACS file in the appropriate subdirectory. The *.TIM file is then deleted.

- Key <F7> to calculate (average) intensity data, write the *.AVE data file and display intensity data. After intensity data are output, the system returns to the main menu.
- Key <F6> to enter the header entry for the next shot, or any of the other allocated function keys.
- If the SUS charge misfires, the ADC 'wait for' trigger will time out after approximately 60 seconds and analog to digital conversion will commence. Processing will proceed to scale the data as for a successful ADC on trigger. The program will return to the main menu screen. The trigger delay recorded in the header file will reflect the actual time elapsed before ADC commenced and will be inappropriate for the next shot.

A.3 First SUS

(U) Prior to the deployment of each SUS, the HEADER was updated by two entries: the SUS number within the SSR (starting with number 1), and the requested delay between reception of the hull transducer trigger and commencement of digitisation (selectable range from 0.0 to 60.0 seconds in multiples of buffer periods).

(U) At the first SUS drop distance, usually one mile after sonobuoy deployment, the procedure was: Order the first SUS drop. Set the VCR to record mode and sensitise the ADC for the direct path trigger via the hull transducer. Monitor the receiver output via loudspeaker to determine when the acoustic signal from the SUS had ceased. At this point the VCR recording was stopped.

(U) Meanwhile the ADC would have registered the trigger pulse and the program automatically acquired an 8 second digitised record. When the digital record was completed, the program, SONOADC, converted the data to a form suitable for later extraction and then wrote the data file.

(U) The acoustic intensity of each conversion within the record was calculated, then blocks of 80 consecutive samples were averaged, with the normalised results stored on disk and displayed in graphic form. Normalisation set the maximum intensity to a value of 10,000. This presentation allows the operator to judge whether the acoustic record had been completely captured, i.e. the trigger delay correctly set, or whether the record must be re-digitised from tape at a later stage. When completed the program returned to the main prompt screen to prepare for the next SUS drop. A typical display of relative acoustic intensity over an 8 second period is shown in Figure 10.

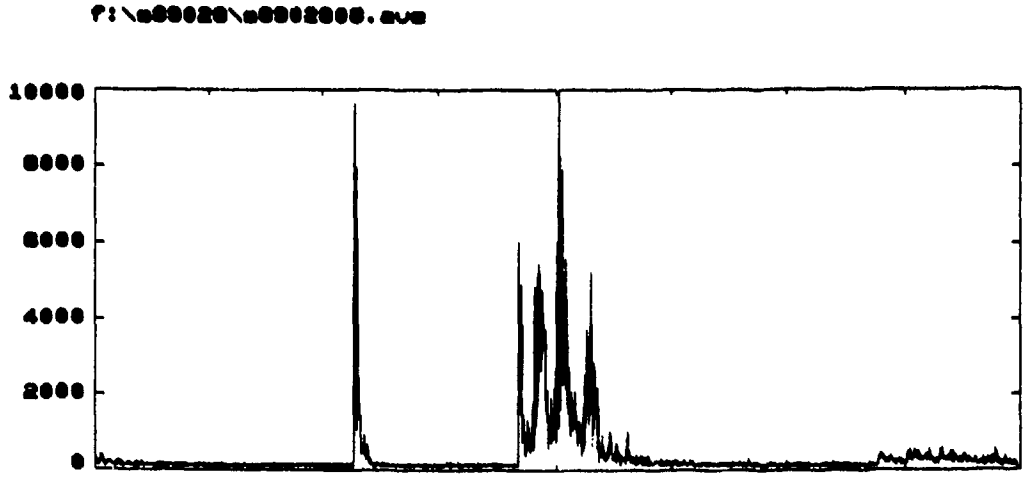

Figure 10: (U) Typical acoustic intensity display from data acquisition program SONOADC. Time, along the horizontal axis, extends over 10 seconds

A.4 Subsequent SUS

(U) The procedure for subsequent SUS drops was the same as for the first SUS. Whilst waiting for the next drop the operator monitored the receiver output to judge whether the radio link performance was adequate. Drops continued until the radio link ceased to be viable, the range reached depending primarily on weather conditions.

(U) It was standard practice throughout these experiments for the Bridge Watchkeeping Officer (OOW) to control the SUS drops. Rather than attempting to drop at exact positions, the OOW monitored the time from the sonobuoy deployment and ordered the SUS drop at specific time intervals corresponding approximately to one mile travelled. At the same time he noted the position from the most accurate available navigation system. Via the SEAMAP program this procedure was found to be more workable than the alternative of attempting exact position drops.

A.5 Filters

(U) Filter functions for the data recording and digitisation systems were provided by Rockland model 852 dual high-pass/low-pass units. Each of these consisted of two independent 4th order filters. The cutoff frequency is at -3 dB signal reduction.

(U) Unless otherwise stated in particular run records, the filters were used with 0 dB gain and flat amplitude characteristic. Acoustic data were recorded via a low-pass filter with a 12 kHz cutoff. Prior to digitisation, whether direct from the receiver or from a tape replay, the data were low-pass filtered to 8 kHz, to provide alias protection.

(U) High-pass filtering to 5 Hz was applied immediately before the pre-digitisation low-pass filter. This filter served to remove low frequency effects, such as that due to hydrophone movement, from the data.

A.6 Hull Transducer

(U) A hydrophone (model Z3B) was installed in a fresh water tank in the hull of the ship and was connected to the recording system via a 20 dB broadband preamplifier. This hydrophone was used to obtain the direct path signal from the SUS explosion in order to provide a trigger point for the analysis of the sonobuoy arrival. This trigger point was vital in accurate determination of the range between SUS explosion and sonobuoy receiver.

(U) No attempt was made to retain any information content from this acoustic signal other than accurate timing. The signal was processed by a 300 Hz to 2 kHz bandpass filter before either direct real time digitisation or recording on tape, .

Annex B Interference of Bottom Bounce Quartet

B.1 (U) Estimates of size of effect of coherent addition

(U) Urick [1983, pp. 131-133] develops a formula for (and gives a graph of) "Lloyd mirror" interference for an isovelocity ocean, using a single-frequency acoustic source. By adapting Urick's approach, we can obtain a guide to the magnitude of the effects in the case of a bottom bounce signal.

(U) Urick's analysis deals with the interference between a signal path directly from source to receiver and one which undergoes a single reflection from the sea surface, on the way from source to receiver. For consideration of the magnitude of this effect, Urick defines a reference distance (acoustic path length) l_0, by

$$l_0 = \frac{4 d_1 d_2}{\lambda}$$

where d_1 is the source depth, d_2 is the receiver depth and λ is the wavelength. Urick defines a "transmission anomaly" as the difference between the interference signal and the signal that would have occurred in the absence of surface reflection.

(U) The significance of the reference distance, l_0, is that it is the slant range (between source and receiver) which entails a half-wavelength, $\lambda/2$, path difference between the two paths. For Urick's case (direct path and surface reflected path) this corresponds to the final peak (up to 6 dB magnitude) of the transmission anomaly. For ranges beyond this, the transmission anomaly decreases asymptotically as the fourth power of the range. There is a minimum in interference signal at all distances derived by dividing the reference distance by even integers.

(U) In the case of a single bottom bounce signal, the interference between any two paths of the quartet may be considered. All of these paths involve a single bottom bounce, but have differing numbers of surface reflections. The behaviour of the transmission anomaly described above applies to all pairs of paths for which the sum of the number of surface reflections is odd. Thus the above behaviour applies to the pair of B (bottom only) and SB (surface reflection, then bottom bounce). It also applies to the pair of B and BS.

(U) However in the case of the pair B and SBS, as well as the pair SB and BS, the sum of the number of surface reflections is even. The behaviour of the

transmission anomaly is different in this case. The reference distance is still the slant range which entails a half-wavelength path difference between the two paths. However, at the reference distance, there is a minimum in the interference signal. At longer ranges, the transmission anomaly asymptotically approaches a maximum (of 6 dB in the ideal case). There is a minimum in interference signal at all distances derived by dividing the reference distance by odd integers.

(U) Use of the technique of image sources allows determination of the following formula for the reference distance, for any pair of paths in the bottom bounce quartet:

$$l_0 = \frac{8hd}{\lambda}$$

where h is the water depth and d is a depth as follows. For the case of B/SB, $d = d_1$, for B/BS, $d = d_2$, for B/SBS, $d = (d_2+d_1)$, and for SB/BS, $d = (d_2-d_1)$. Table B1 sets out these values. The slant range is the average range along the acoustic path, including the bottom bounce. The assumption that $2h >> d$ is used in deriving this result. It is trivial to avoid this assumption, but the extra complexity of the formulae is not useful for current purposes.

(U) Taking this result further, gives a formula for the horizontal range, r_0, to the point at which the phase difference between the two paths is a half wavelength:

$$r_0 = 2h\left\{\left(\frac{4d}{\lambda}\right)^2 - 1\right\}^{\frac{1}{2}}$$

By analogy with the reference distance, we call this a reference range.

(U) In order to determine what influence this interference has on the results given in this report, we consider the cases in which there is most potential for affecting the results. Since the reference range increases approximately linearly with frequency, it is the lowest frequencies, and with the smallest d values, that need investigating.

(U) Choosing the lowest frequency, 16 Hz, used in the analysis and taking typical values for various parameters ($d_1 = 244$ m, $d_2 = 305$ m, $h = 5000$ m, $c = 1520$ m/sec), and using the formula $c = \lambda f$, allows determination of the reference range, as set out in Table B1.

Table B1 (U): For various arrival pair combinations, the form of d, and the reference ranges at a frequency of 16 Hz.

Arrival Pair	Depth d	Reference Range (km) for frequency 16 Hz
B/SB	d_1	102
B/BS	d_2	128
B/SBS	(d_2+d_1)	231
BS/SB	(d_2-d_1)	24

(U) In the data analysis, the signal is averaged over a full-octave frequency band. The oscillations in the transmission anomaly have a period of at most a full octave. Thus, full-octave band averaging goes a long way to eliminating surface interference as a problem, provided the maximum range of the data analysed is not beyond the reference range. Even for ranges out to twice the reference range full-octave band averaging will achieve a result which is not greatly different from that in the absence of interference.

(U) The bottom bounce signal observed is, of course, generated by all four members of the quartet interfering together. Different arrival pairs are on different parts of their interference curves at any one frequency and range. Hence, on addition of the effects of the pairs, there will be some cancellation of any residual interference effects.

(U) From Table B1, in the worst situation, the most closely spaced pair of arrivals (BS/SB) have a reference range of 24 km at 16 Hz. The experimental results often extend to a range of 40 km. While this is beyond the reference range for this particular case, it is not beyond double the reference range.

(U) The above analysis was for a water depth of 5 km. For shallower water depths, the reference range will be proportionally reduced. At these smaller water depths, the propagation runs were truncated at shorter ranges than for the deep water runs.

(U) Examination of the configurations reported here shows that surface interference should have not been a problem for any of the reported results. That is, the incoherent summation used in the water path transmission loss calculation is adequate. For a frequency of 16 Hz, however, the limit of applicability of incoherent summation is being approached. Third-octave band averaging would have provided too little averaging for the lowest frequencies.

B.2 Difficulties in modelling the coherent summation process

(U) Although coherent summation was not used in the analysis, the difficulties associated with implementing it were addressed. In order to accurately model the coherent summation process, the relative phases and amplitudes must be known accurately. Also, there are complexities arising from the pulse nature of the signals. These issues are discussed in this section.

B.2.1 Estimation of relative phases

(U) In order to successfully combine the various member paths coherently, the relative phases of each member must be known to within about 20 degrees. The relative phases depend on both accurate estimation of relative path length and of relative discrete phase changes.

(U) Keeping track of these phase changes requires very accurate environmental information. Sound speed profile in the water and in the sea bed need to be known accurately at all ranges.

(U) There can be considerable separation of the points on the bottom that are struck by the different members of the quartet. The range separation between the B and the SB bottom strike points is approximately given by:

$$\delta r = \frac{rd}{2h}$$

At a range of 40 km, for water depth 5 km, this range separation is 1.0 km.

(U) Errors in path length difference cause errors in the relative phases. In order to accurately calculate path length, parameters that need to be known accurately are sea-floor depth, sediment structure and bottom slope at each bottom hit, as well as depths of source and receiver. The relative path lengths have to be calculated to an accuracy of a few percent of a wavelength. At the high frequencies this is not possible, but band averaging makes it unnecessary. At the lower frequencies the problem is more tractable, but still imprecise. The problem is made worse for the case in which the bottom has considerable horizontal variation (in depth or in sediment layering) or is rough.

(U) Discrete phase changes occur due to a number of processes:
(a) Surface reflection to sub-surface refraction. As range increases, surface reflections (π rad phase shift) will become sub-surface refractions. The transition range must be known very accurately, otherwise a major calculational error will occur.
(b) Bottom interface reflection. A phase change will frequently occur on reflection from the bottom interface. The magnitude of the phase change

depends on the acoustic properties on each side of the interface. If the sea-bed properties change over the separation of the bottom strikes of the various members of the quartet, the relative phases of the quartet members will also change.
(c) Caustic phase changes. A phase change of $\pi/2$ rad occurs at a caustic. There may be caustics on the sub-surface refraction paths.

B.2.2 Amplitude effects

(U) Roughness of the sea surface will reduce the surface reflection and cause scattering. The reduced amplitude is important in any sum of the constituent signals. The scattered energy causes complications through scattered paths contributing to the signal summation process. The effect of sea surface roughness will be least evident at the lowest frequencies.

B.2.3 Pulse nature of signals

(U) The Fourier transform of signals that do not overlap is different to that of overlapping signals (even for the same relative phases). Energy will appear at the frequency corresponding to the time separation of the pulses (after allowing for phase changes due to reflections and caustics). To effectively deal with this problem, a model is required which will generate the total time series (including phase) over the measurement interval. This has not been attempted here.

Annex C Data from Each Propagation Run

Shot-Run Title :	SSR89.005
Position of receiver :	32°20S 155°01E
Physiographic Province :	Tasman Abyssal Plain
Ship :	HMAS Cook
Cruise :	MSD 15/89 winter (MSD 15/89)
Time/Date of start :	0842K 09 MAY 89 (128 2242Z)
Heading :	026
Sound-speed profile :	XBT
Position of ssp :	32°20S 155°08E
Time/Date of ssp :	0850K 09 MAY 89 (128 2250Z)
Source depth :	244 m
Receiver depth :	305 m
Sea State :	3
Swell :	0.5 m, 2 sec, 120° to ship

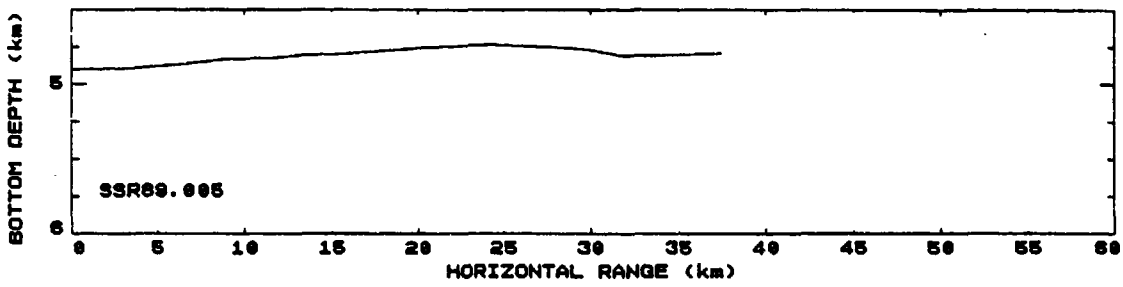

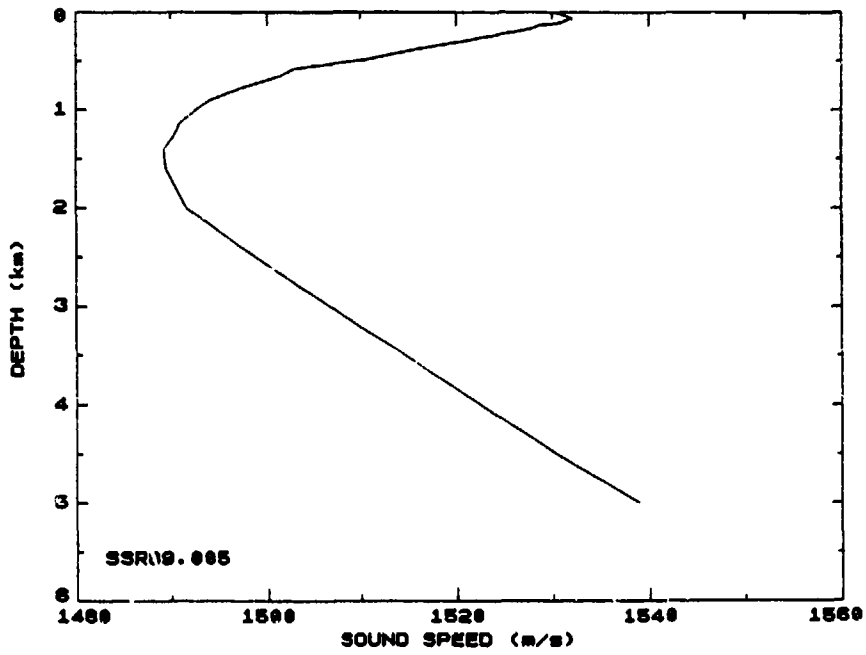

Figure S.1: (U) Summary page for propagation run SSR89.005, containing ancillary information, the bottom profile, and the sound speed profile. (U)

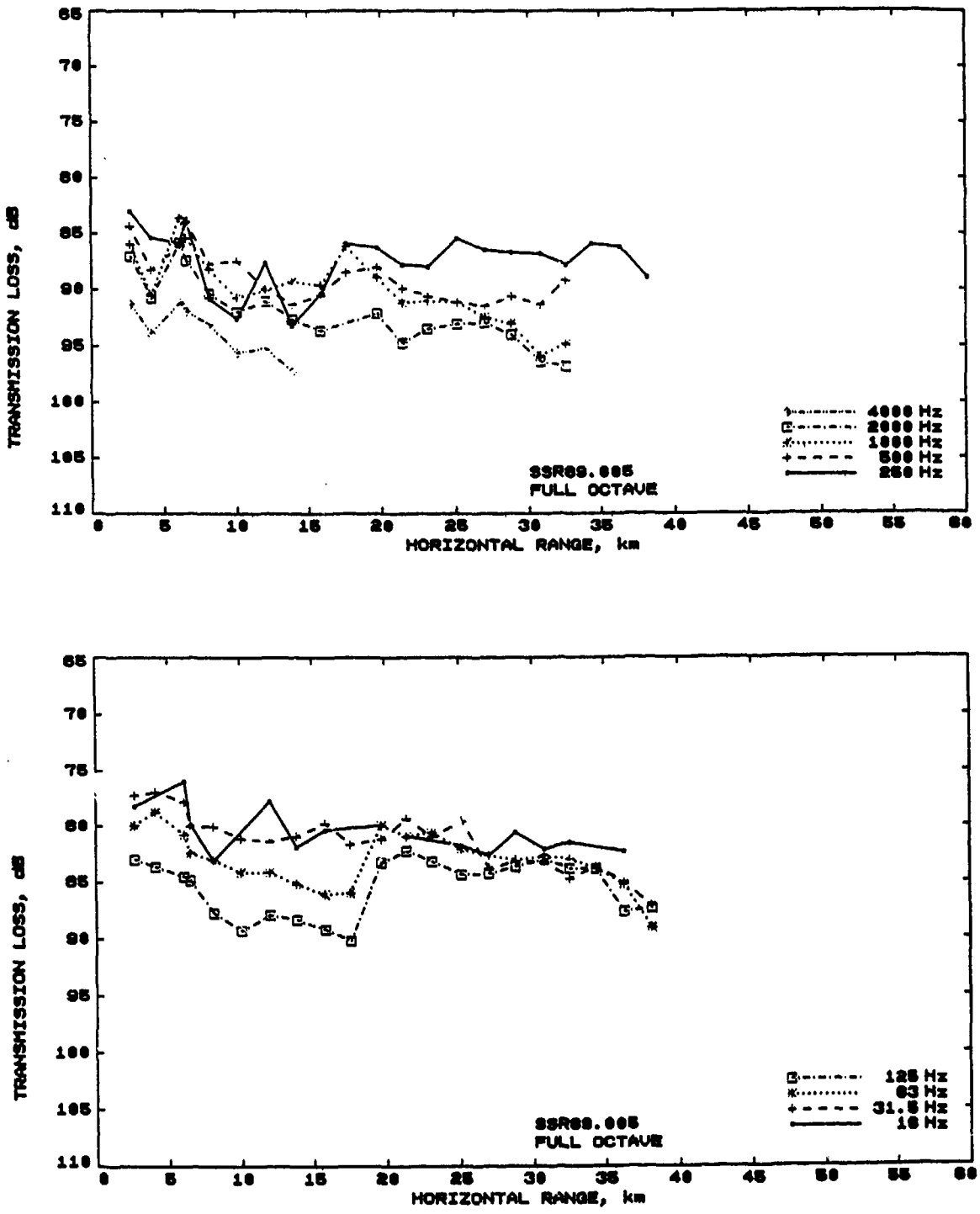

Figure T.1: (C) Measured transmission loss as a function of range, for propagation run SSR89.005.

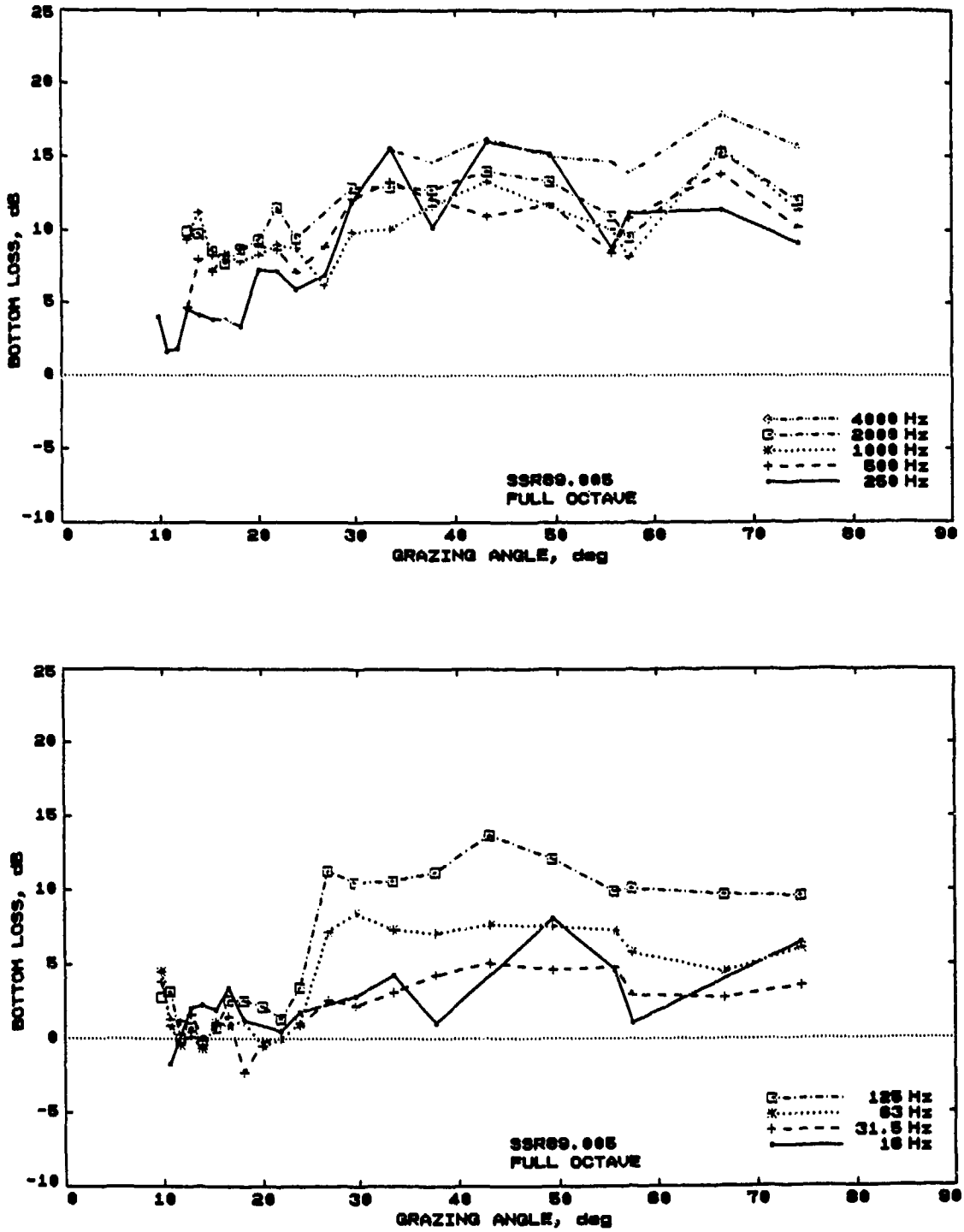

Figure B.1: (C) Bottom loss as a function of grazing angle, for propagation run SSR89.005.

Shot-Run Title :	SSR89.006
Position of receiver :	31°04S 155°28E
Physiographic Province :	Tasman Abyssal Plain
Ship :	HMAS Cook
Cruise :	MSD 15/89 (winter)
Time/Date of start :	1517K 09 MAY 89 (129 0517Z)
Heading :	023
Sound-speed profile :	XBT
Position of ssp :	31°04S 155°28E
Time/Date of ssp :	1519K 09 MAY 89 (129 0519Z)
Source depth :	244 m
Receiver depth :	305 m
Sea State :	3
Swell :	0.5 m, 5 sec, 120°to ship

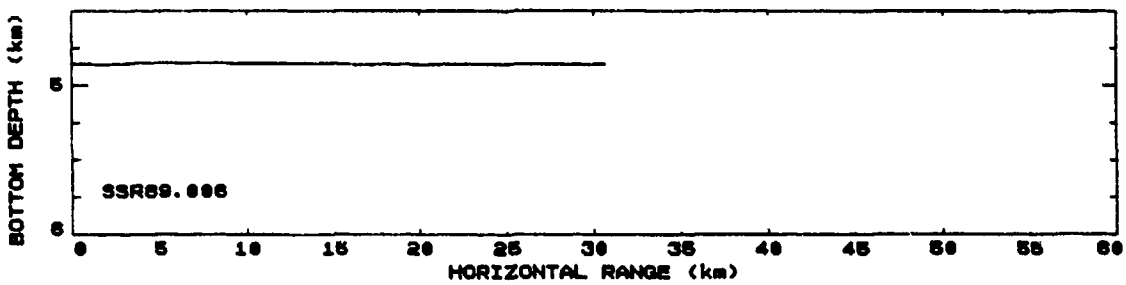

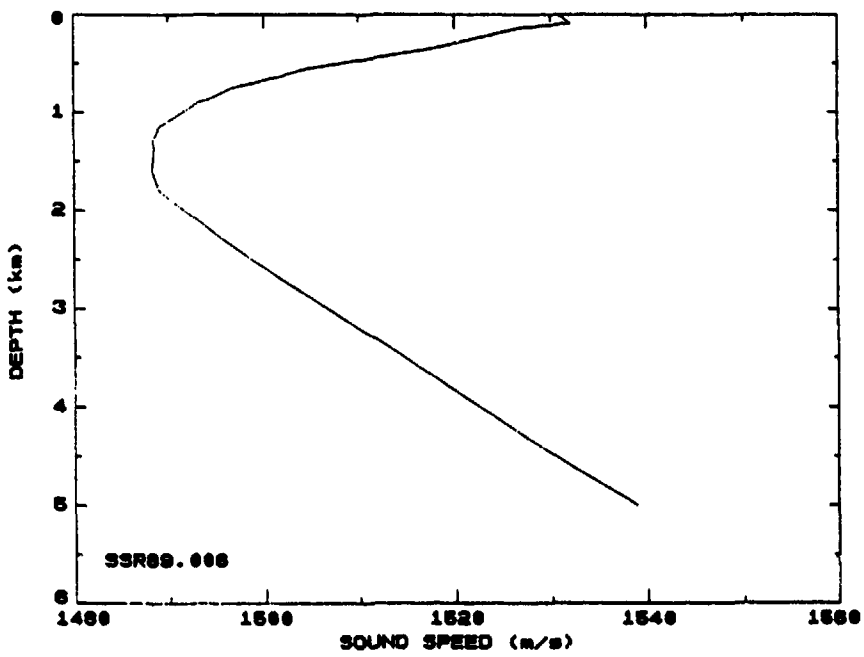

Figure S.2: (U) Summary page for propagation run SSR89.006, containing ancillary information, the bottom profile, and the sound speed profile.

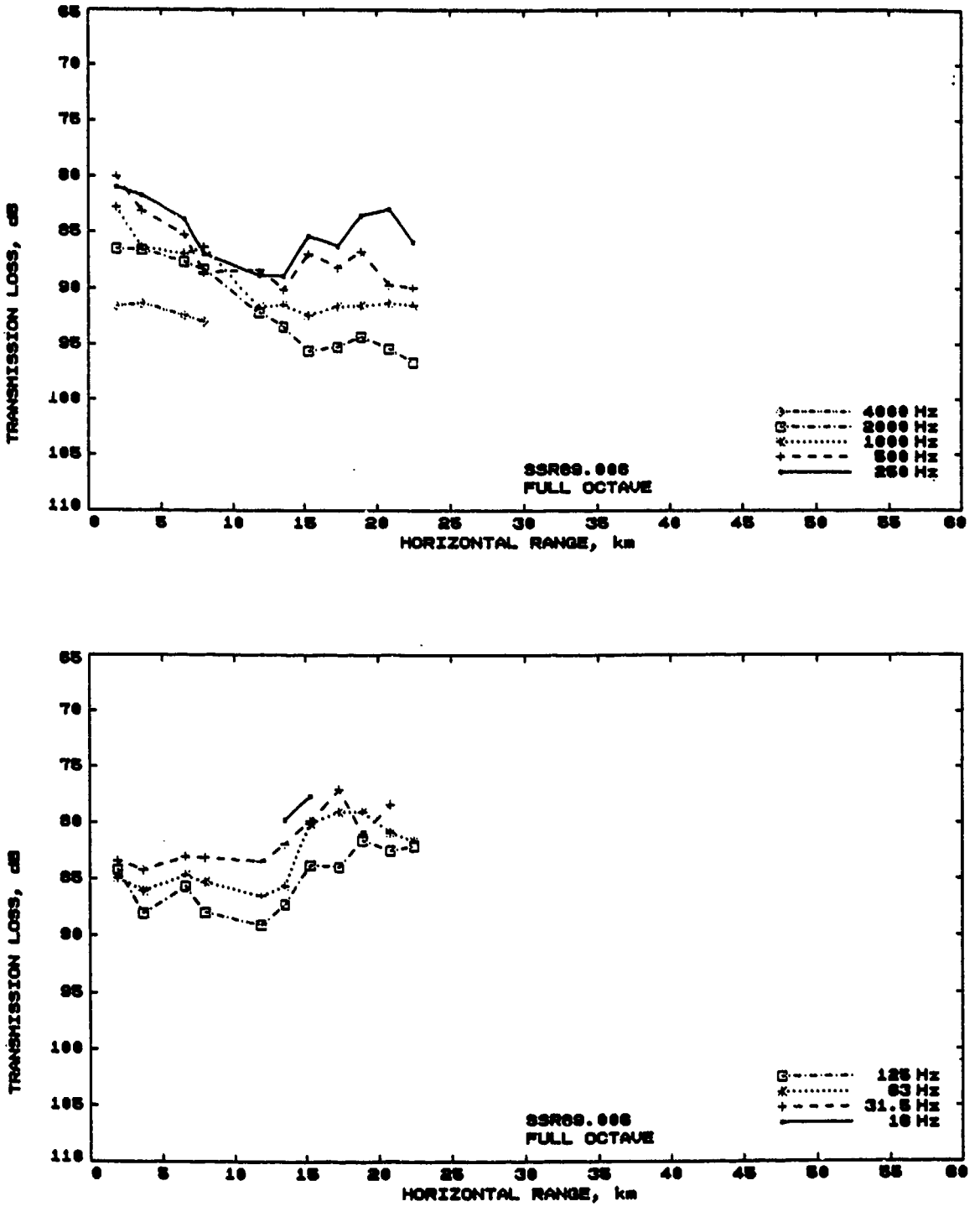

Figure T.2: (C) Measured transmission loss as a function of range, for propagation run SSR89.006.

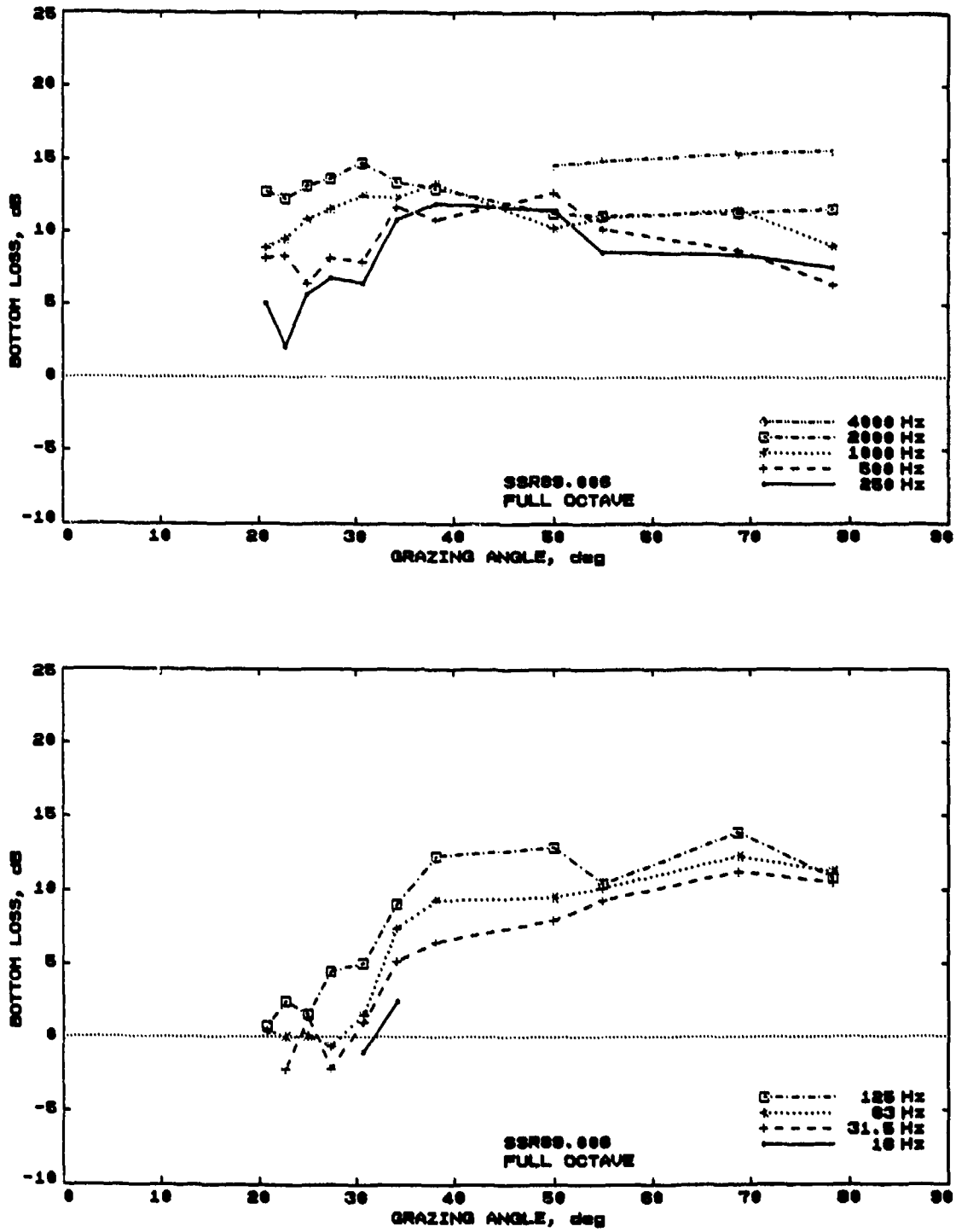

Figure B.2: (C) Bottom loss as a function of grazing angle, for propagation run SSR89.006.

Shot-Run Title :	SSR89.007
Position of receiver :	29°56S 155°47E
Physiographic Province :	Tasman Abyssal Plain
Ship :	HMAS Cook
Cruise :	MSD 15/89 (winter)
Time/Date of start :	2209K 09 MAY 89 (129 1209Z)
Heading :	018
Sound-speed profile :	XBT
Position of ssp :	29°56S 155°47E
Time/Date of ssp :	2216K 09 MAY 89 (129 1216Z)
Source depth :	244 m
Receiver depth :	305 m
Sea State :	3
Swell :	2 m, 3 sec, 120° to ship

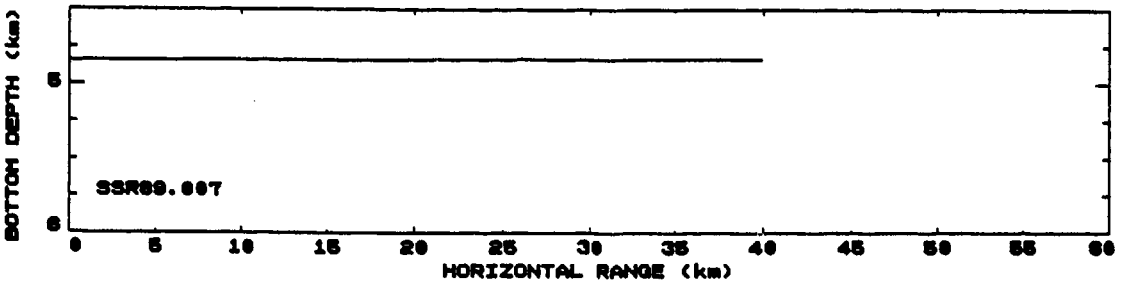

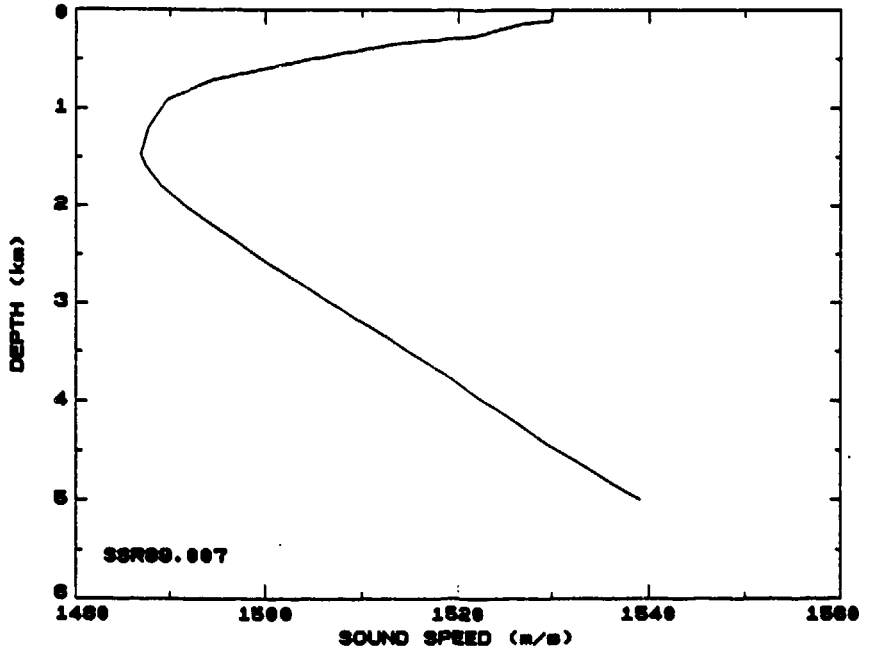

Figure S.3: (U) Summary page for propagation run SSR89.007, containing ancillary information, the bottom profile, and the sound speed profile.

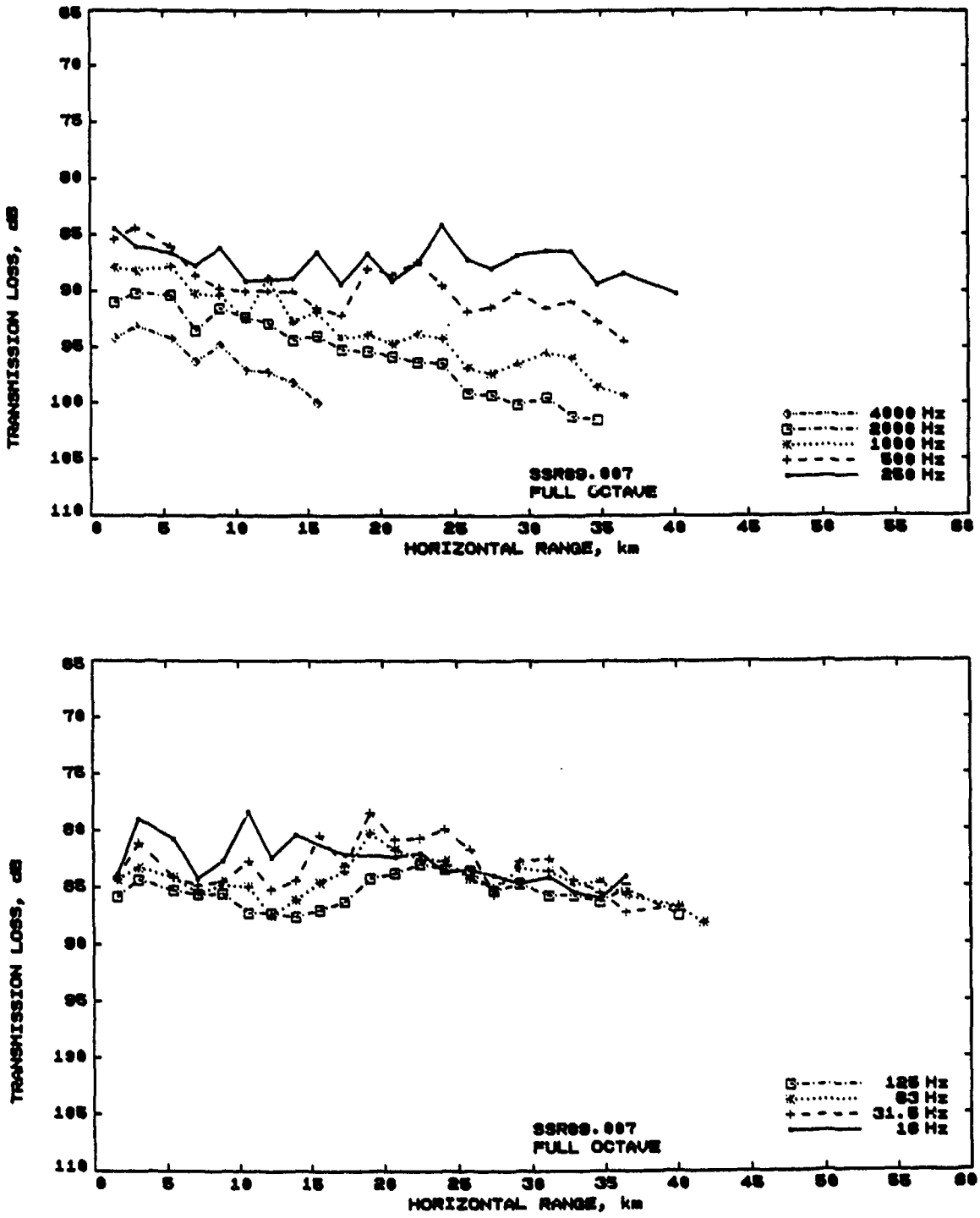

Figure T.3: (C)Measured transmission loss as a function of range, for propagation run SSR89.007.

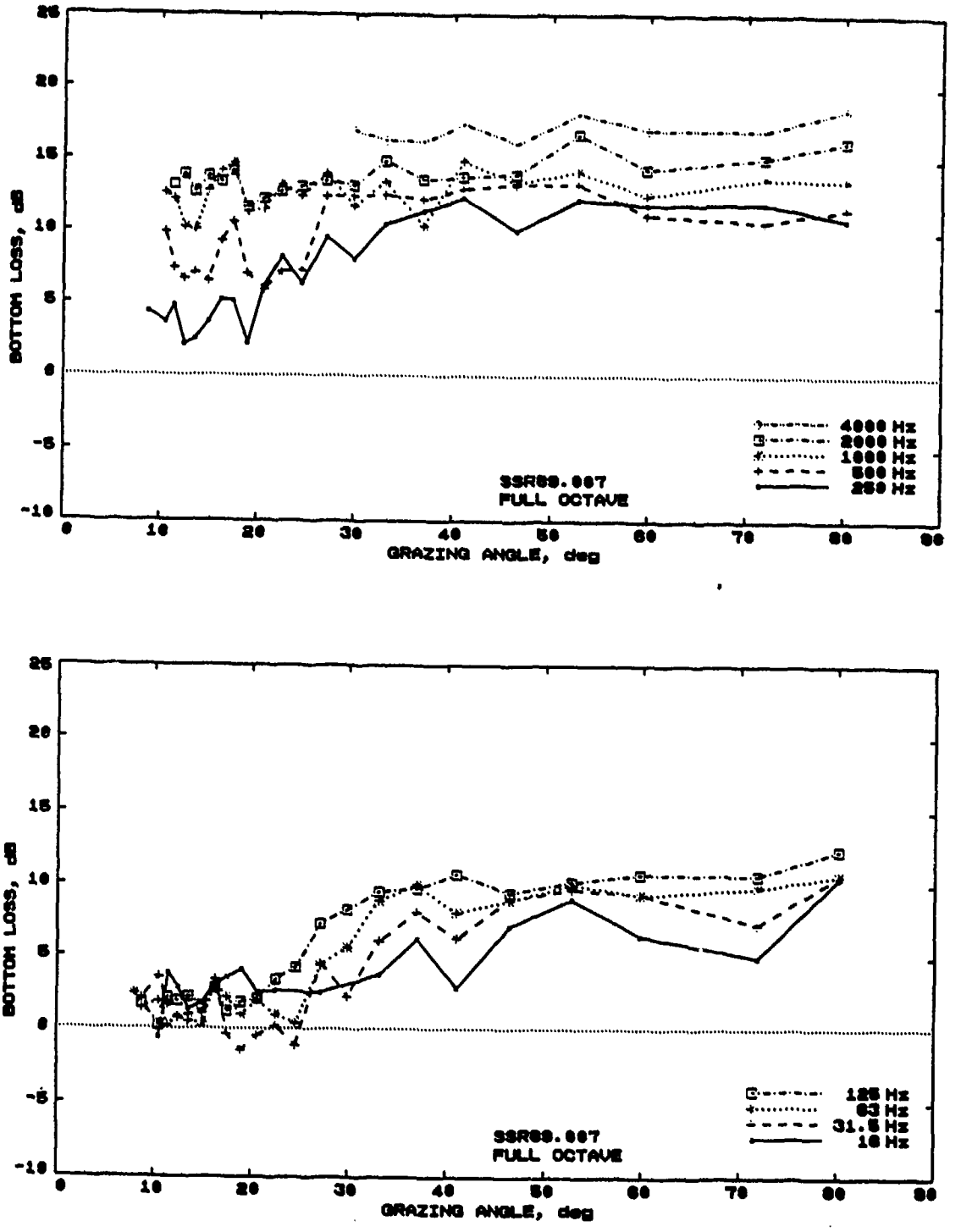

Figure B.3: (C) Bottom loss as a function of grazing angle, for propagation run SSR89.007.

Shot-Run Title :	SSR89.010
Position of receiver :	21°53S 155°09E
Physiographic Province :	Cato trough
Ship :	HMAS Cook
Cruise :	MSD 15/89 (winter)
Time/Date of start :	2009L 11 MAY 89 (131 0909Z)
Heading :	002
Sound-speed profile :	XBT
Position of ssp :	21°31S 154°60E
Time/Date of ssp :	2221L 11 MAY 89 (131 1121Z)
Source depth :	244 m
Receiver depth :	305 m
Sea State :	2
Swell :	1 m, 5 sec, 130° to ship

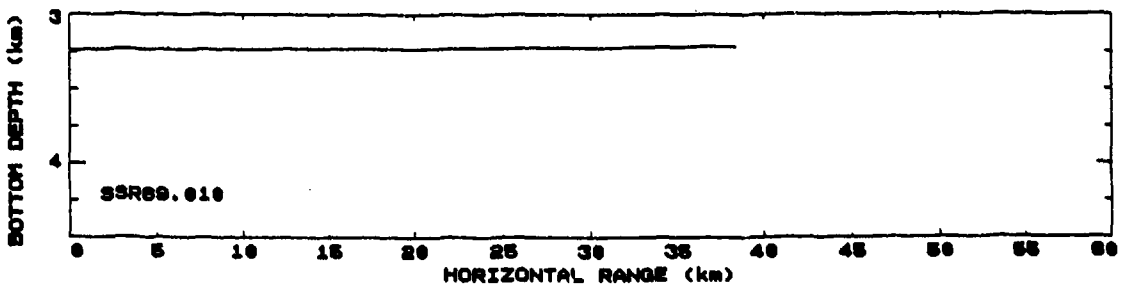

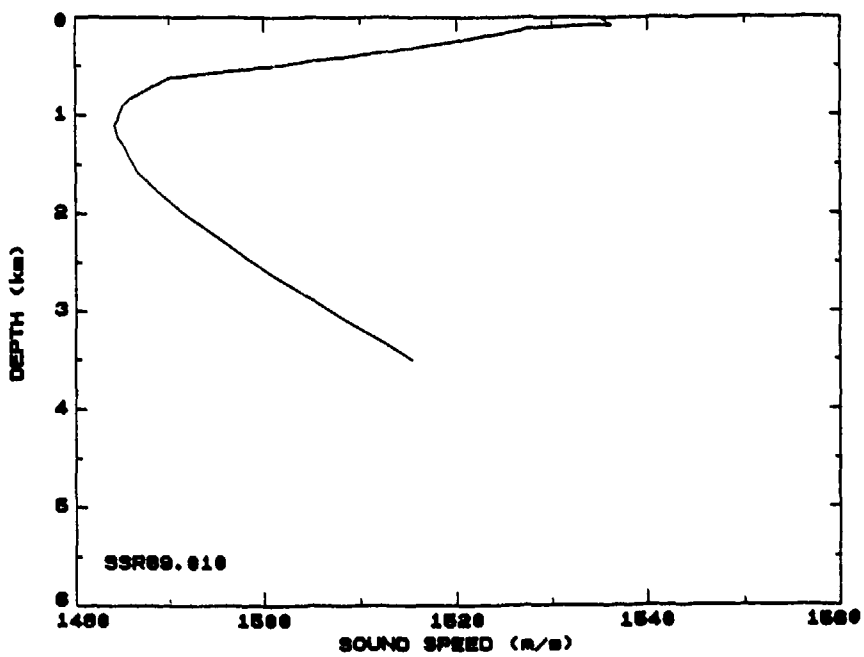

Figure S.4: (U) Summary page for propagation run SSR89.010, containing ancillary information, the bottom profile, and the sound speed profile.

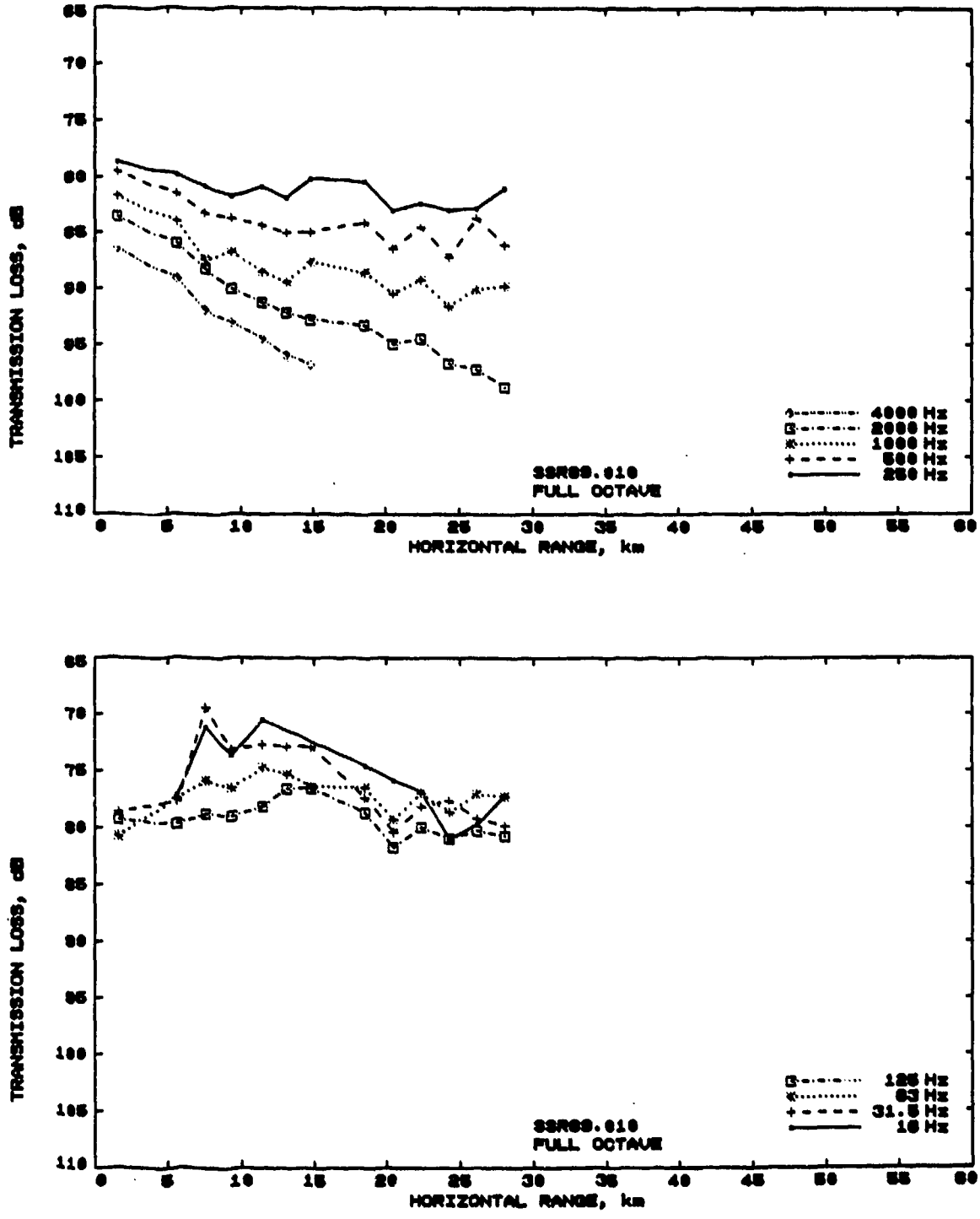

Figure T.4: (C) Measured transmission loss as a function of range, for propagation run SSR89.010.

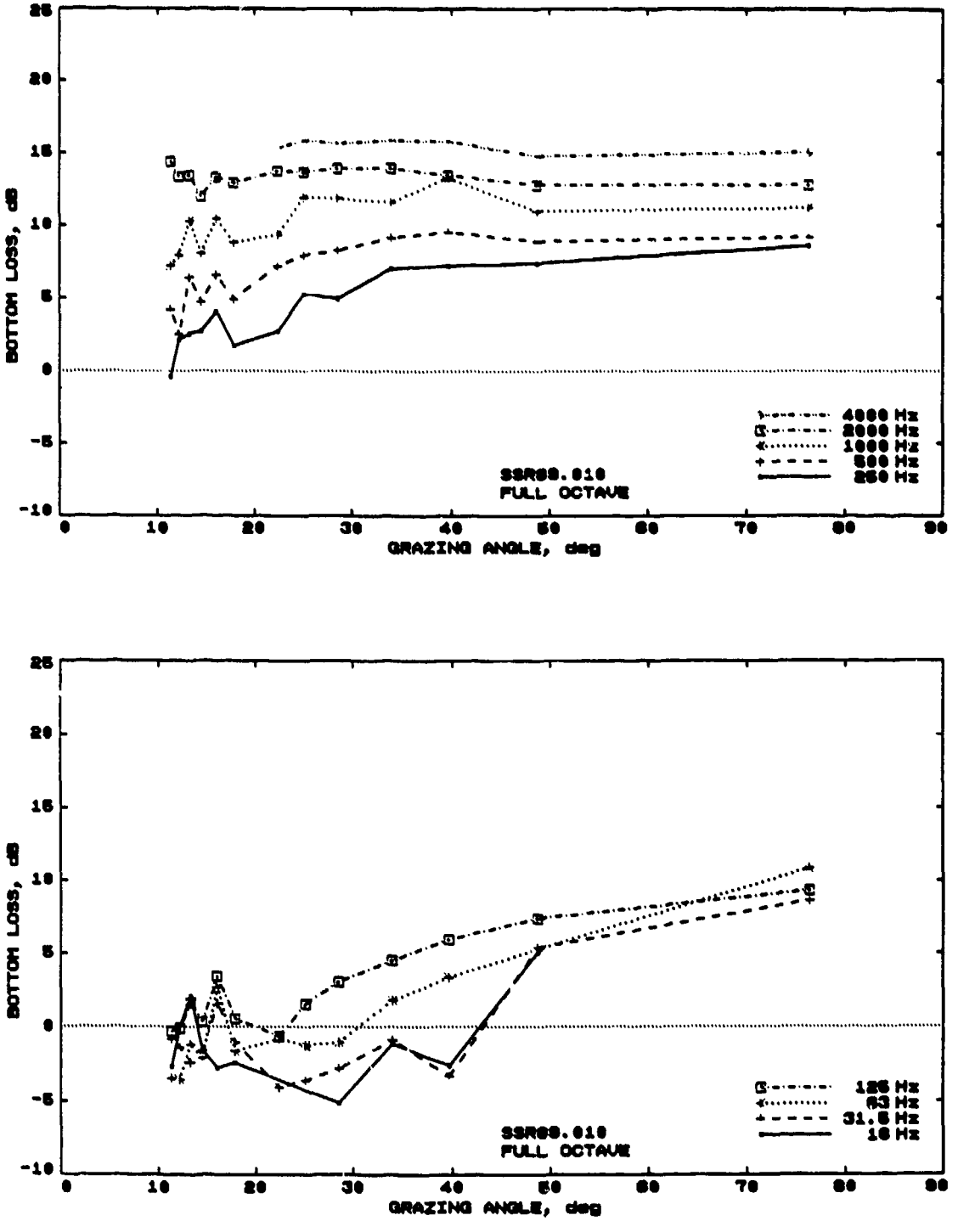

Figure B.4: (C) Bottom loss as a function of grazing angle, for propagation run SSR89.010.

Shot-Run Title :	SSR89.013
Position of receiver :	15°14S 154°46E
Physiographic Province :	Coral Sea Abyssal Plain
Ship :	HMAS Cook
Cruise :	MSD 15/89 (winter)
Time/Date of start :	2058L 15 MAY 89 (135 0958Z)
Heading :	001
Sound-speed profile :	XBT
Position of ssp :	15°16S 154°46E
Time/Date of ssp :	2240L 15 MAY 89 (135 1140Z)
Source depth :	244 m
Receiver depth :	305 m
Sea State :	2
Swell :	0.5 m, 5 sec, 100° to ship

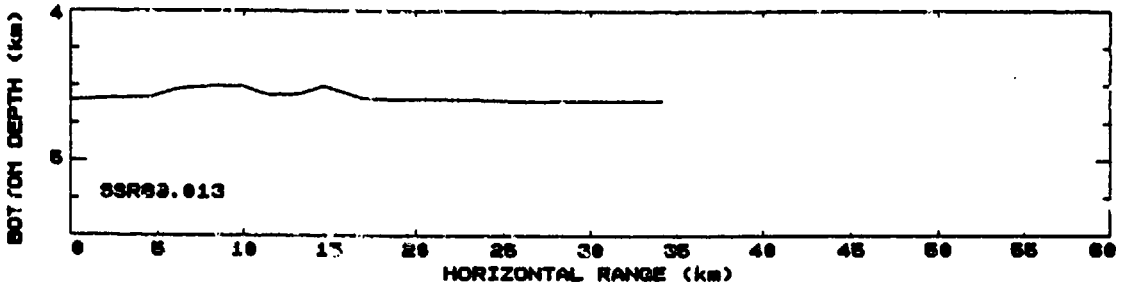

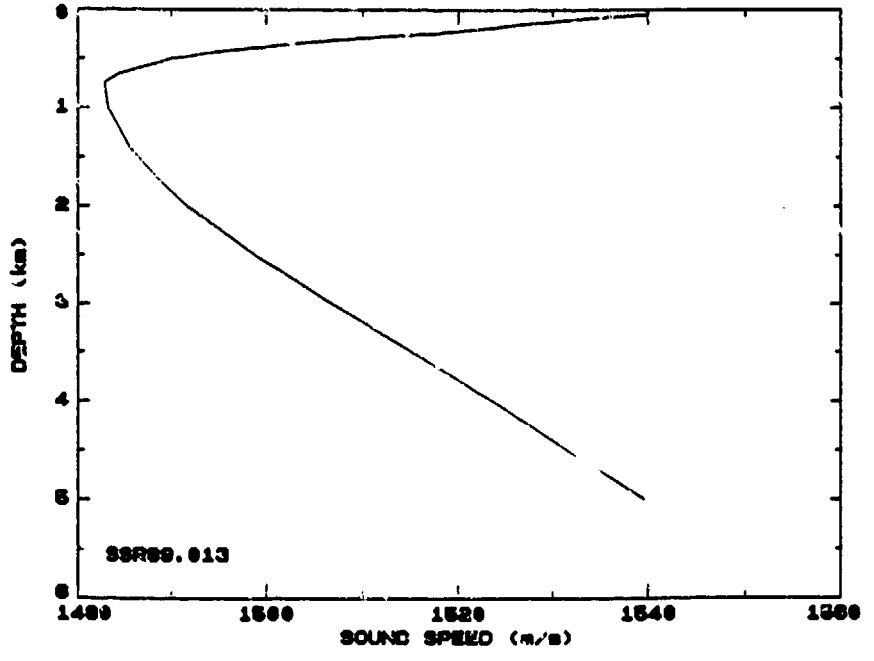

Figure S.5: (U) Summary page for propagation run SSR89.013, containing ancillary information, the bottom profile, and the sound speed profile.

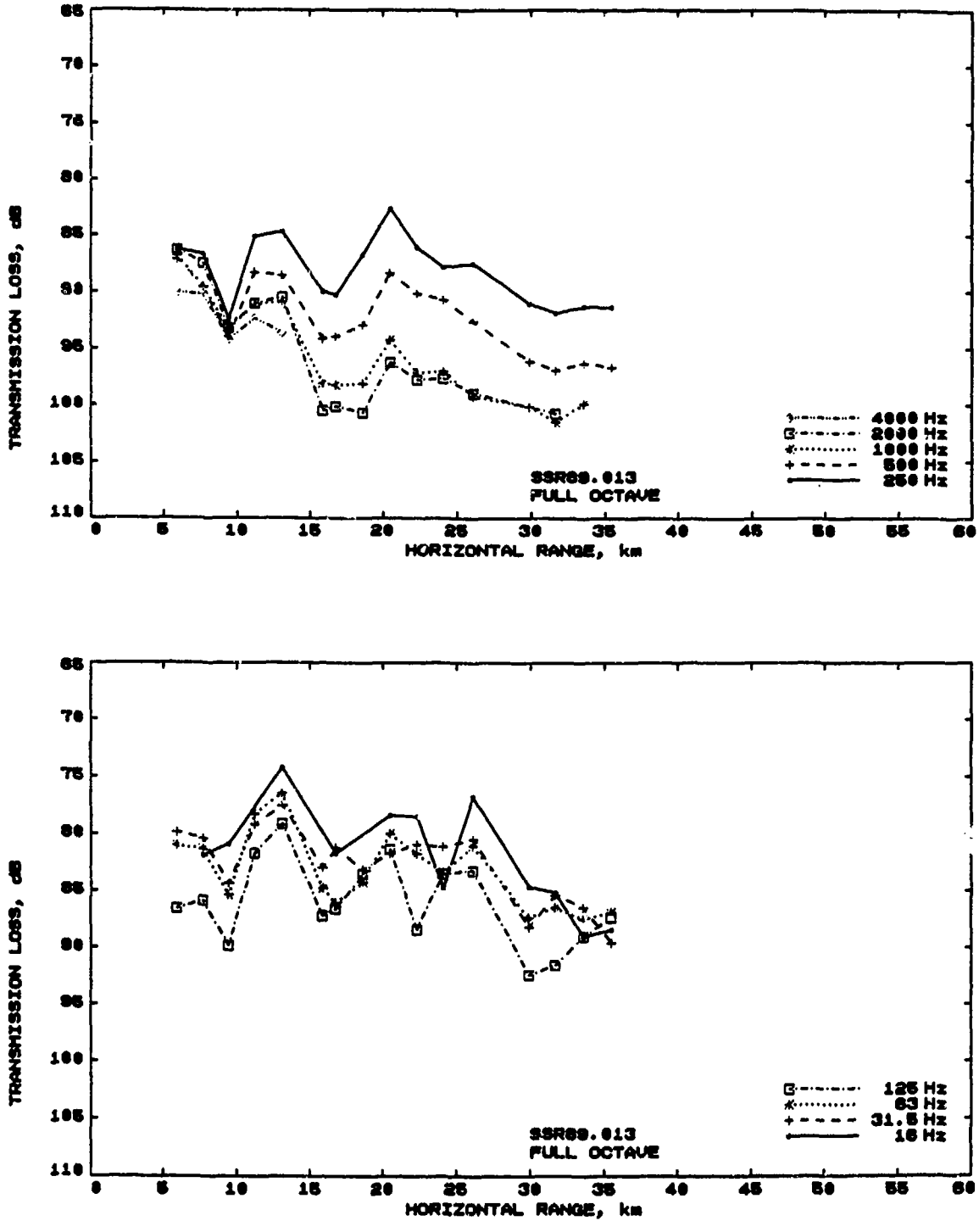

Figure T.5: (C) Measured transmission loss as a function of range, for propagation run SSR89.013.

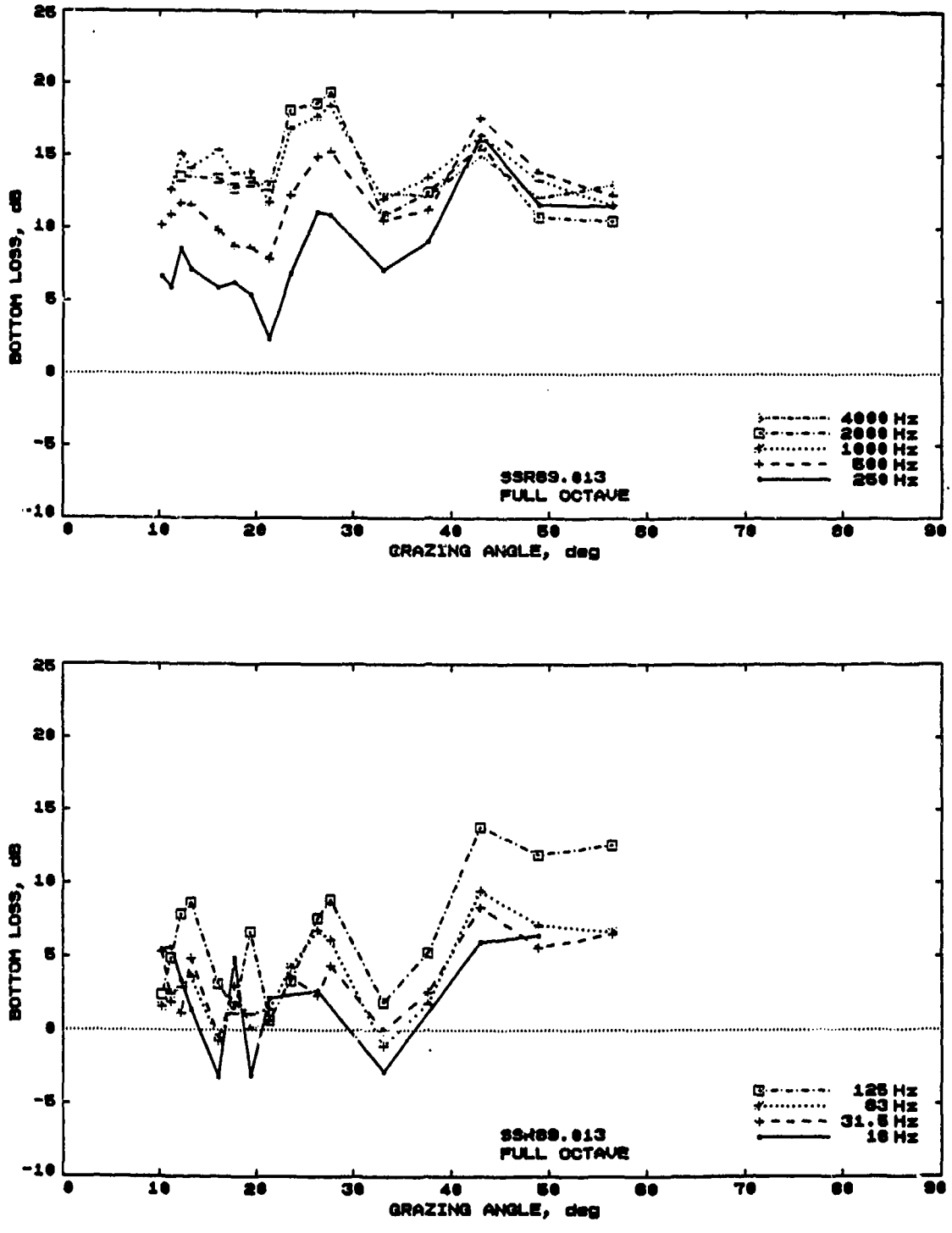

Figure B.5: (C) Bottom loss as a function of grazing angle, for propagation run SSR89.013.

Shot-Run Title :	SSR89.016
Position of receiver :	10°45S 154°25E
Physiographic Province :	Woodlark Basin
Ship :	HMAS Cook
Cruise :	MSD 15/89 (winter)
Time/Date of start :	1909L 16 MAY 89 (136 0809Z)
Heading :	343
Sound-speed profile :	XBT
Position of ssp :	10°45S 154°25E
Time/Date of ssp :	1913L 16 MAY 89 (136 0813Z)
Source depth :	244 m
Receiver depth :	305 m
Sea State :	2
Swell :	0.5 m, 5 sec, 100° to ship

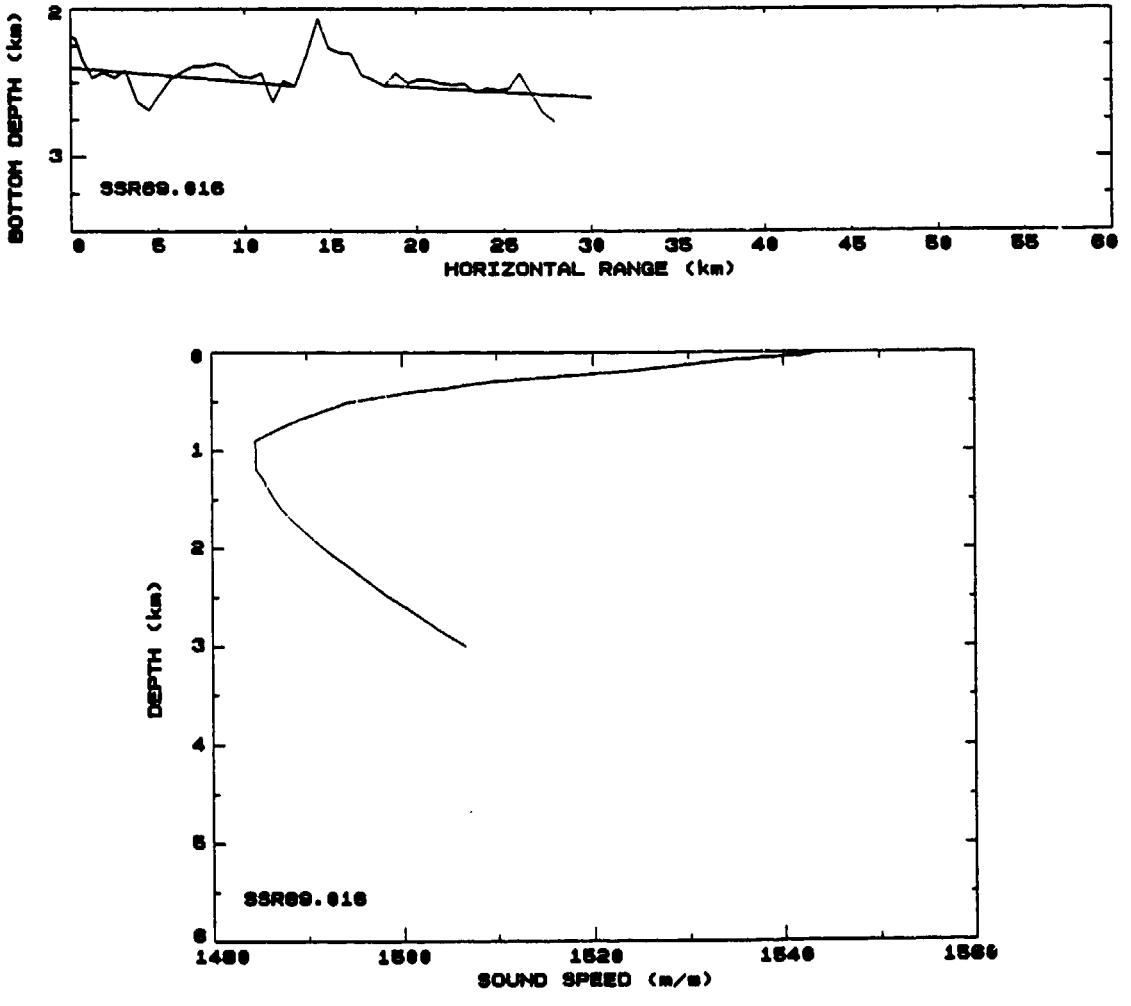

Figure S.6: (U) Summary page for propagation run SSR89.016, containing ancillary information, the bottom profile, and the sound speed profile.

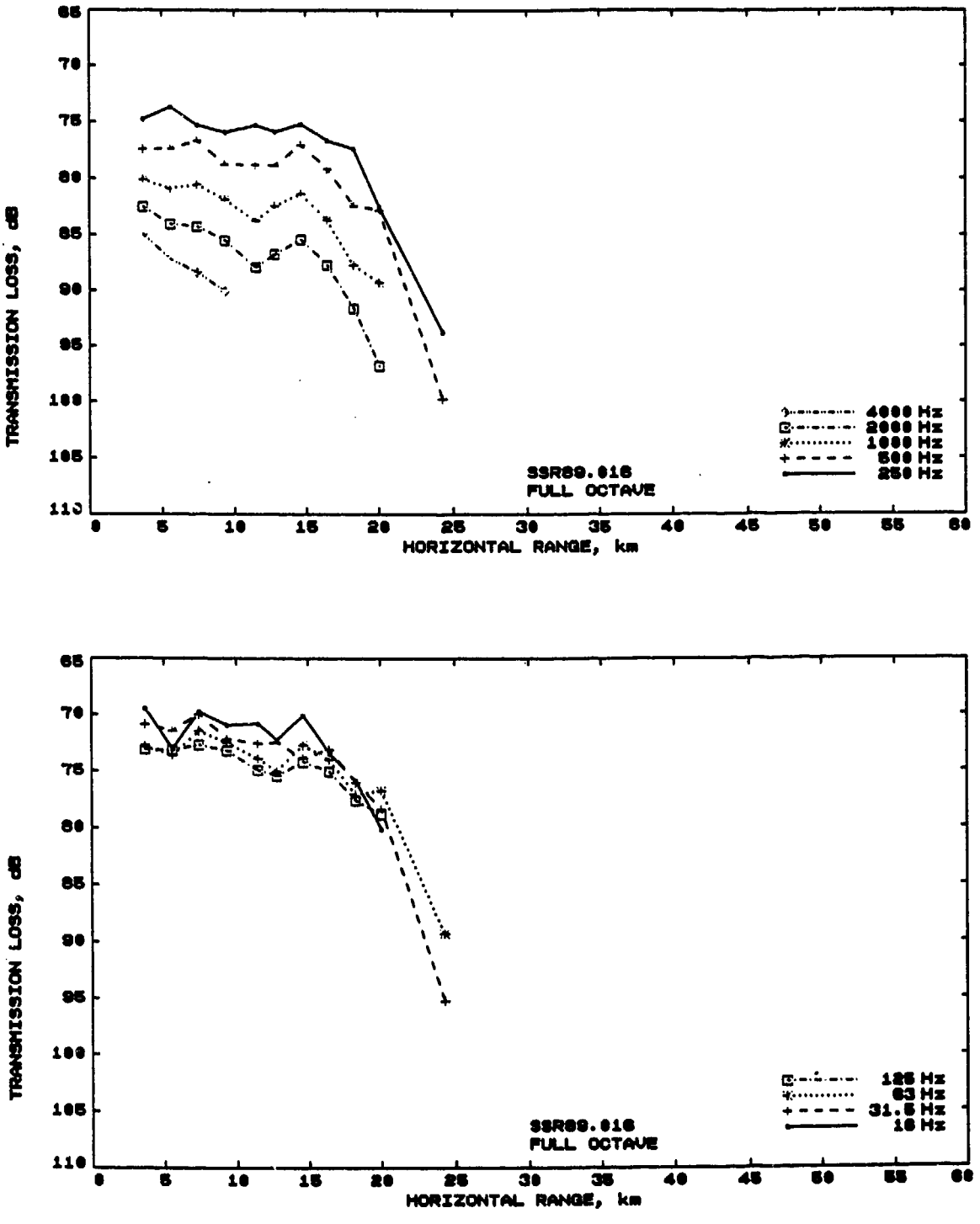

Figure T.6: (C) Measured transmission loss as a function of range, for propagation run SSR89.016.

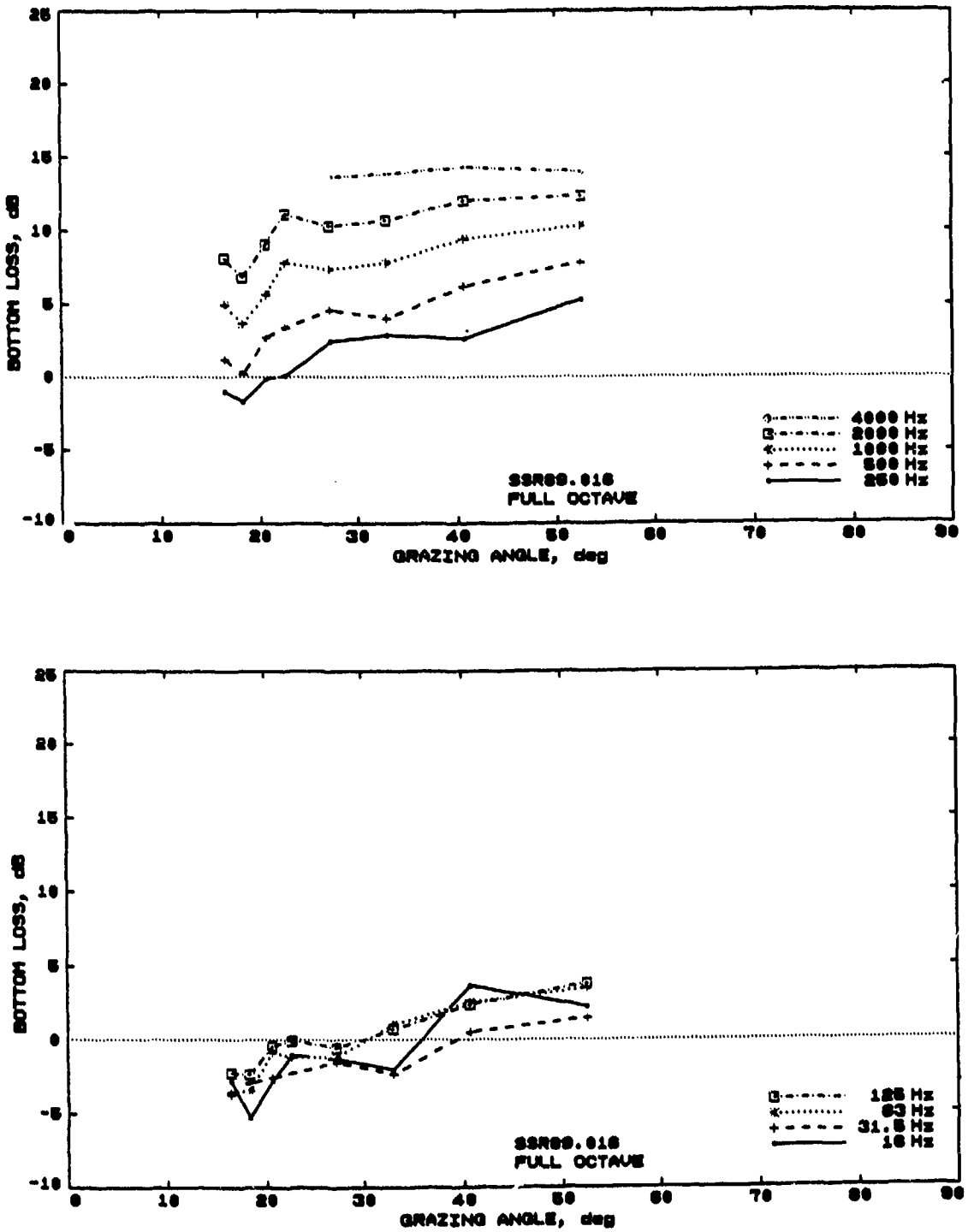

Figure B.6: (C) Bottom loss as a function of grazing angle, for propagation run SSR89.016.

Shot-Run Title :	SSR89.017
Position of receiver :	08°42S 154°07E
Physiographic Province :	Trobriand Ridge
Ship :	HMAS Cook
Cruise :	MSD 15/89 (winter)
Time/Date of start :	0725L 17 MAY 89 (136 2025Z)
Heading :	355.1
Sound-speed profile :	XBT
Position of ssp :	08°42S 154°07E
Time/Date of ssp :	0729L 17 MAY 89 (136 2029Z)
Source depth :	244 m
Receiver depth :	305 m
Sea State :	2
Swell :	0.25 m,10 sec, 110° to ship

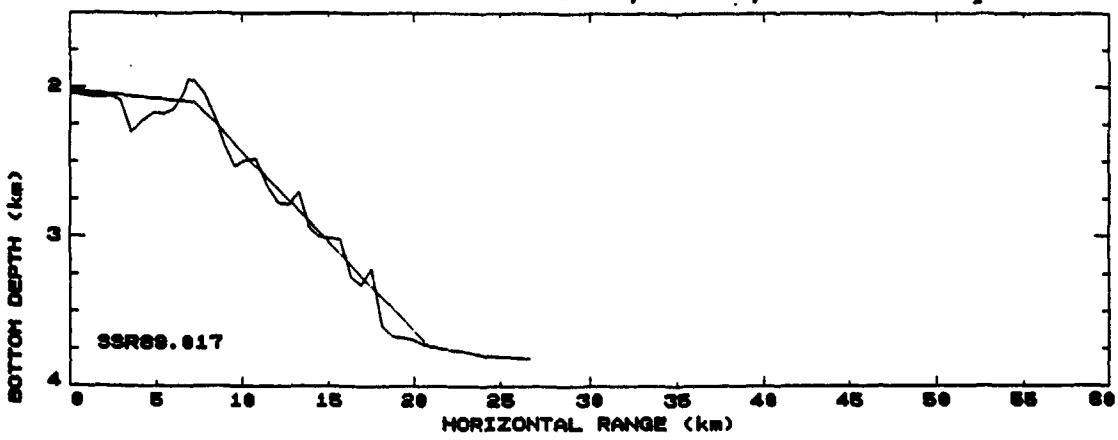

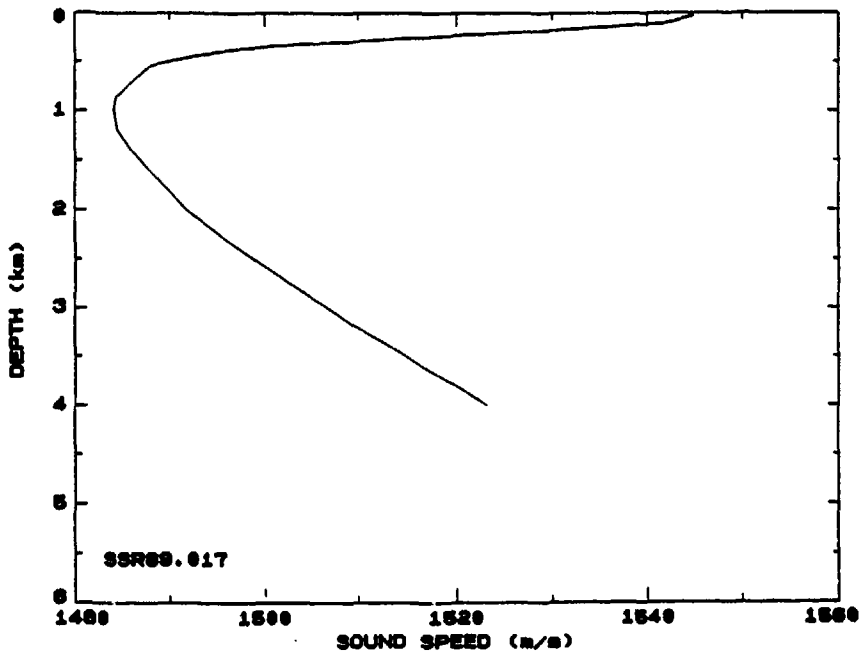

Figure S.7: (U) Summary page for propagation run SSR89.017, containing ancillary information, the bottom profile, and the sound speed profile.

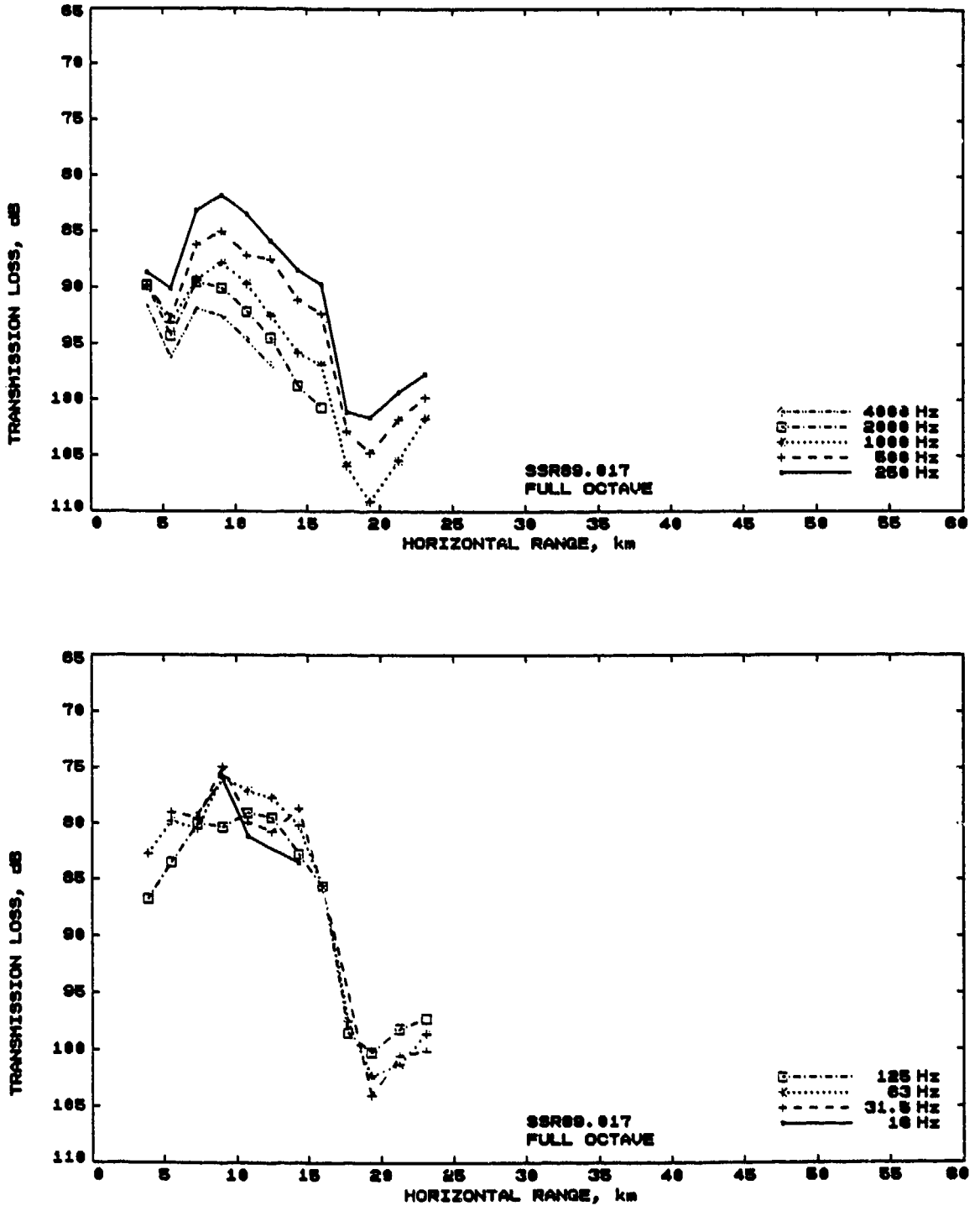

Figure T.7: (C) Measured transmission loss as a function of range, for propagation run SSR89.017.

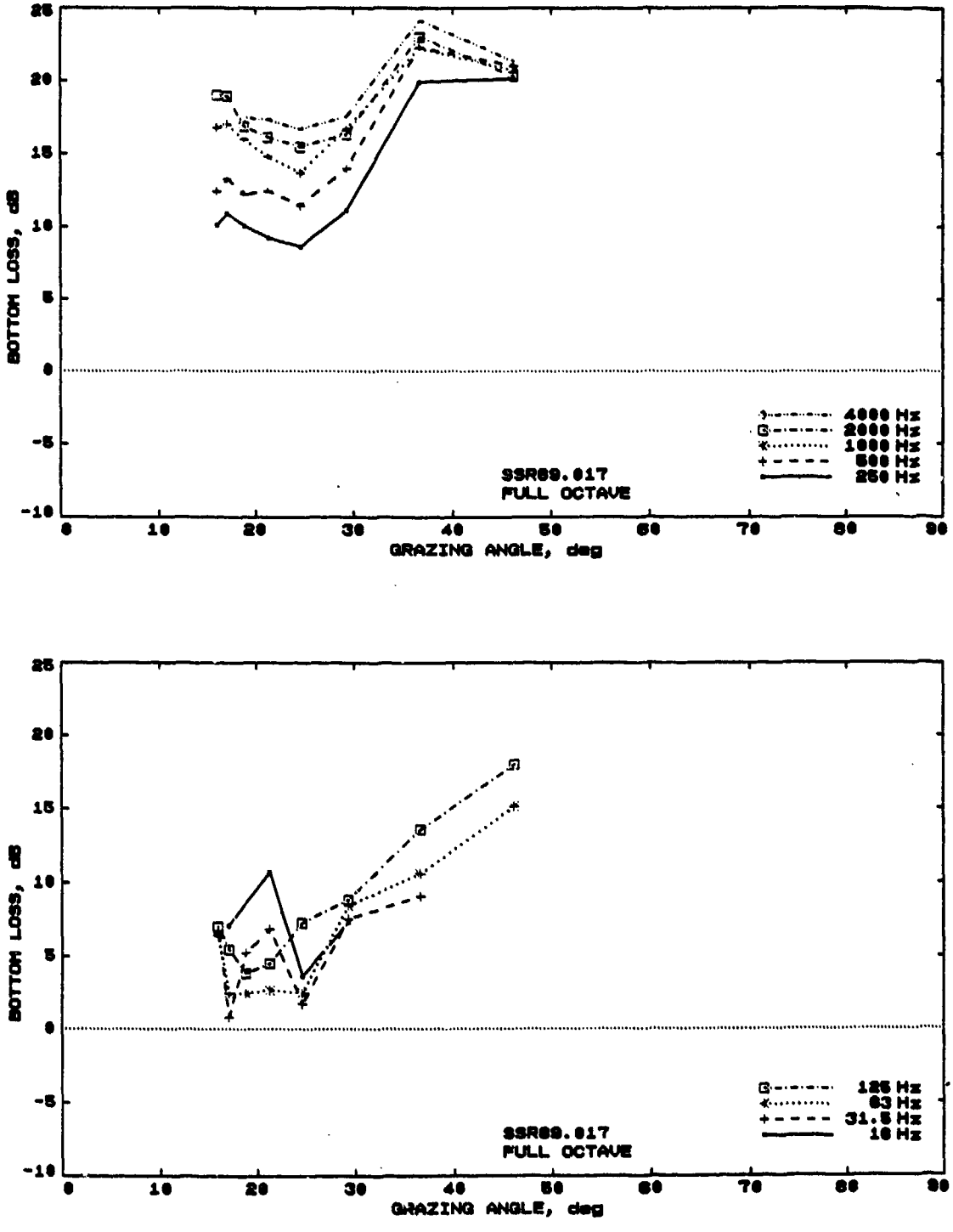

Figure B.7: (C) Bottom loss as a function of grazing angle, for propagation run SSR89.017.

Shot-Run Title :	SSR89.018
Position of receiver :	07°31S 154°54E
Physiographic Province :	Woodlark Basin
Ship :	HMAS Cook
Cruise :	MSD 15/89 (winter)
Time/Date of start :	1636L 17 MAY 89 (137 0536Z)
Heading :	353
Sound-speed profile :	XBT
Position of ssp :	07°30S 153°55E
Time/Date of ssp :	1639L 17 MAY 89 (137 0539Z)
Source depth :	244 m
Receiver depth :	305 m
Sea State :	2
Swell :	0.5 m, 4 sec, 140° to ship

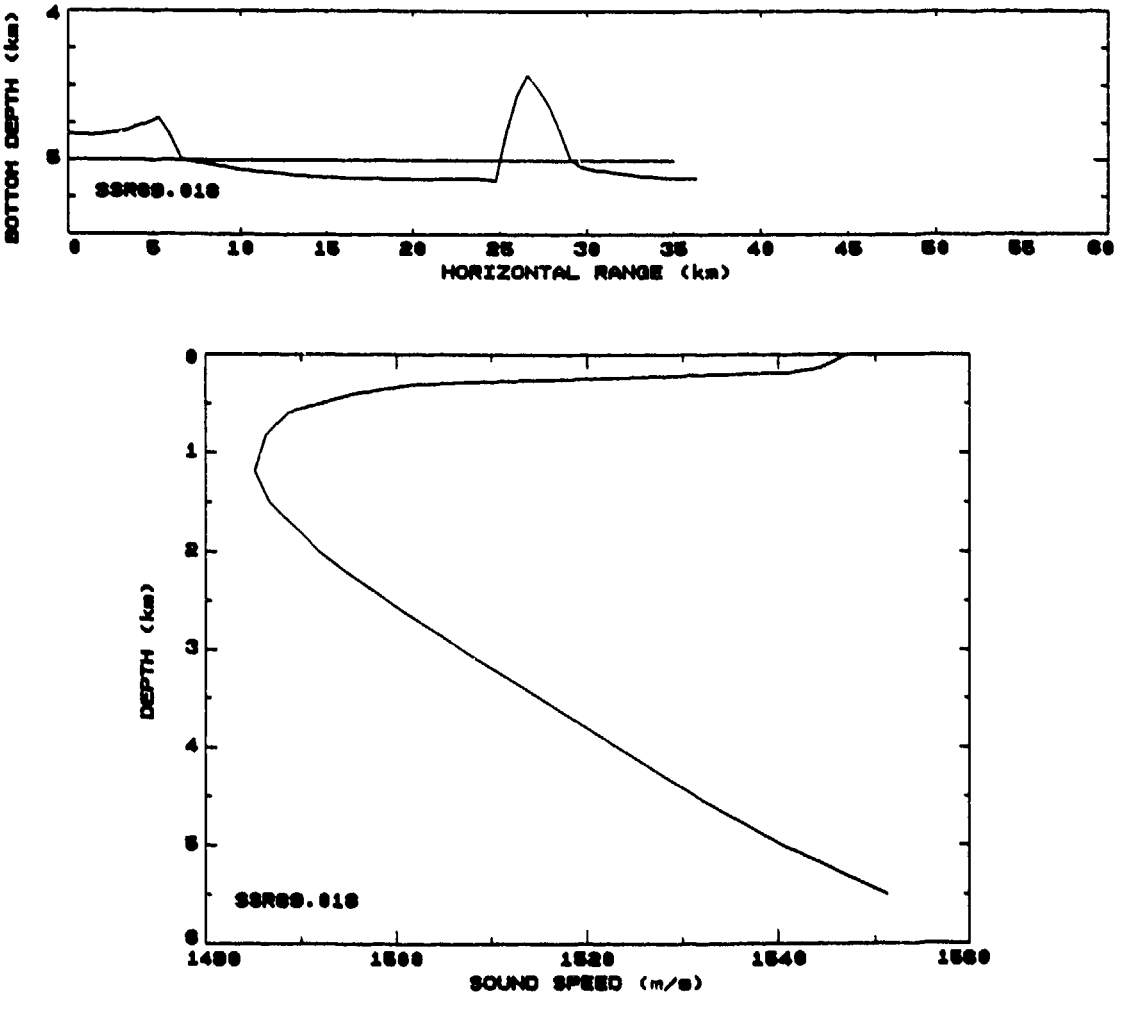

Figure S.8: (U) Summary page for propagation run SSR89.018, containing ancillary information, the bottom profile, and the sound speed profile.

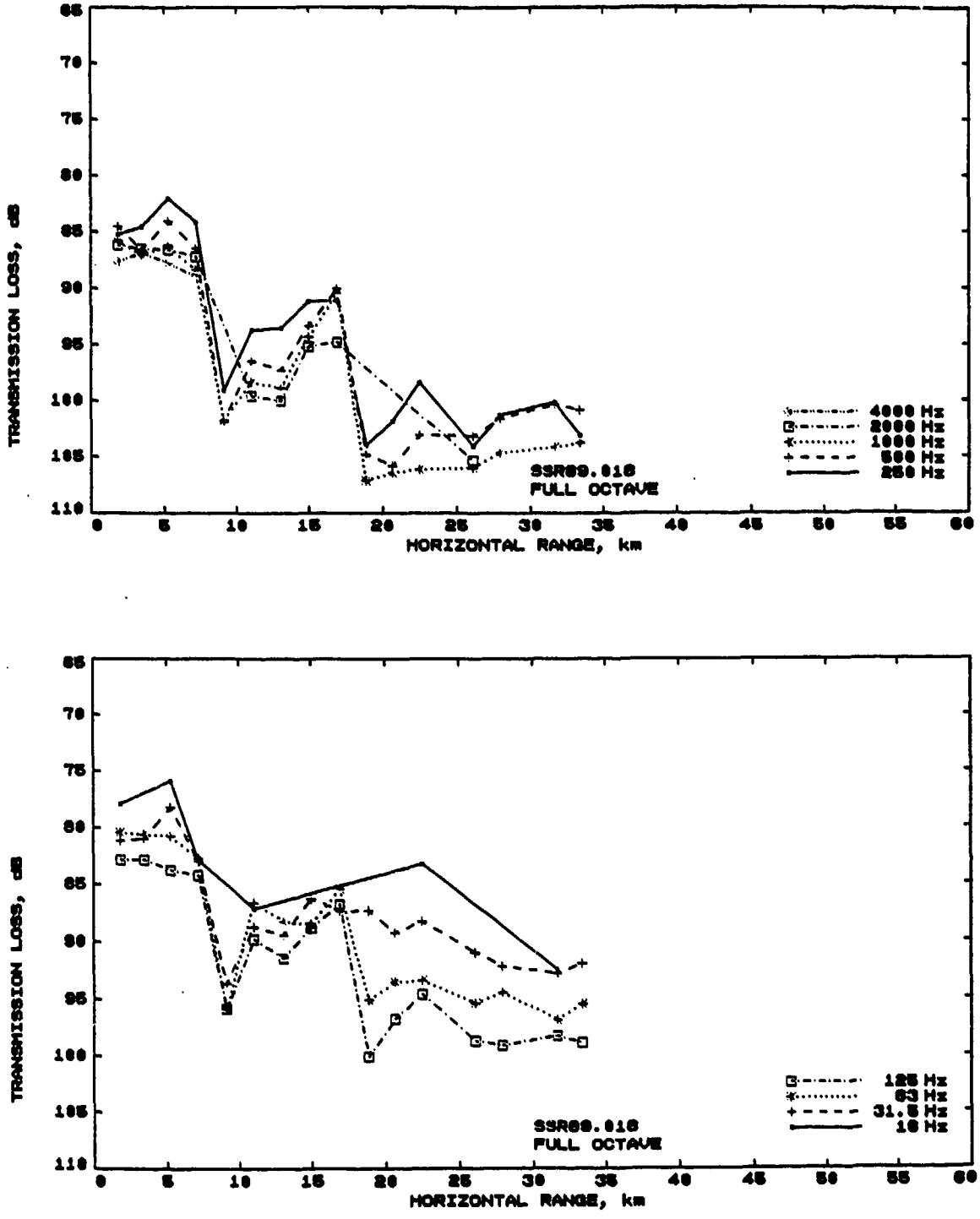

Figure T.8: (C) Measured transmission loss as a function of range, for propagation run SSR89.018.

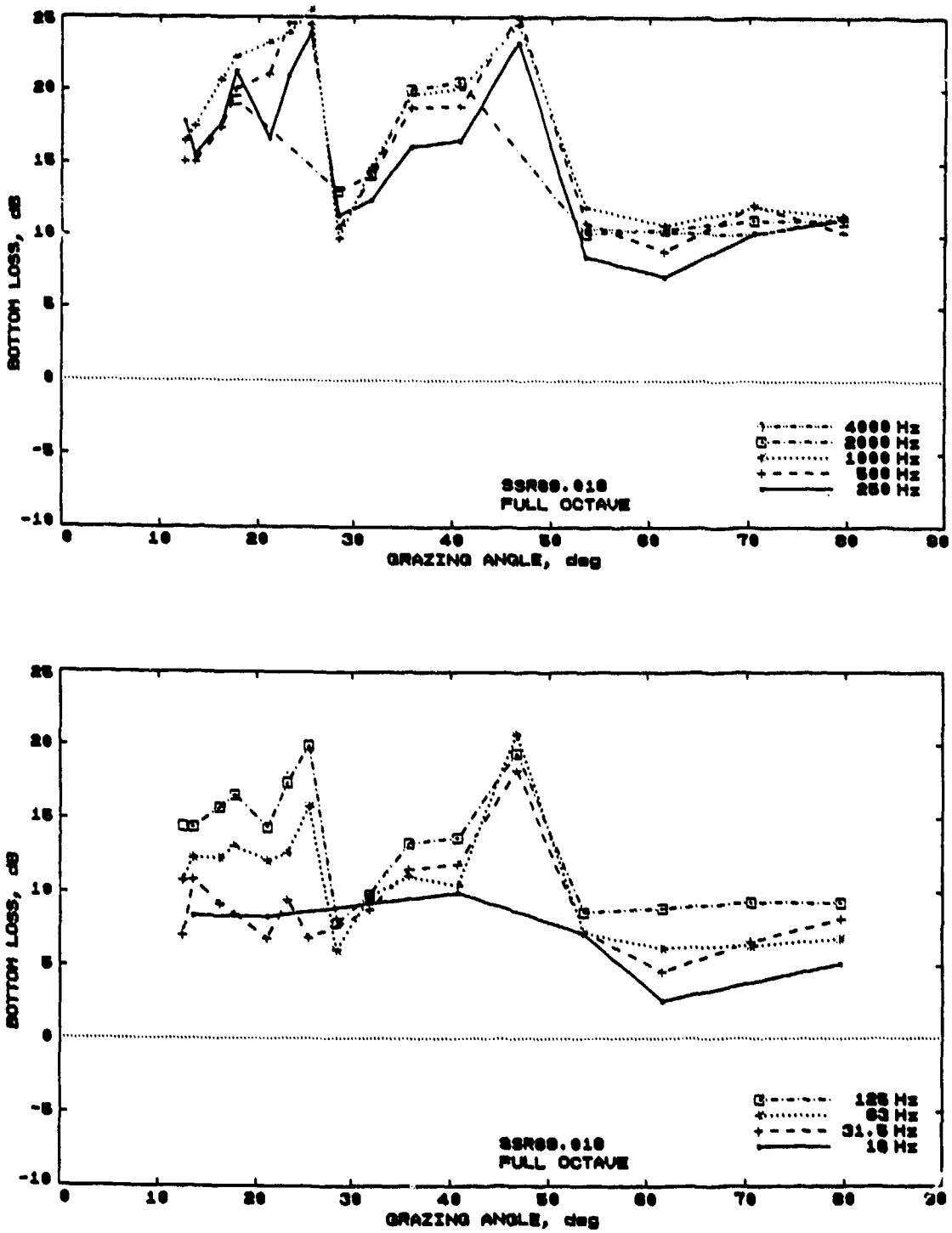

Figure B.8: (C) Bottom loss as a function of grazing angle, for propagation run SSR89.018.

Shot-Run Title :	SSR89.019
Position of receiver :	06°13S 153°45E
Physiographic Province :	Inner Trench Slope
Ship :	HMAS Cook
Cruise :	MSD 15/89 (winter)
Time/Date of start :	0706L 18 MAY 89 (137 2006Z)
Heading :	347
Sound-speed profile :	XBT
Position of ssp :	06°13S 153°45E
Time/Date of ssp :	0708L 18 MAY 89 (137 2008Z)
Source depth :	244 m
Receiver depth :	305 m
Sea State :	2
Swell :	0.0 m, 0 sec, 000° to ship

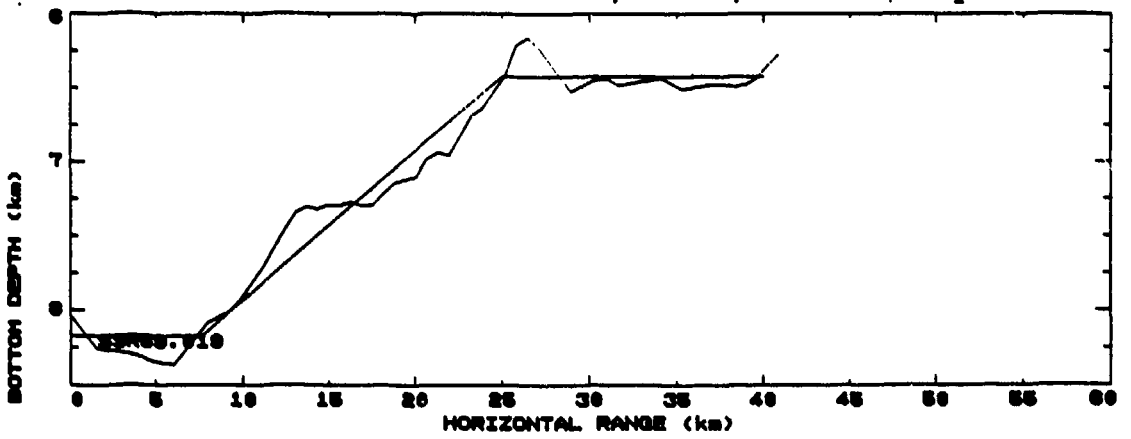

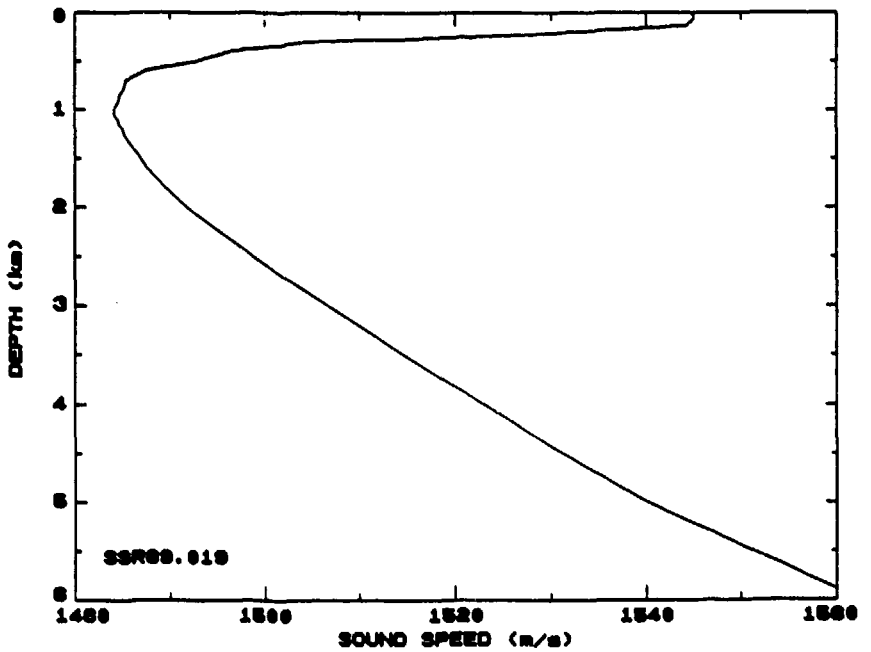

Figure S.9: (U) Summary page for propagation run SSR89.019, containing ancillary information, the bottom profile, and the sound speed profile.

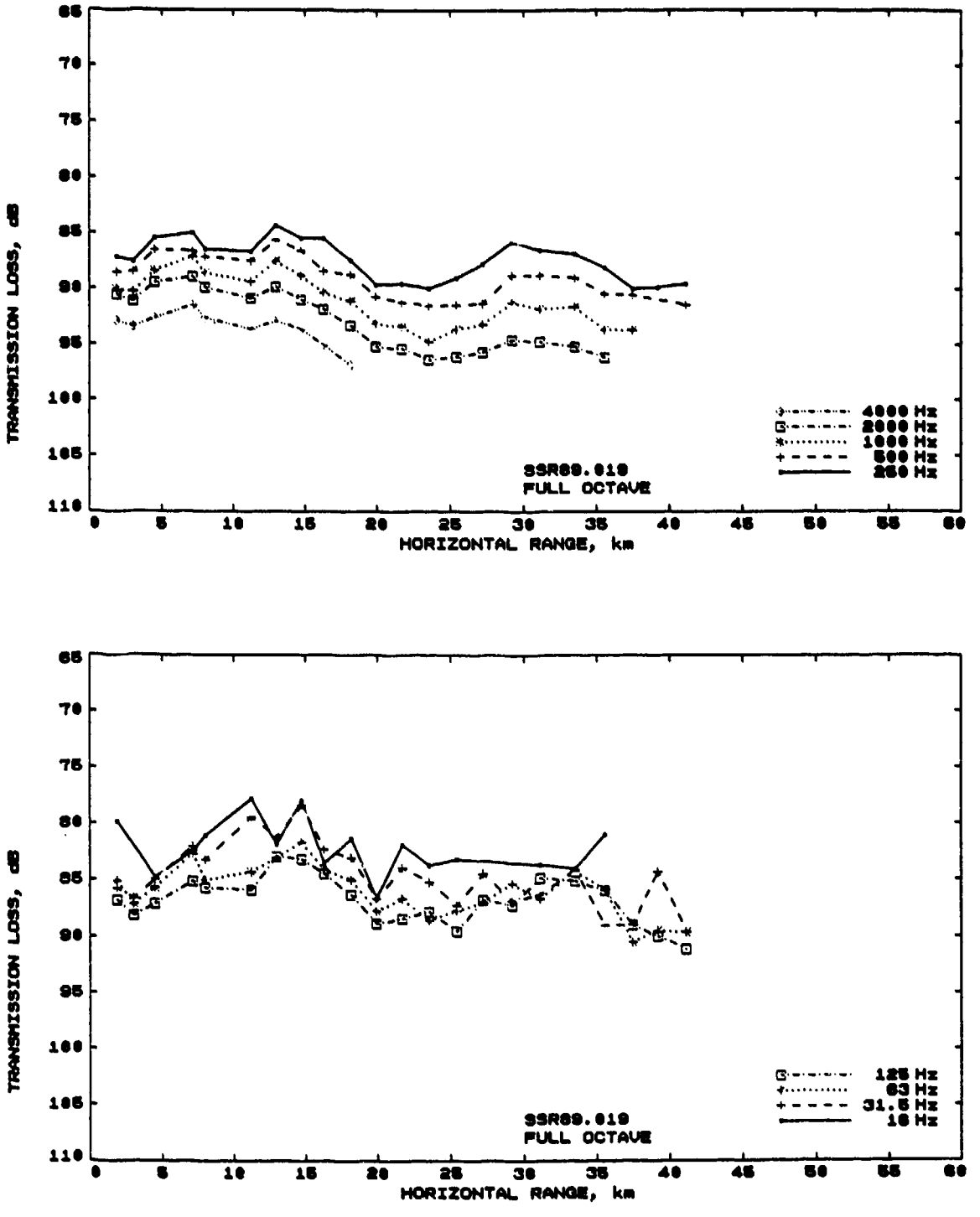

Figure T.9: (C) Measured transmission loss as a function of range, for propagation run SSR89.019.

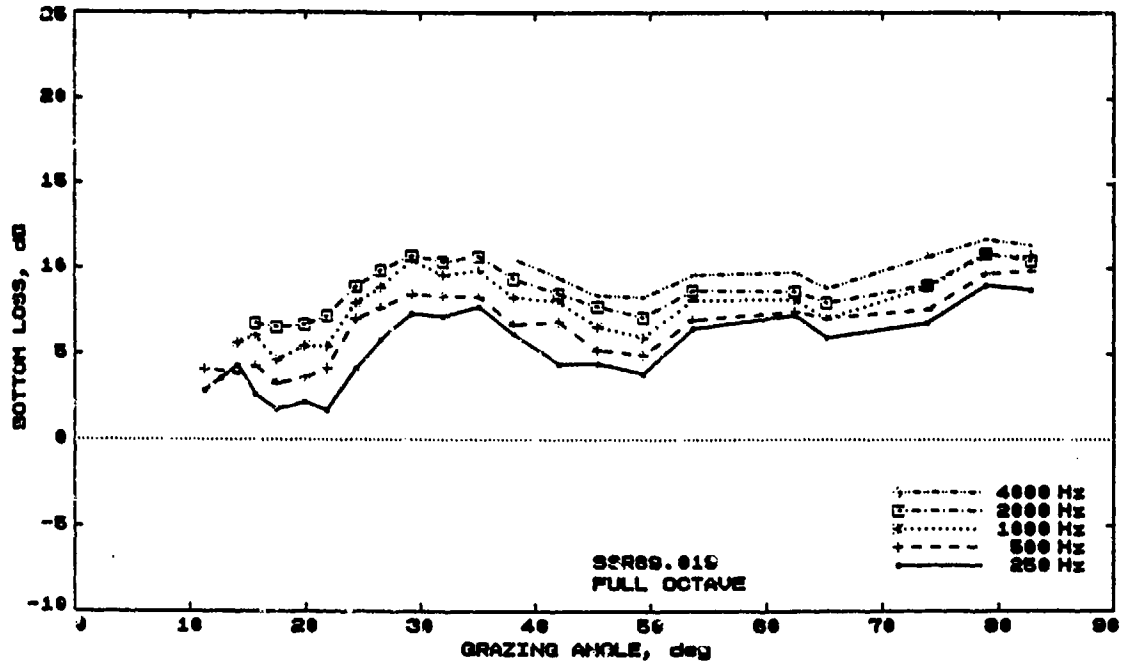

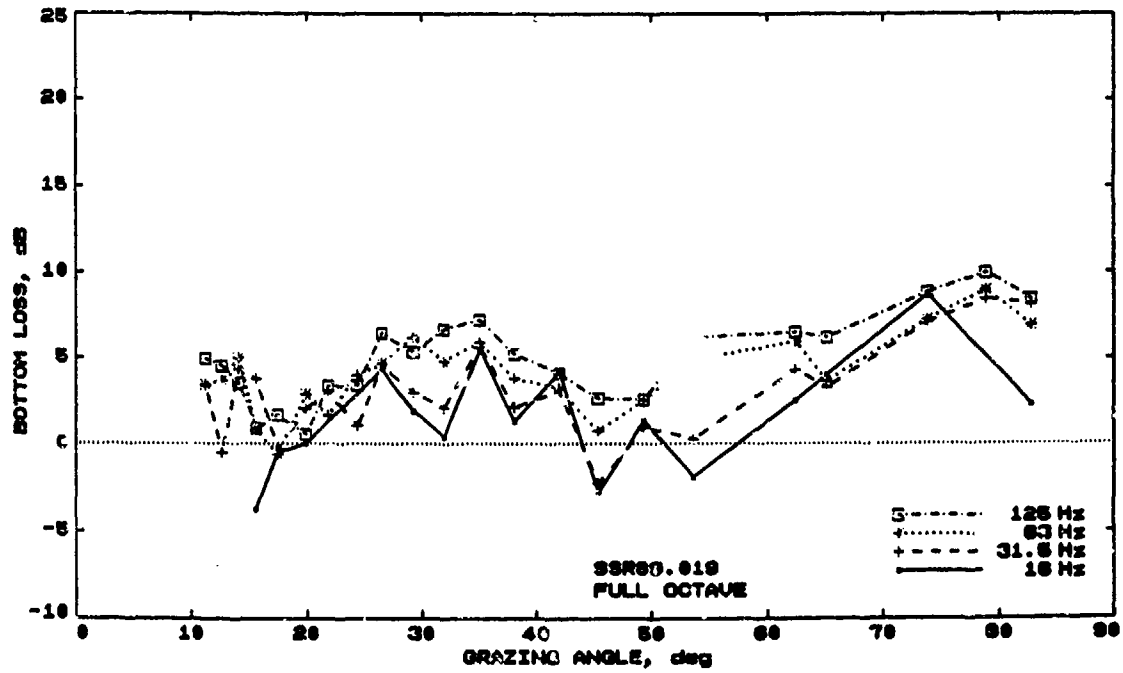

Figure B.9: (C) Bottom loss as a function of grazing angle, for propagation run SSR89.019.

Shot-Run Title :	SSR89.020
Position of receiver :	04°49S 153°28E
Physiographic Province :	South East New Island Basin
Ship :	HMAS Cook
Cruise :	MSD 15/89 (winter)
Time/Date of start :	2100L 18 MAY 89 (138 1000Z)
Heading :	354
Sound-speed profile :	XBT
Position of ssp :	04°49S 153°28E
Time/Date of ssp :	2104L 18 MAY 89 (138 1004Z)
Source depth :	244 m
Receiver depth :	305 m
Sea State :	2
Swell :	0.0 m, 0 sec, 000° to ship

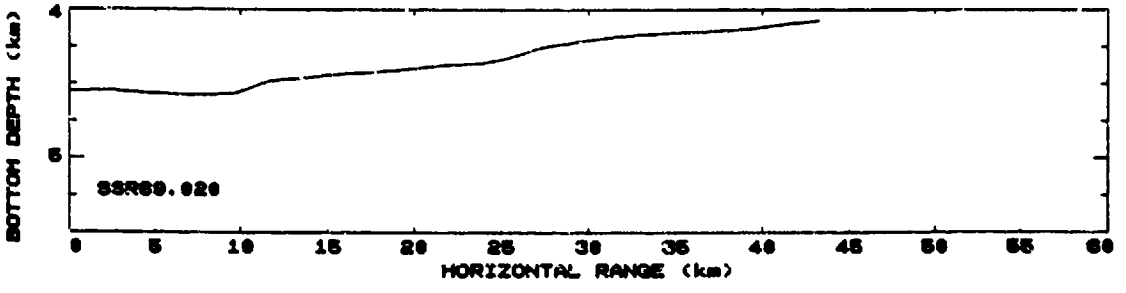

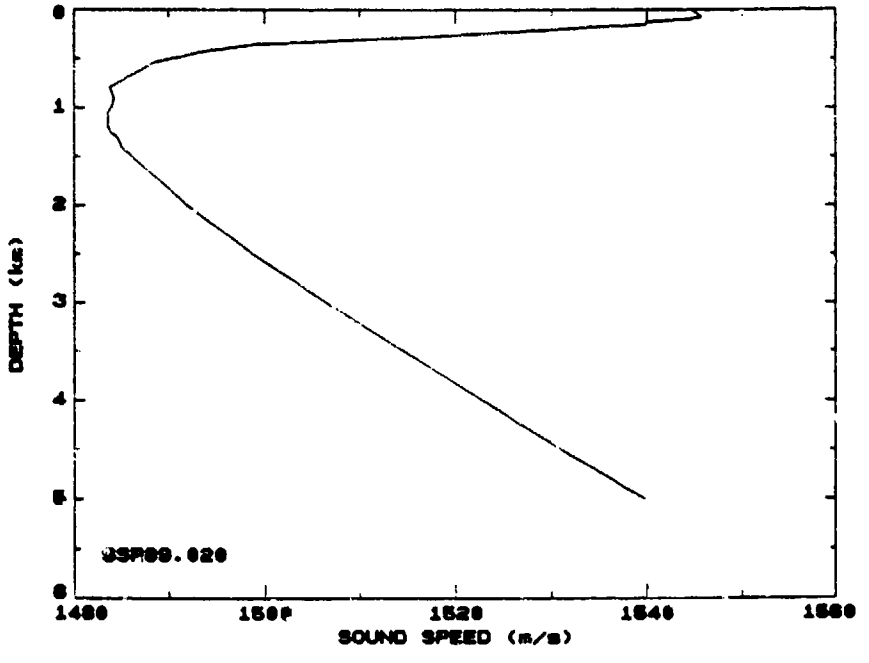

Figure S.10: (U) Summary page for propagation run SSR89.020, containing ancillary information, the bottom profile, and the sound speed profile.

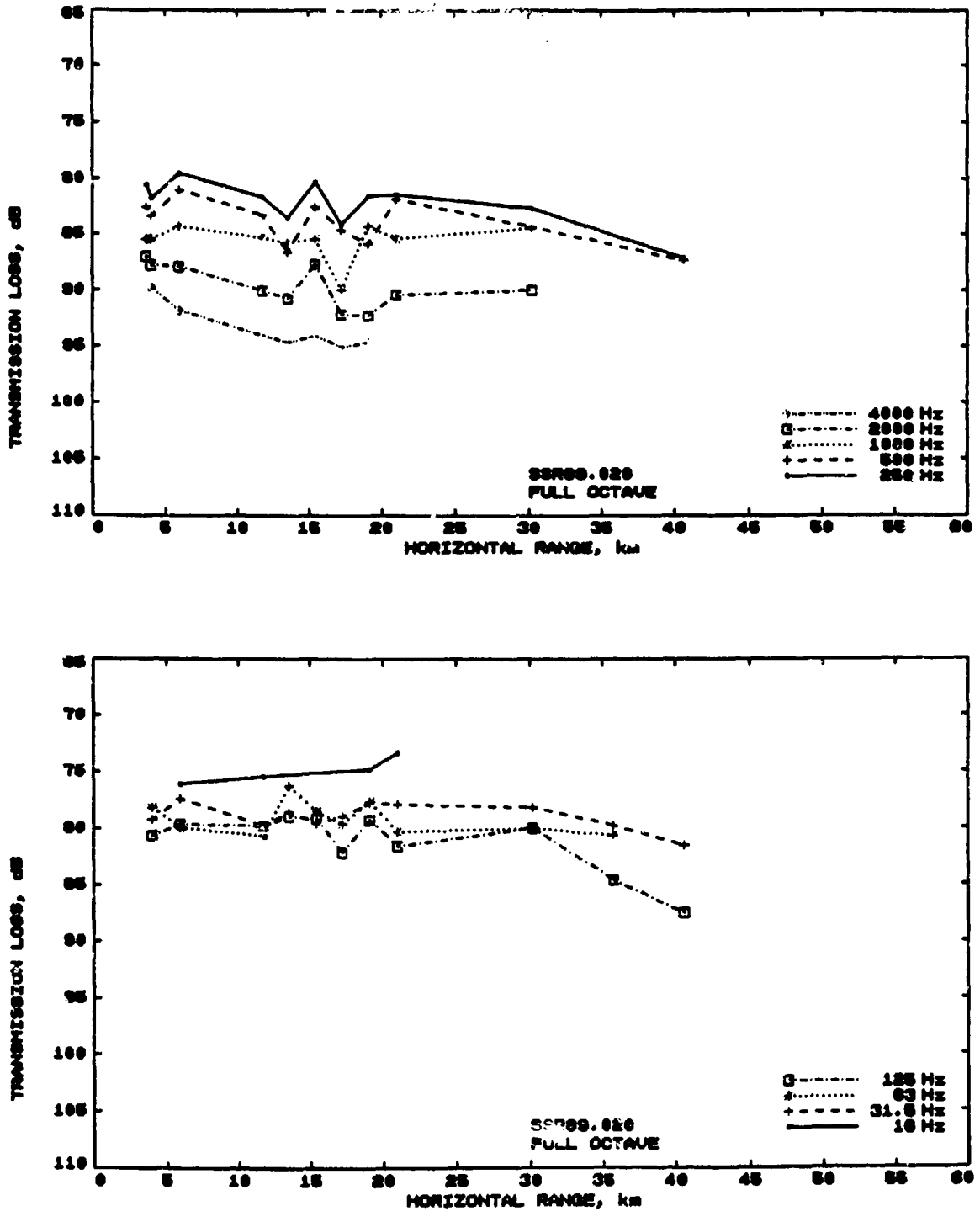

Figure T.10: (C) Measured transmission loss as a function of range, for propagation run SSR89.020.

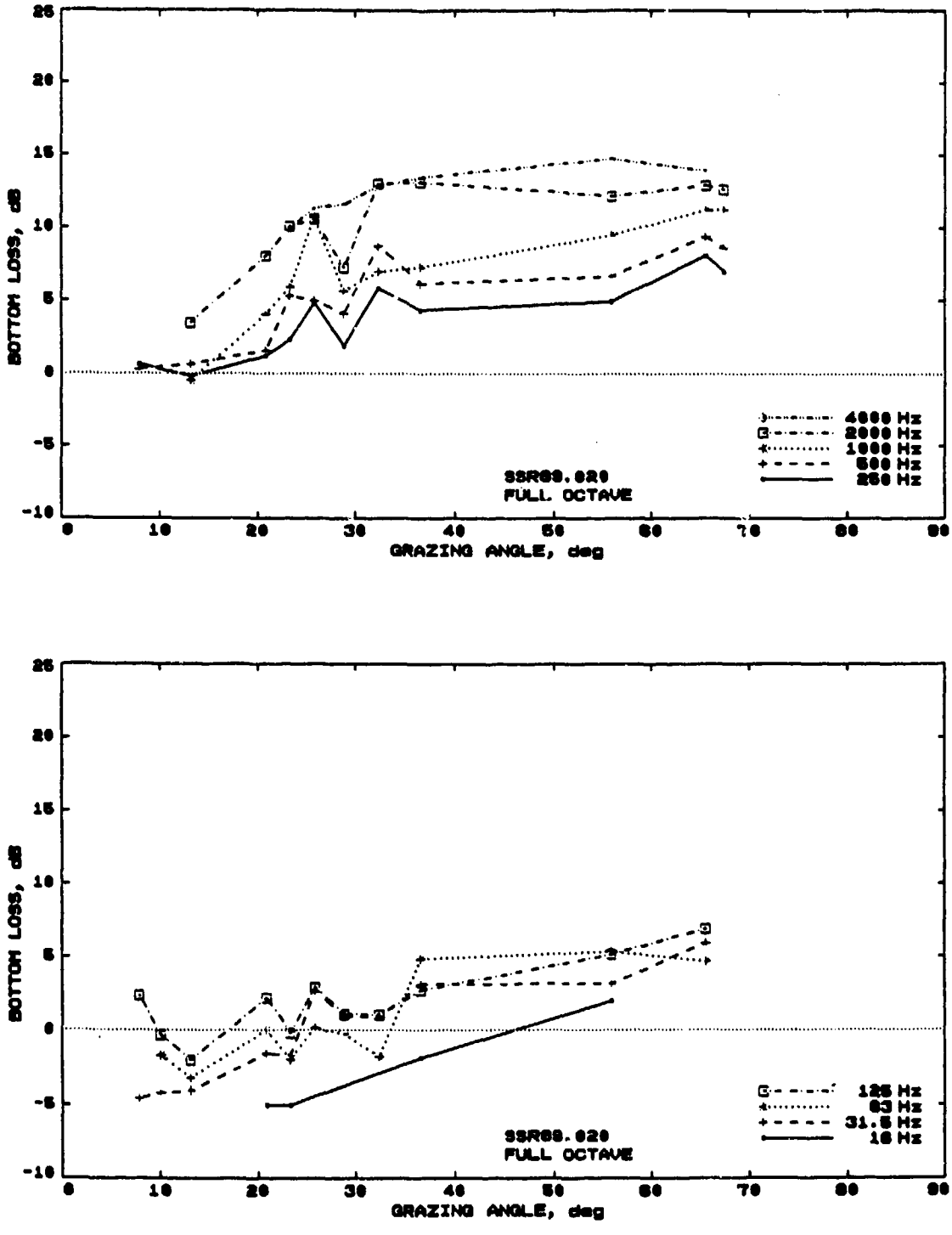

Figure B.10: (C) Bottom loss as a function of grazing angle, for propagation run SSR89.020.

Shot-Run Title :	SSR89.021
Position of receiver :	05°40S 152°13E
Physiographic Province :	Inner Trench Slope
Ship :	HMAS Cook
Cruise :	MSD 15/89 (winter)
Time/Date of start :	0136L 23 MAY 89 (142 1436Z)
Heading :	200
Sound-speed profile :	XBT
Position of ssp :	05°40S 152°13E
Time/Date of ssp :	0115L 23 MAY 89 (142 1415Z)
Source depth :	244 m
Receiver depth :	305 m
Sea State :	2
Swell :	000 m, 0 sec, 000° to ship

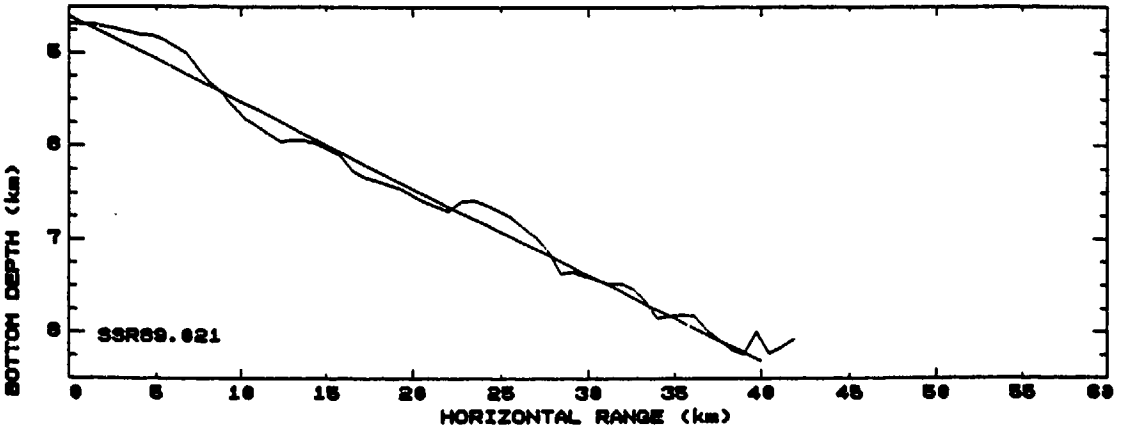

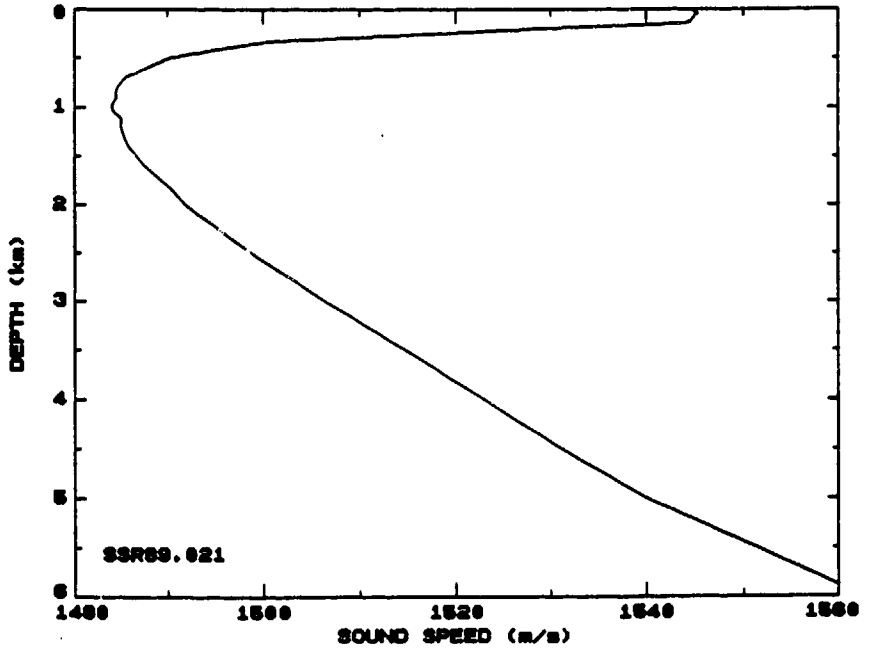

Figure S.11: (U) Summary page for propagation run SSR89.021, containing ancillary information, the bottom profile, and the sound speed profile.

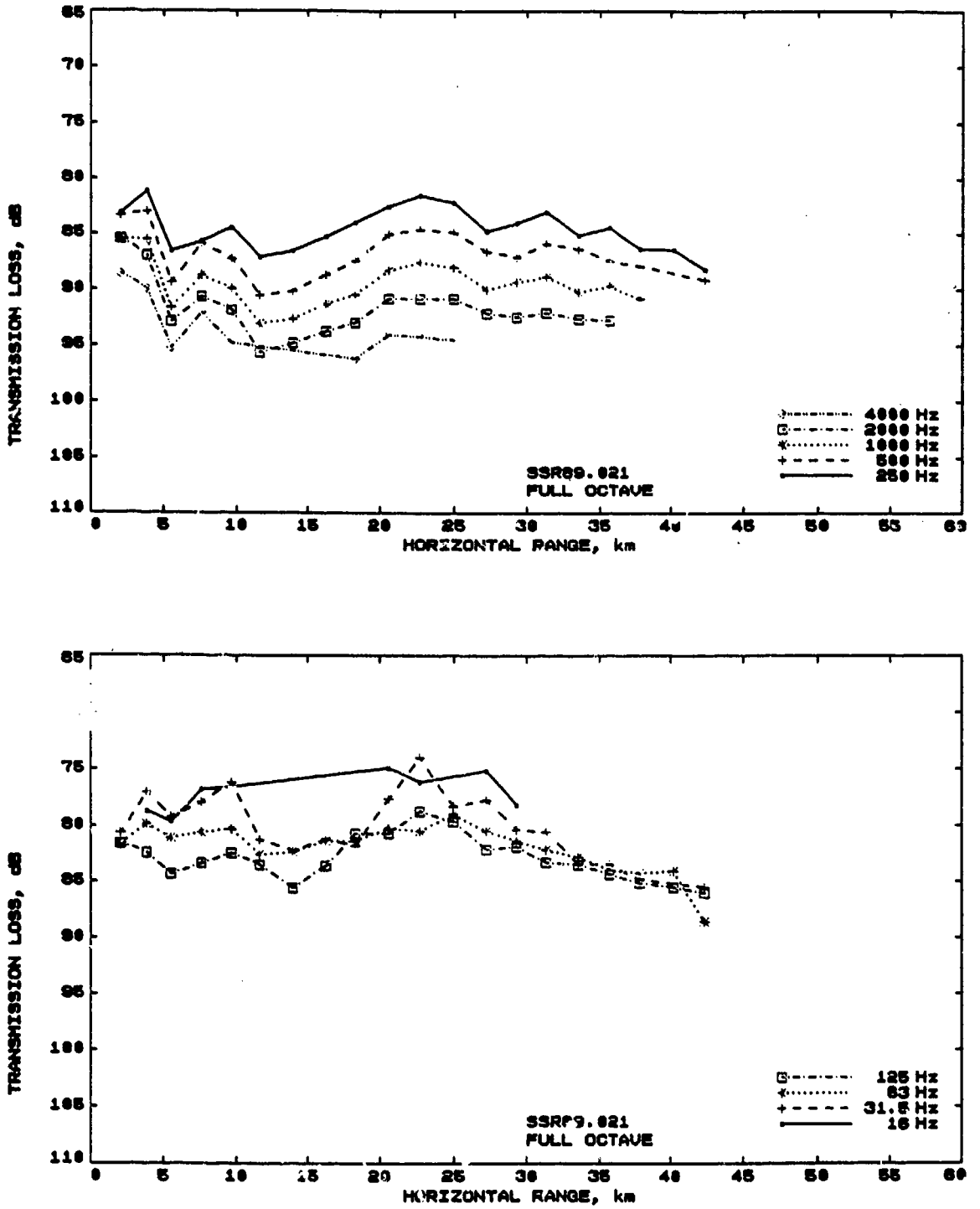

Figure T.11: (C) Measured transmission loss as a function of range, for propagation run SSR89.021.

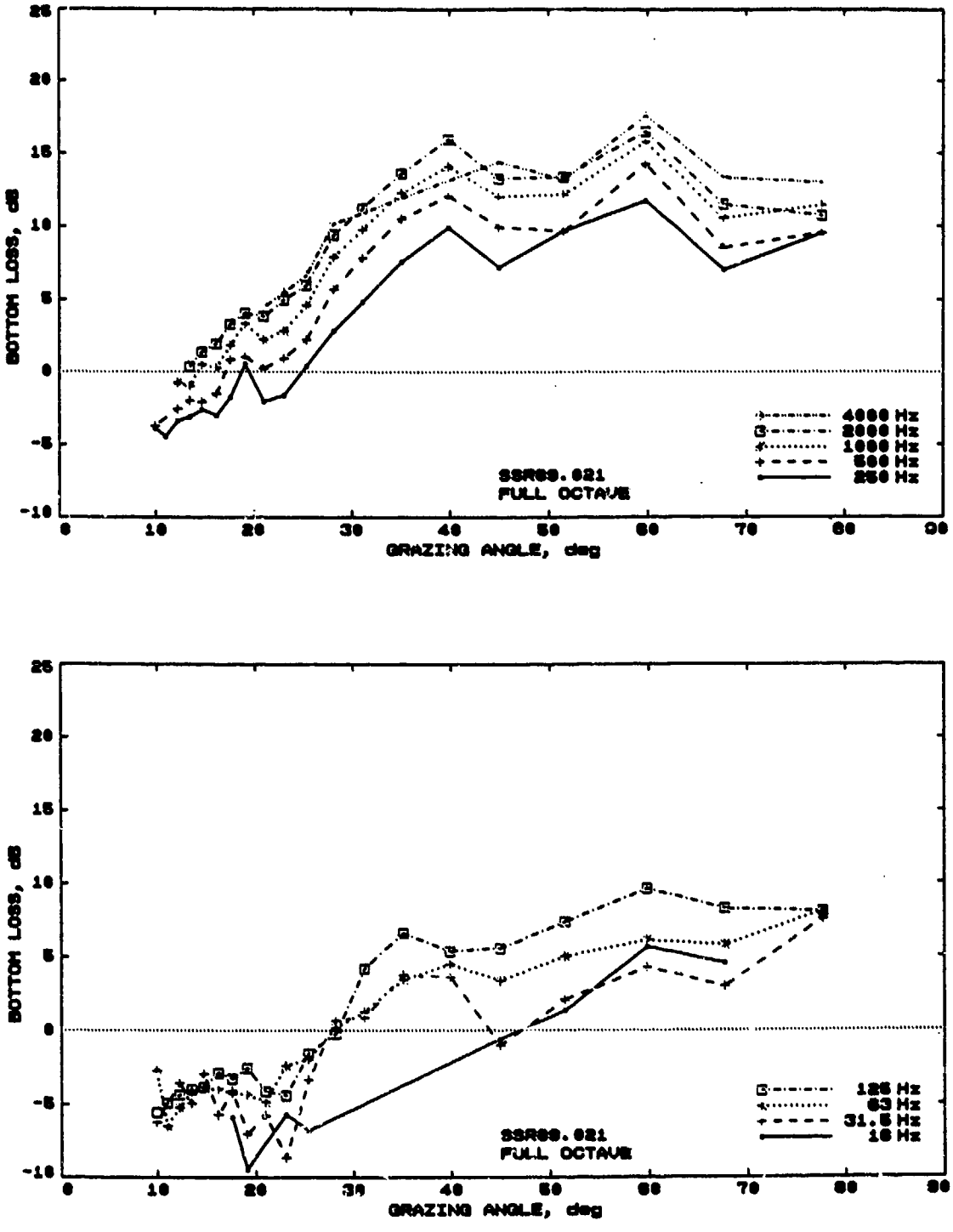

Figure B.11: (C) Bottom loss as a function of grazing angle, for propagation run SSR89.021.

Shot-Run Title :	SSR89.022
Position of receiver :	06°32S 151°57E
Physiographic Province :	Outer Trench Slope
Ship :	HMAS Cook
Cruise :	MSD 15/89 (winter)
Time/Date of start :	1256L 23 MAY 89 (143 0156Z)
Heading :	207
Sound-speed profile :	XBT
Position of ssp :	06°33S 151°57E
Time/Date of ssp :	1259L 23 MAY 89 (143 0159Z)
Source depth :	244 m
Receiver depth :	305 m
Sea State :	2
Swell :	0 m, 0 sec, 000° to ship

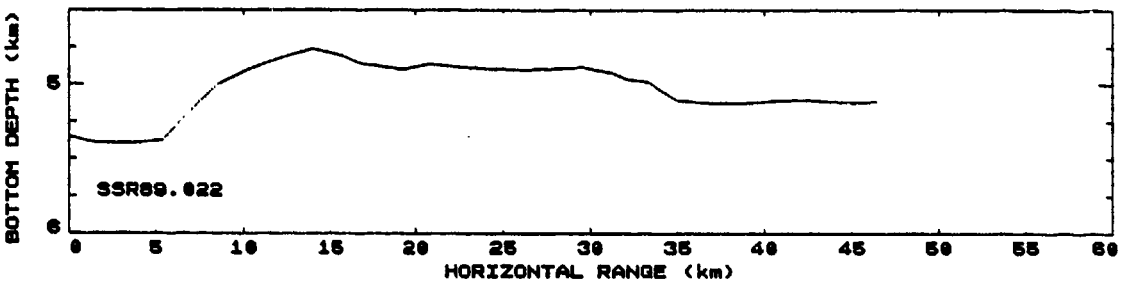

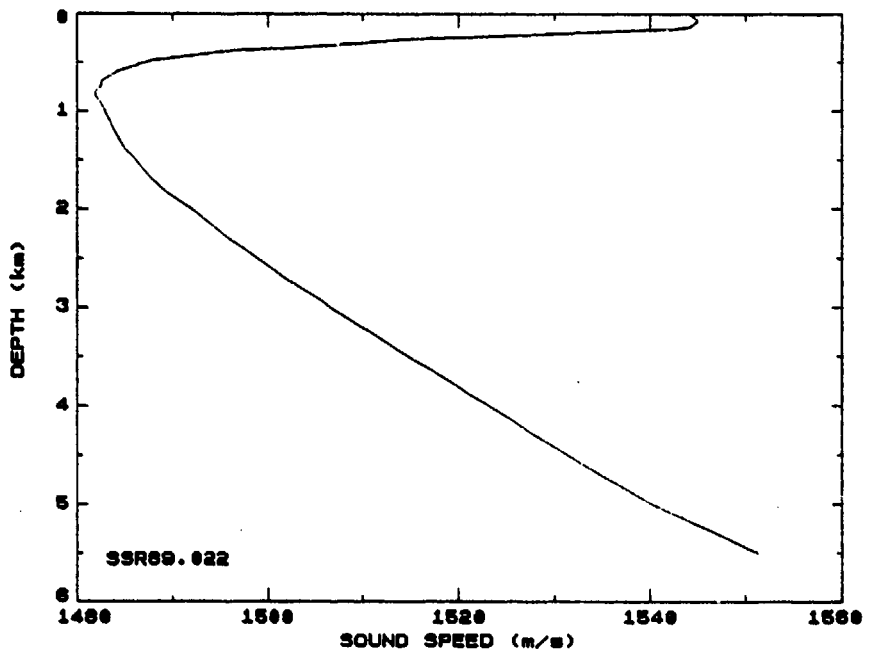

Figure S.12: (U) Summary page for propagation run SSR89.022, containing ancillary information, the bottom profile, and the sound speed profile.

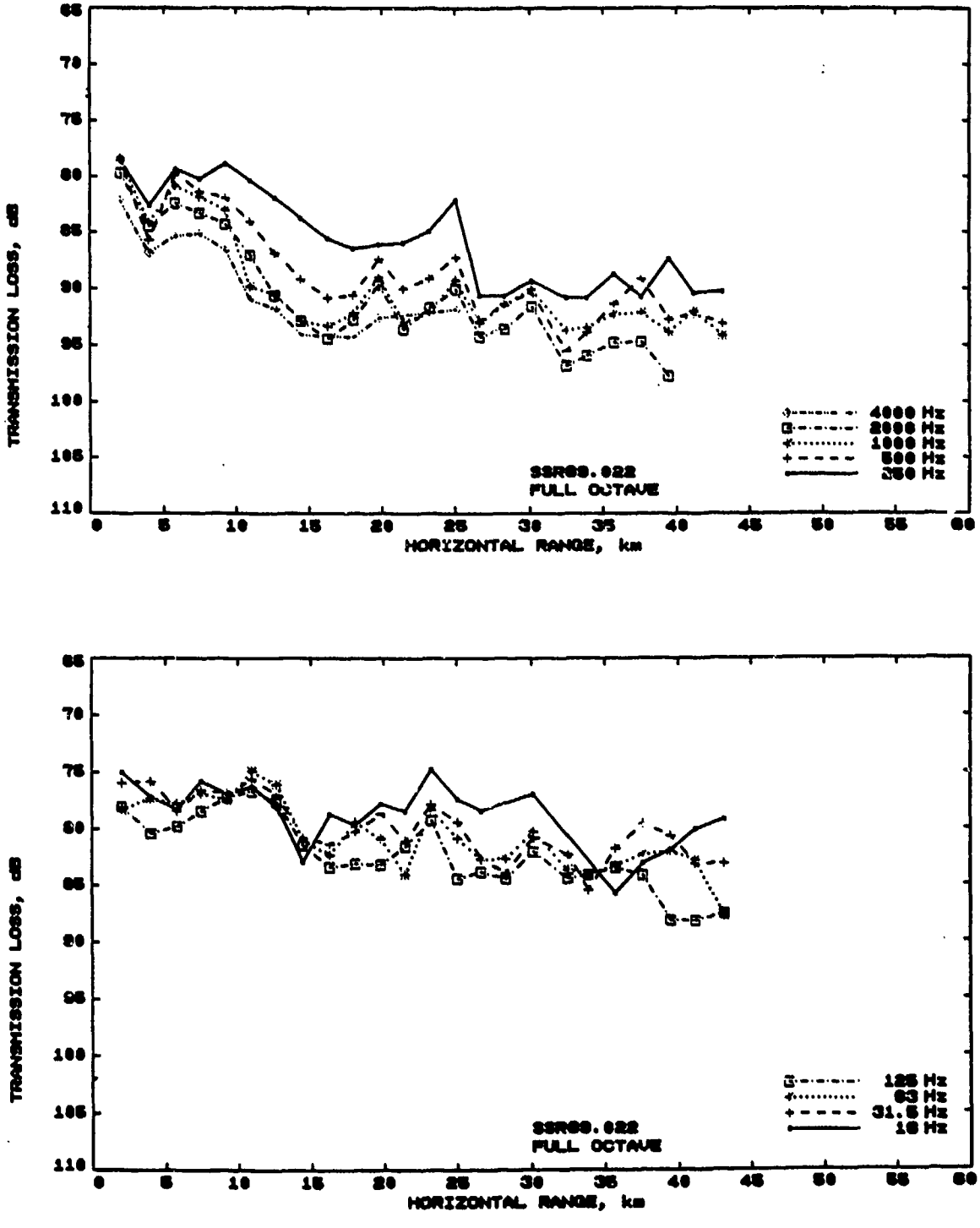

Figure T.12: (C) Measured transmission loss as a function of range, for propagation run SSR89.022.

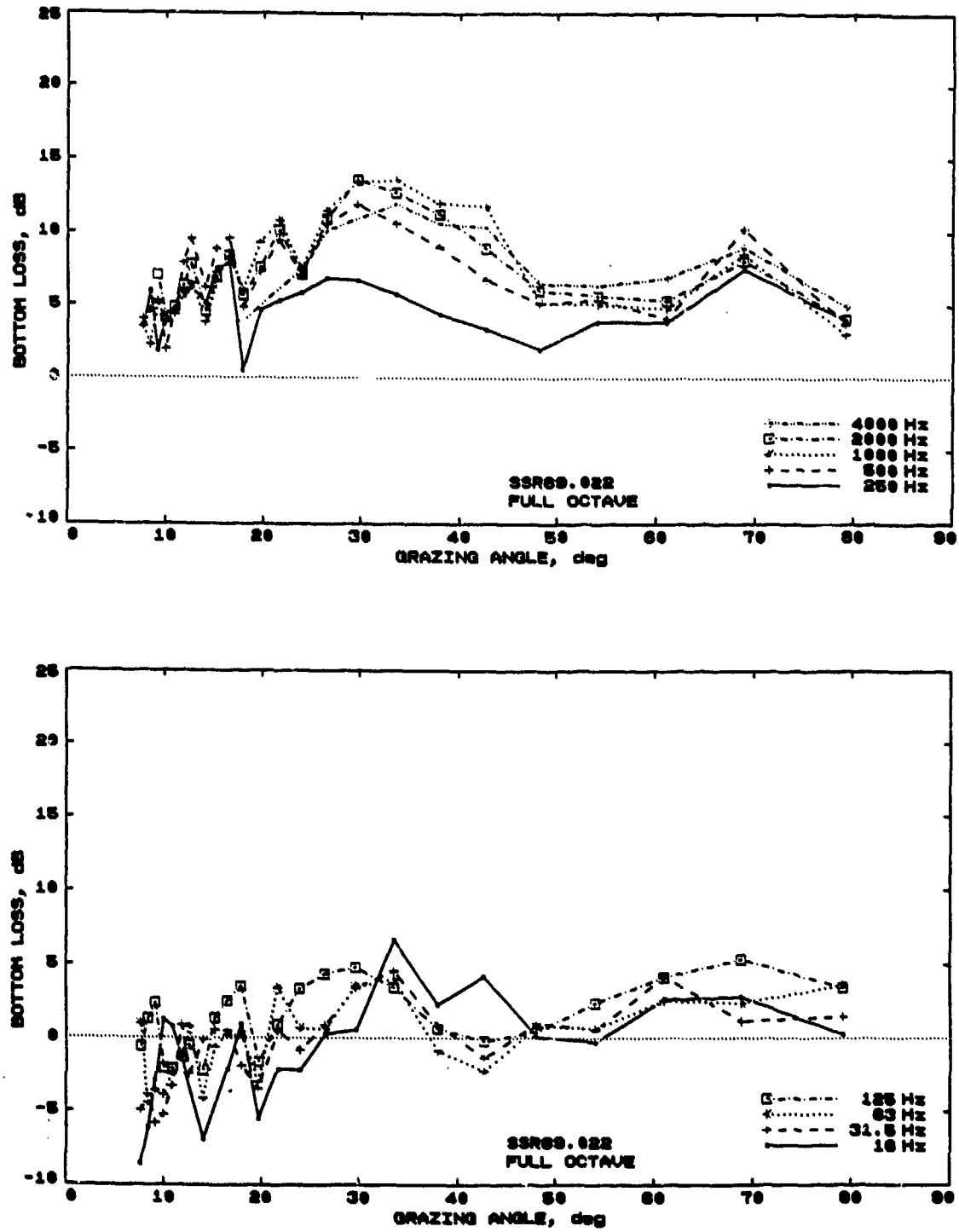

Figure B.12: (C) Bottom loss as a function of grazing angle, for propagation run SSR89.022.

Shot-Run Title :	SSR89.025
Position of receiver :	13°14S 150°05E
Physiographic Province :	Coral Sea Abyssal Plain
Ship :	HMAS Cook
Cruise :	MSD 15/89 (winter)
Time/Date of start :	1251L 27 MAY 89 (147 0151Z)
Heading :	342
Sound-speed profile :	XBT
Position of ssp :	13°15S 150°07E
Time/Date of ssp :	1307L 27 MAY 89 (147 0207Z)
Source depth :	244 m
Receiver depth :	305 m
Sea State :	1
Swell :	0.25 m, 6 sec, 130° to ship

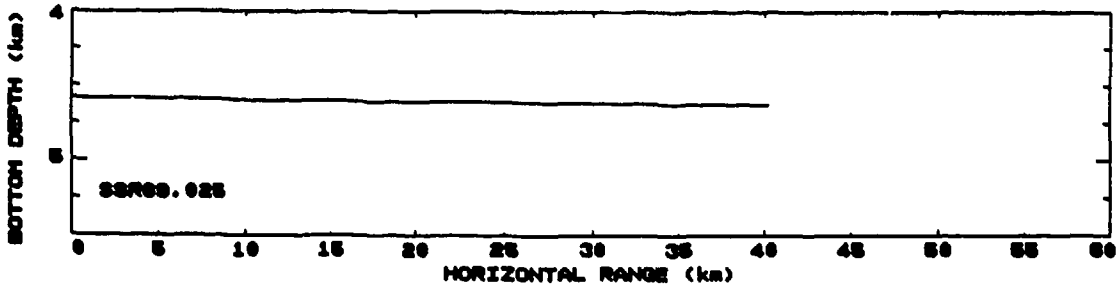

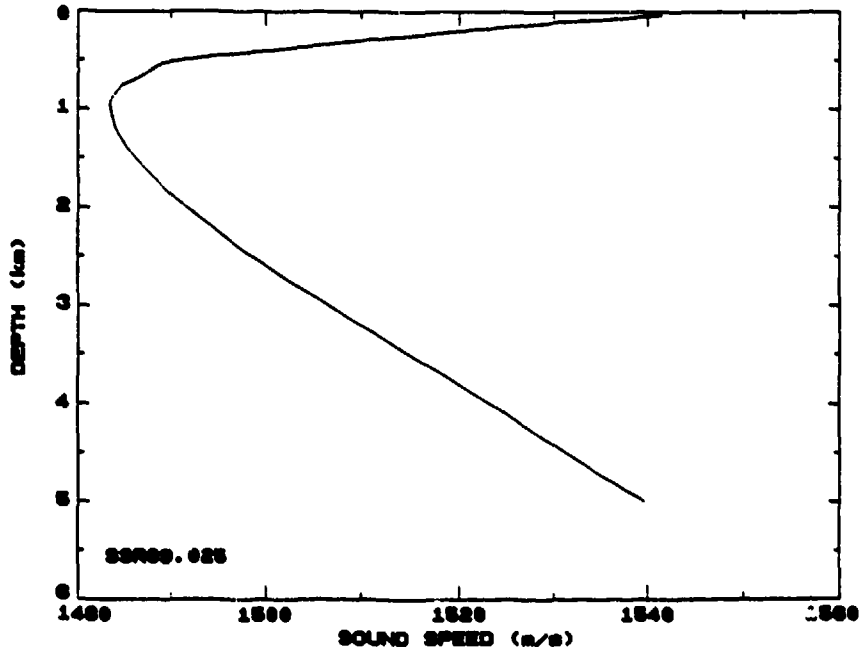

Figure S.13: (U) Summary page for propagation run SSR89.025, containing ancillary information, the bottom profile, and the sound speed profile.

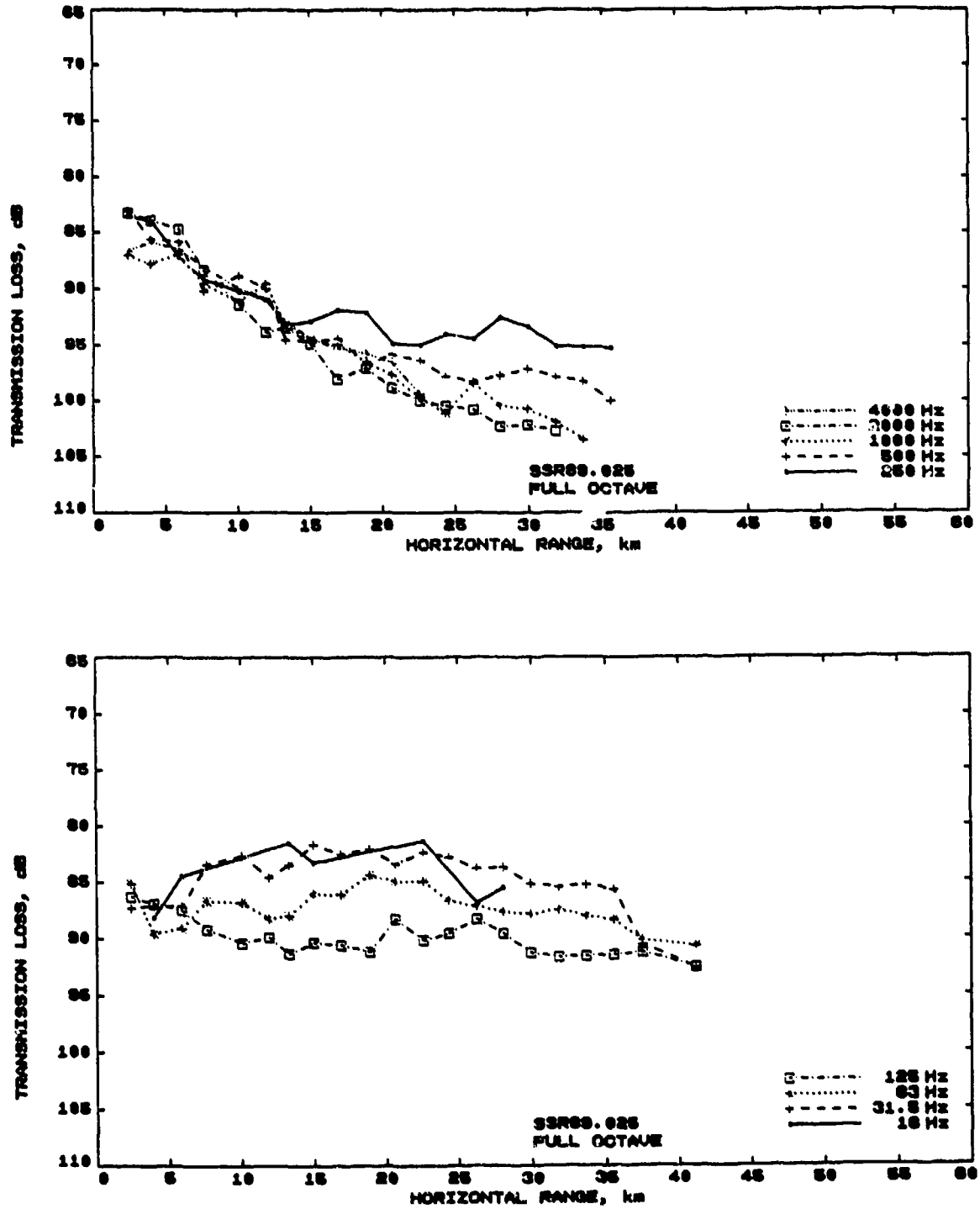

Figure T.13: (C) Measured transmission loss as a function of range, for propagation run SSR89.025.

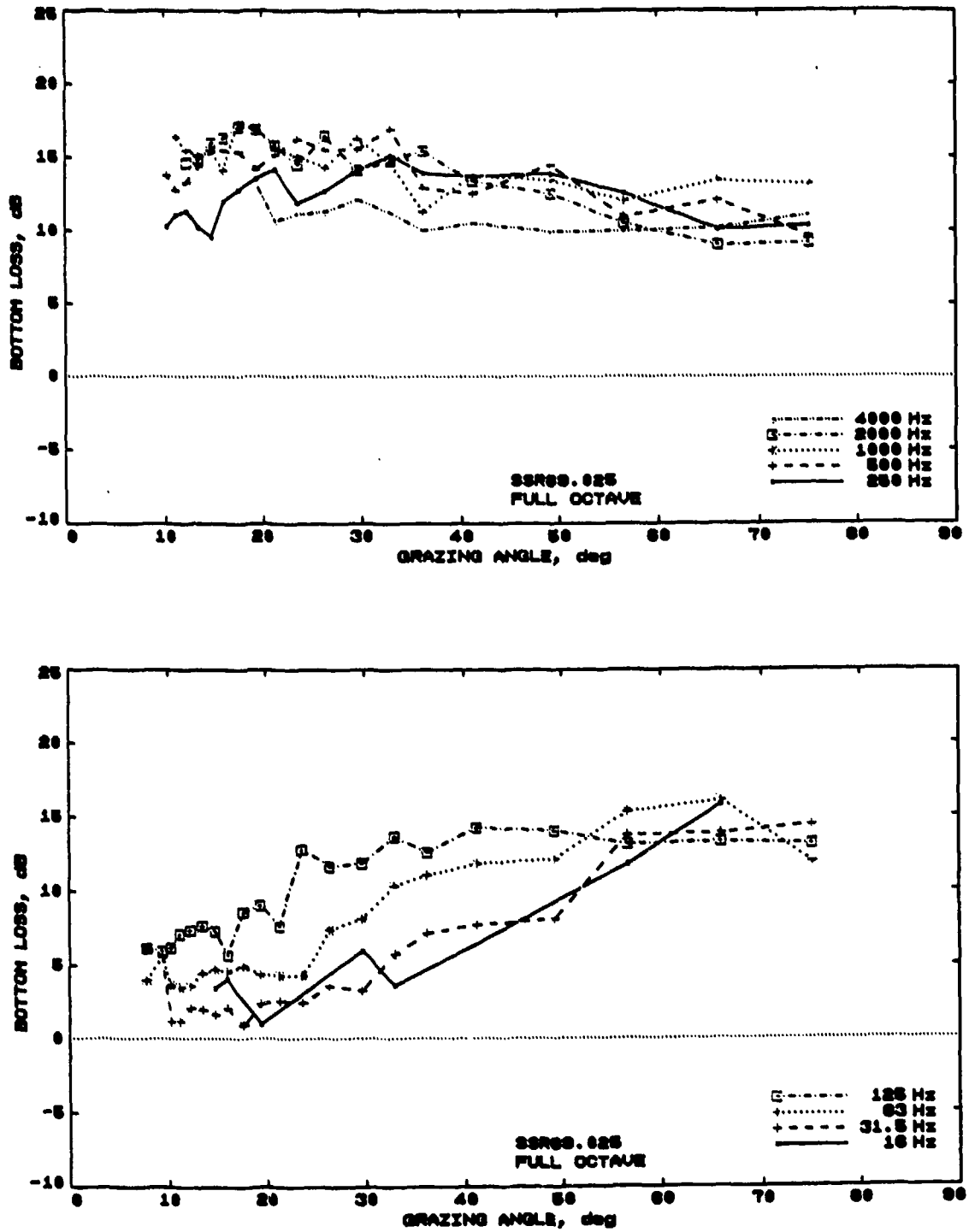

Figure B.13: (C) Bottom loss as a function of grazing angle, for propagation run SSR89.025.

Shot-Run Title :	SSR89.026
Position of receiver :	14°30S 151°37E
Physiographic Province :	Coral Sea Abyssal Plain
Ship :	HMAS Cook
Cruise :	MSD 15/89 (winter)
Time/Date of start :	0209L 28 MAY 89 (147 1509Z)
Heading :	103
Sound-speed profile :	XBT
Position of ssp :	14°35S 151°59E
Time/Date of ssp :	0423L 28 MAY 89 (147 1723Z)
Source depth :	244 m
Receiver depth :	305 m
Sea State :	1
Swell :	0.25 m, 6 sec, 110° to ship

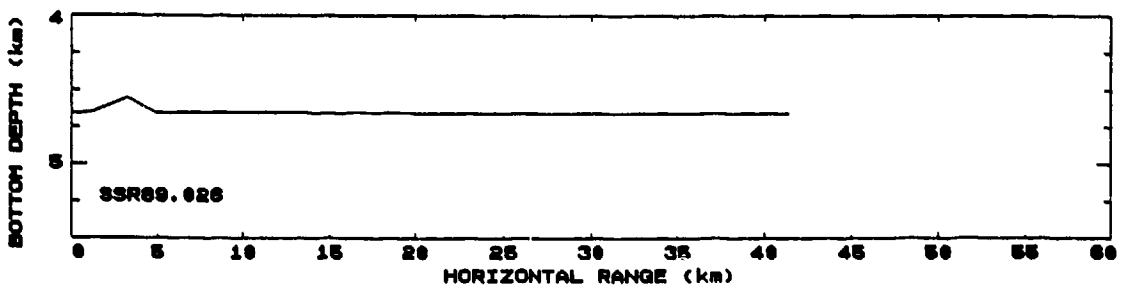

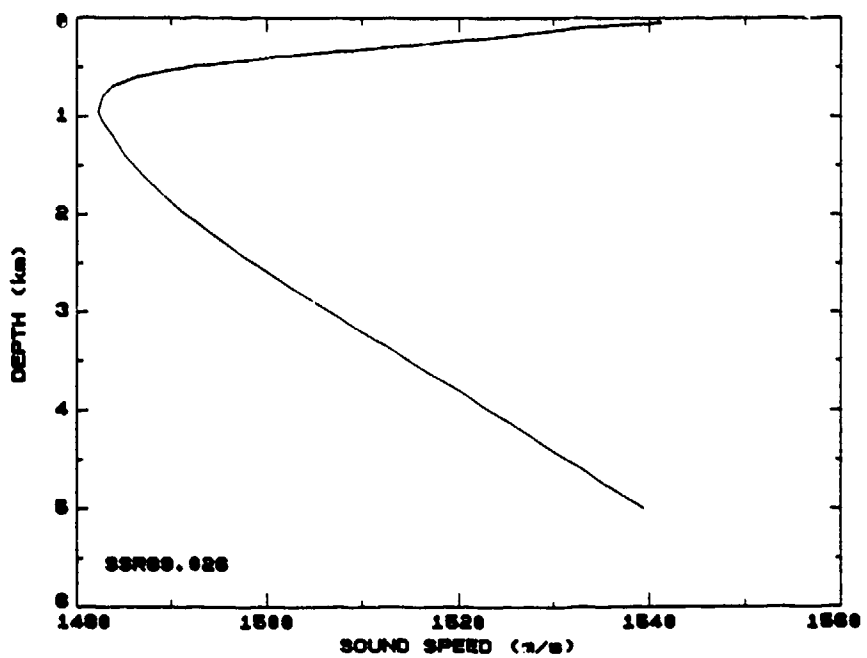

Figure S.14.: (U) Summary page for propagation run SSR89.026, containing ancillary information, the bottom profile, and the sound speed profile.

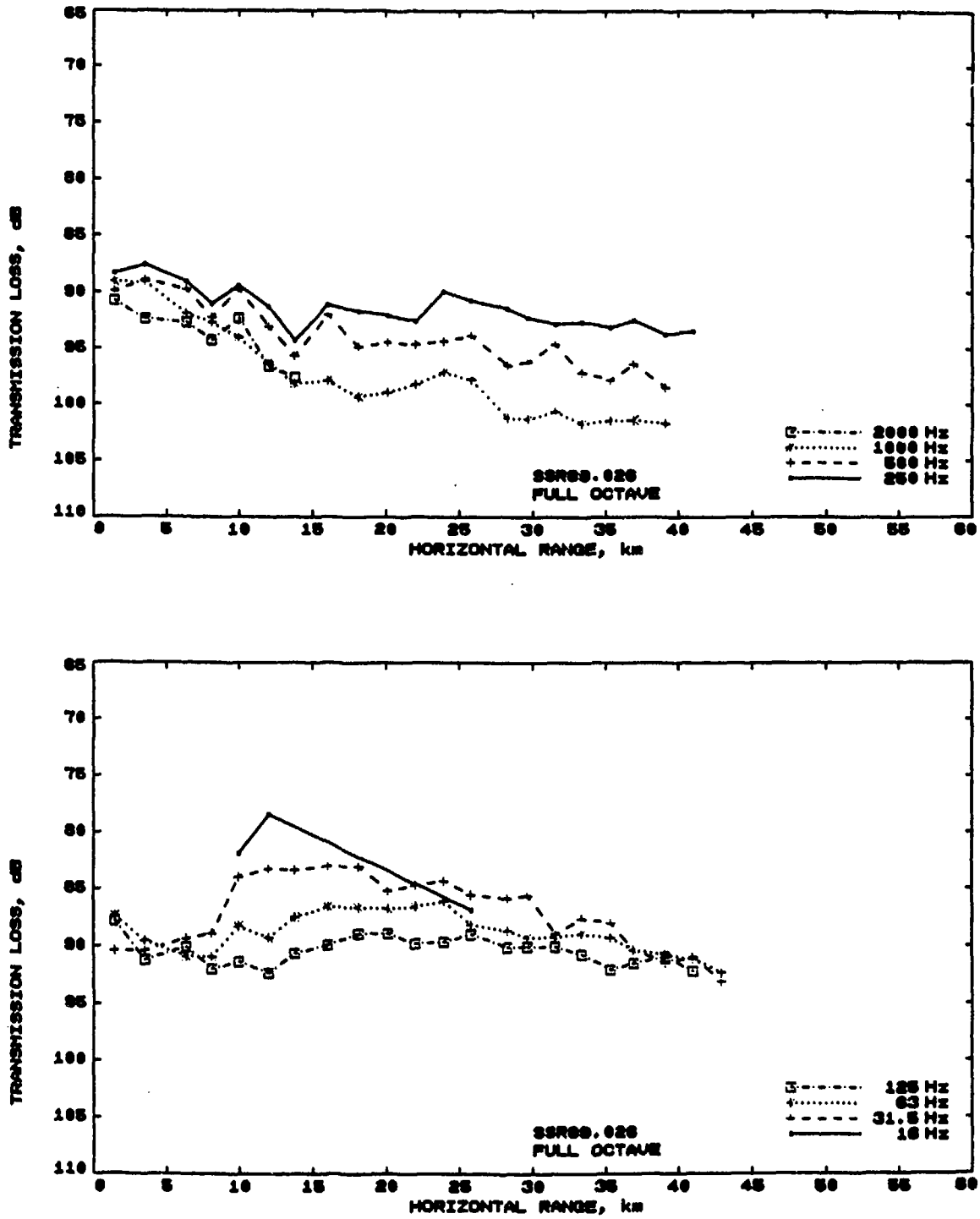

Figure T.14: (C) Measured transmission loss as a function of range, for propagation run SSR89.026.

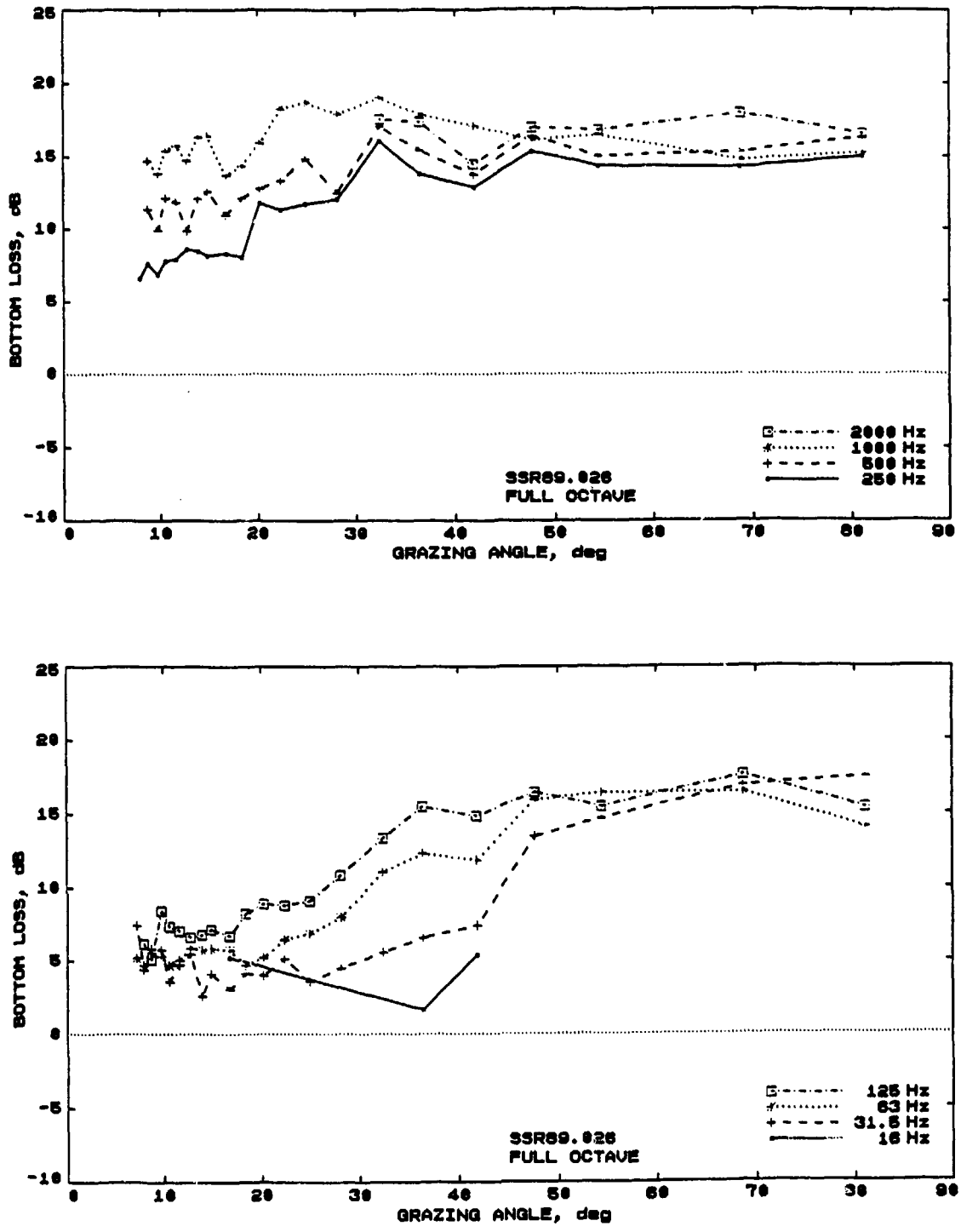

Figure B.14: (C) Bottom loss as a function of grazing angle, for propagation run SSR89.026.

Shot-Run Title :	SSR89.027
Position of receiver :	18°00S 155°00E
Physiographic Province :	Mellish Plateau
Ship :	HMAS Cook
Cruise :	MSD 15/89 (winter)
Time/Date of start :	0915L 29 MAY 89 (148 2215Z)
Heading :	174
Sound-speed profile :	XBT
Position of ssp :	17°59S 155°00E
Time/Date of ssp :	0911L 29 MAY 89 (148 2211Z)
Source depth :	244 m
Receiver depth :	305 m
Sea State :	3
Swell :	3.5 m, 5 sec, 180° to ship

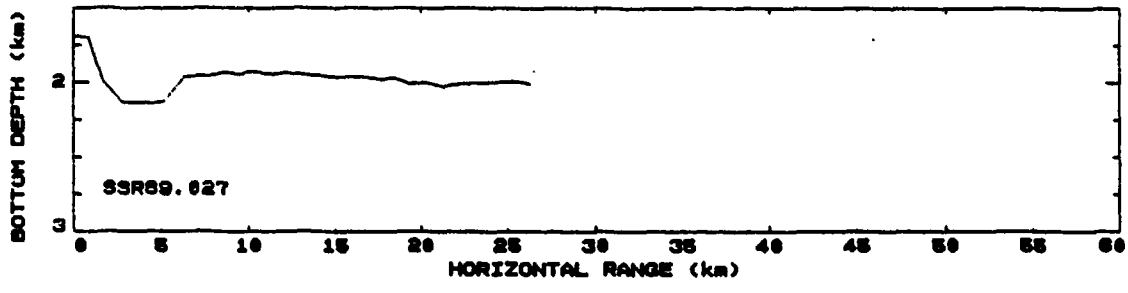

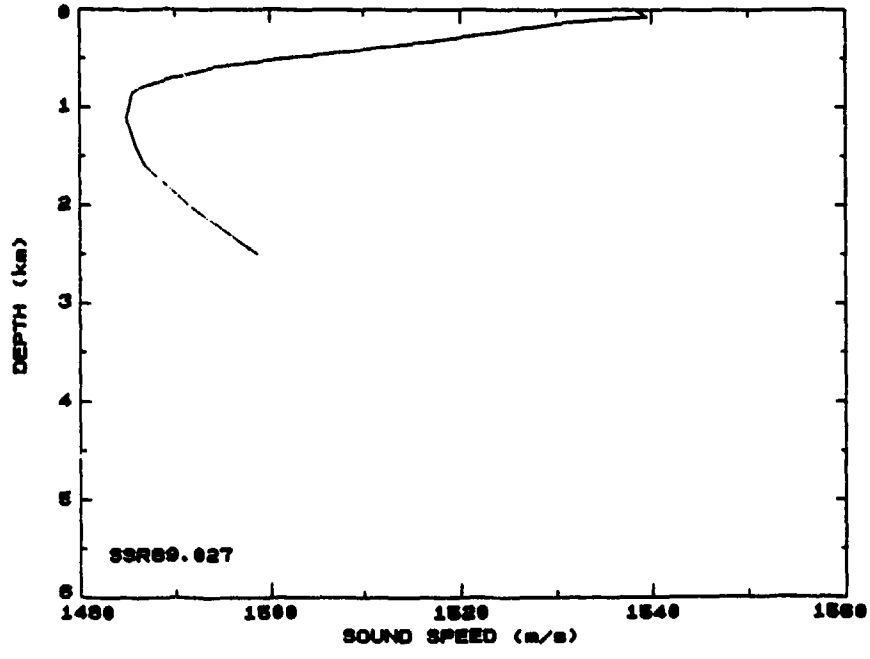

Figure S.15: (U) Summary page for propagation run SSR89.027, containing ancillary information, the bottom profile, and the sound speed profile.

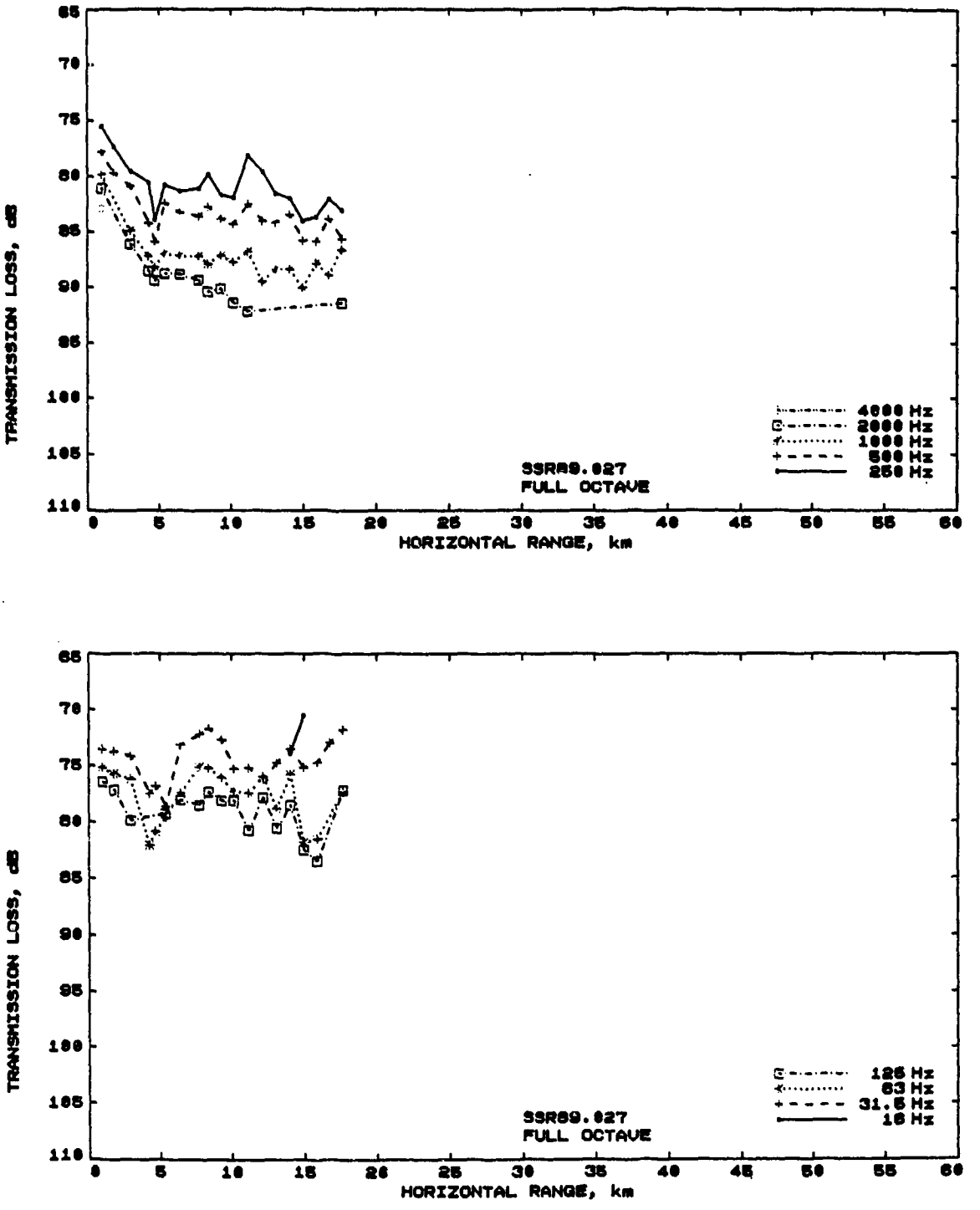

Figure T.15: (C) Measured transmission loss as a function of range, for propagation run SSR89.027.

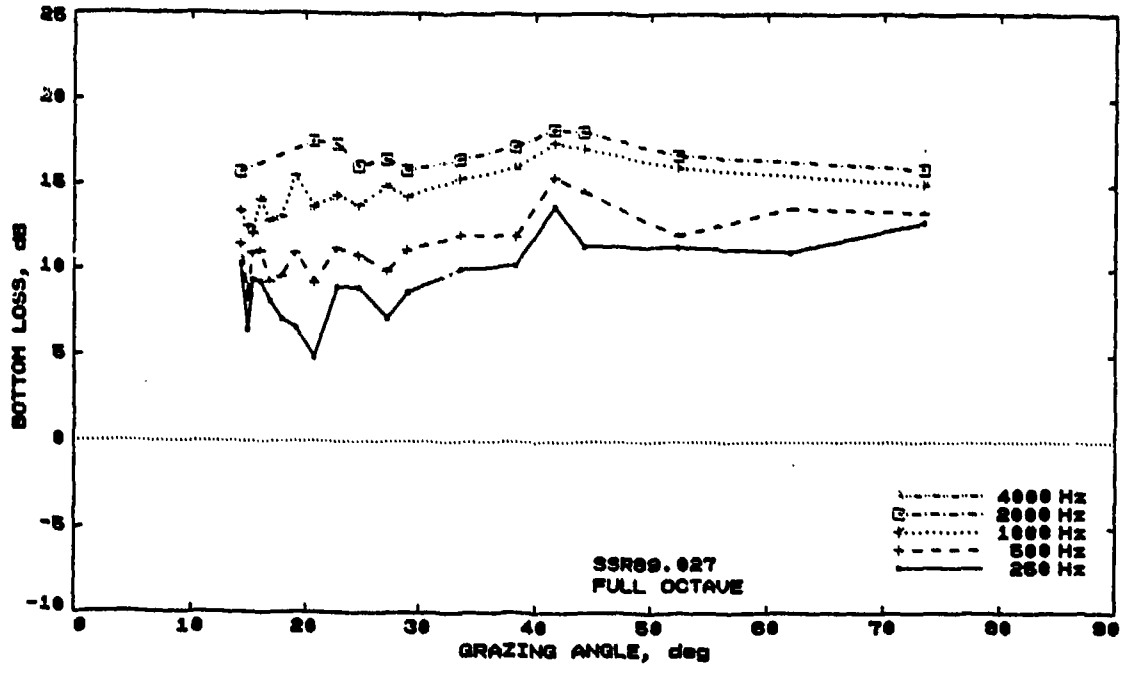

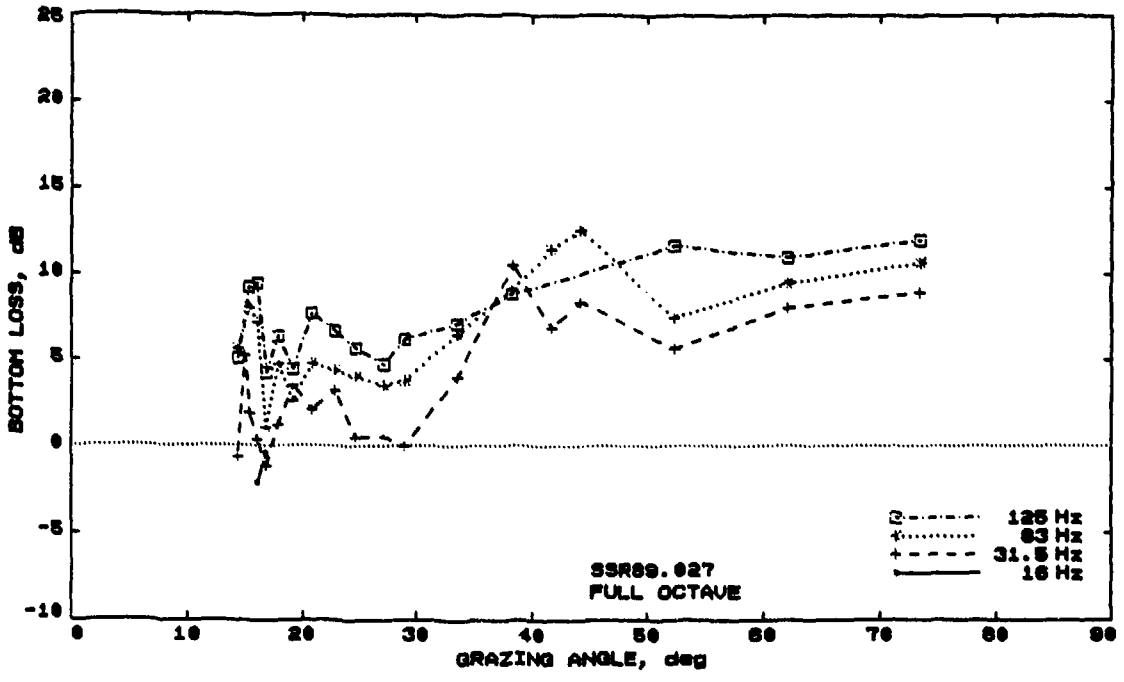

Figure B.15: (C) Bottom loss as a function of grazing angle, for propagation run SSR89.027.

Shot-Run Title :	SSR89.028
Position of receiver :	20°00S 155°00E
Physiographic Province :	Cato Trough
Ship :	HMAS Cook
Cruise :	MSD 15/89 (winter)
Time/Date of start :	2237L 29 MAY 89 (149 1137Z)
Heading :	174
Sound-speed profile :	XBT
Position of ssp :	20°18S 154°57E
Time/Date of ssp :	0038L 30 MAY 89 (149 1338Z)
Source depth :	244 m
Receiver depth :	305 m
Sea State :	4
Swell :	4 m, 5 sec, 180° to ship

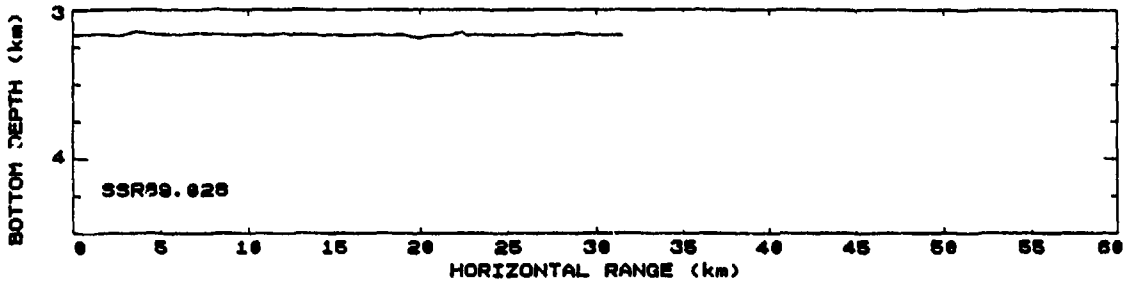

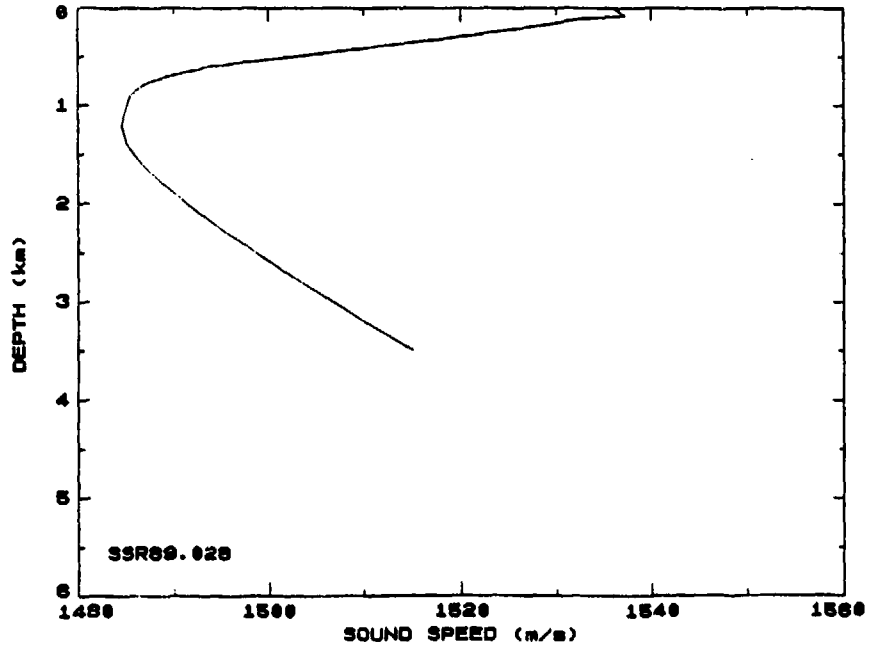

Figure S.16: (U) Summary page for propagation run SSR89.028, containing ancillary information, the bottom profile, and the sound speed profile.

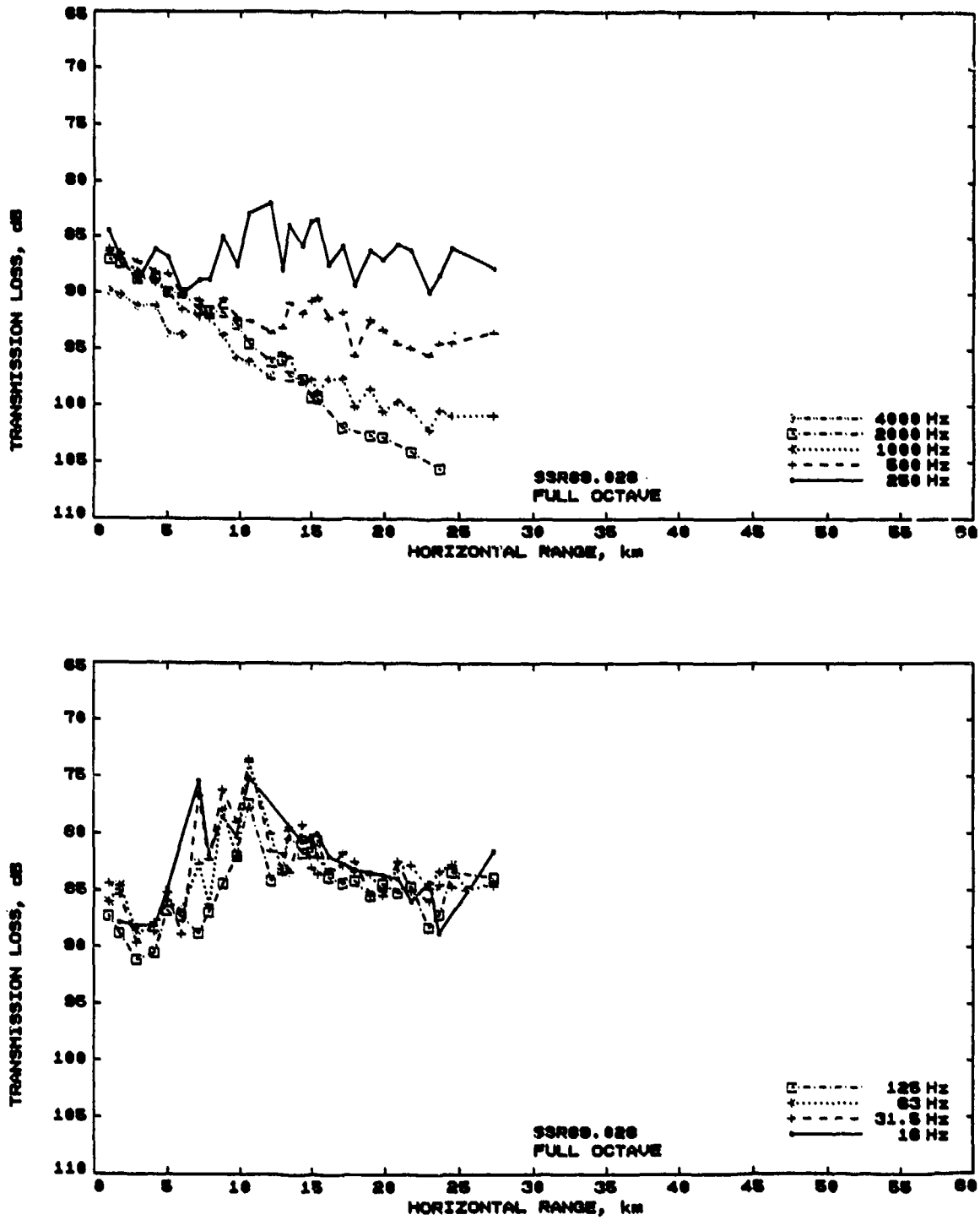

Figure T.16: (C) Measured transmission loss as a function of range, for propagation run SSR89.028.

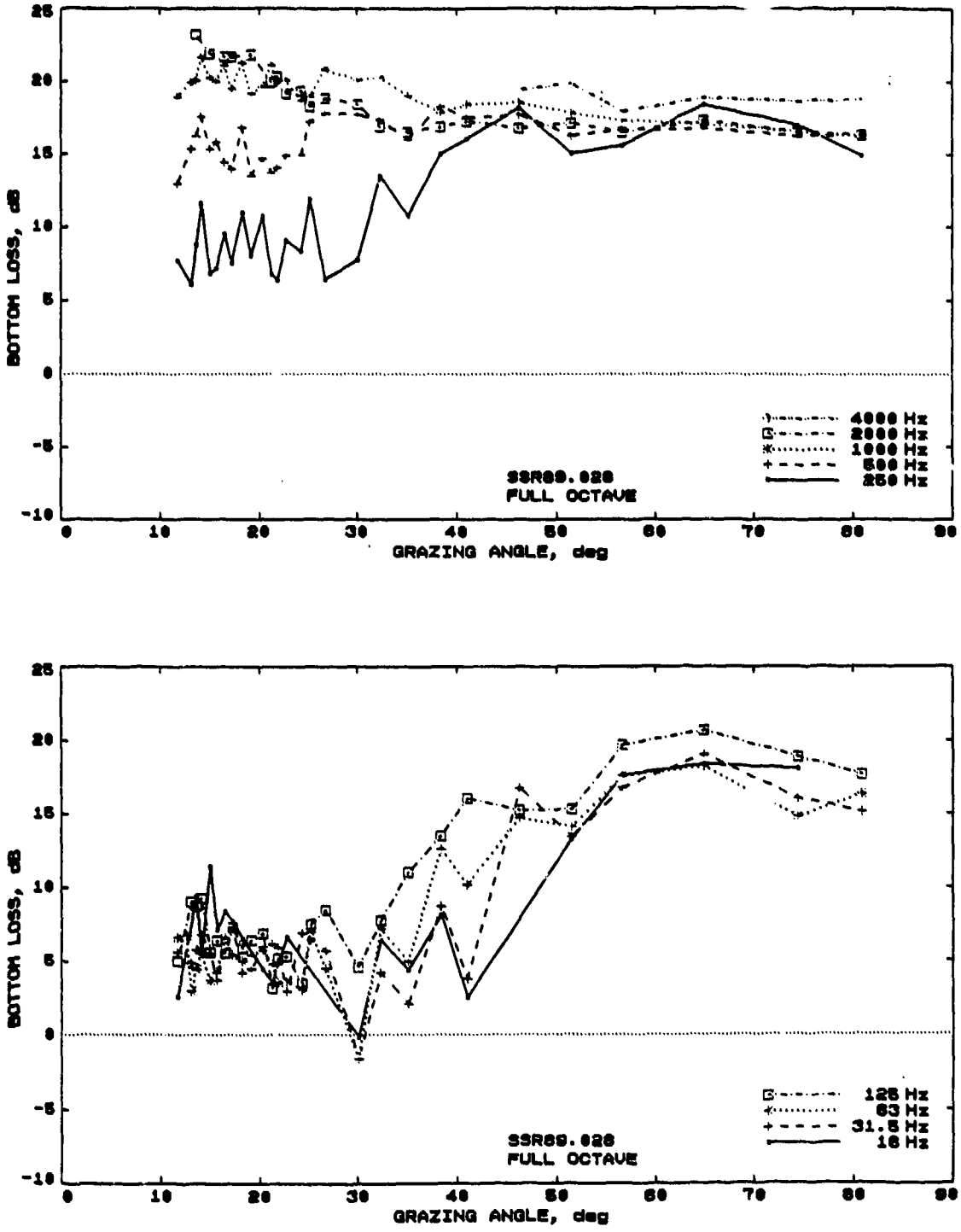

Figure B.16: (C) Bottom loss as a function of grazing angle, for propagation run SSR89.028.

SECURITY CLASSIFICATION OF THIS PAGE **UNCLASSIFIED**

REPORT NO.	AR NO.	REPORT SECURITY CLASSIFICATION
DSTO-TR-0034	AR-008-549	Confidential

TITLE

Acoustic propagation by bottom bounce mode to the North East of Australia (U)

AUTHOR(S)
M.W. Lawrence, M.J. Bell
and S. Prenc

CORPORATE AUTHOR
Aeronautical and Maritime Research
Laboratory
GPO Box 4331
Melbourne Victoria 3001

REPORT DATE	TASK NO.	SPONSOR
July 1994	DST 89/252	DSTO

FILE NO.	REFERENCES	PAGES
G6 4/8-4342	22	104

CLASSIFICATION/LIMITATION REVIEW DATE
July 1997

CLASSIFICATION/RELEASE AUTHORITY
Chief, Maritime Operations Division

SECONDARY DISTRIBUTION

Distribution additional to the initial list is limited to qualified officers of the Defence Department and the Defence Force of Australia and their equivalent in US, UK, Canada and NZ. Other requests should be referred to Chief, Maritime Operations Division, AMRL.

ANNOUNCEMENT

Qualified officers of the Defence Department and the Defence Force of Australia and their equivalent in US, UK, Canada and NZ.

KEYWORDS

Bottom Bounce	Acoustic measurements
Sound propagation	Acoustic bottom loss

ABSTRACT

(U) Underwater acoustic propagation measurements have been made to the north east of Australia, primarily in the Coral and Solomon Seas. A few measurements were made in the Tasman Sea. The resulting data set has been analysed to provide acoustic bottom loss as a function of frequency and grazing angle for a range of sites. The experiments and the analysis are described, together with the results. The variability from site to site is considerable, sometimes even in areas which are geologically of the same province.

DSTO-TR-0034

Acoustic Propagation by Bottom Bounce Mode to the North East of Australia (U)

M.W. Lawrence, M.J. Bell and S. Prenc

DISTRIBUTION LIST

	Copy Nos.
Director, AMRL	1
Chief, Maritime Operations Division	2
Research Leader Submarine and Ship Sonar	3
Research Leader, Maritime Operations Research	4
Research Leader, Airborne Systems	5
D.H. Cato, MOD, Pymont, NSW	6
M.W. Lawrence, MOD, Pyrmont, NSW	7
M.J. Bell, MOD, Pyrmont, NSW	8
S. Tavener, MOD, Pyrmont, NSW	9
G.C.L. Searle, MOD, Pyrmont, NSW	10
L. Booth, MOD, Pyrmont, NSW	11
A.D. Jones, MOD, Salisbury, SA	12
A.I. Larsson, MOD, Salisbury, SA	13
G.J. Day, MOD, Salisbury, SA	14
Library, AMRL Maribyrong	15
Library, AMRL Fishermens Bend	16
Chief Defence Scientist (for CDS, FASSP, ASSCM) 1 copy only	17
Director, ESRL	18
Senior Librarian, Main Library DSTOS	19
Head, Information Centre, Defence Intelligence Organisation	20
OIC, Technical Reports Centre, Defence Central Library	21
Officer in Charge, Document Exchange Centre 7 copies	22-28
Scientific Adviser Army, Russell Offices	29
Air Force Scientific Adviser, Russell Offices	30
Navy Scientific Adviser, Russell Offices	31
Scientific Adviser, Policy and Command	32
Senior Defence Scientific Adviser	33
Librarian, DSTO-Sydney (2 copies)	34-35
Director General Force Development (Sea)	36
Director General Force Development (Air)	37
Director, Oceanography and Meteorology, Potts Point NSW	38
Head, Australian Oceanographic Data Centre, Potts Point NSW	39
Director, Australian Joint Acoustic Analysis Centre, Nowra NSW	40
Counsellor, Defence Science, Embassy of Australia - DCDS only	
Counseller, Defence Science, Australian High Commission - DCDS only	
Spares	41-45

DEPARTMENT OF DEFENCE
DEFENCE SCIENCE & TECHNOLOGY ORGANISATION
DSTO

SCIENCE CORPORATE MANAGEMENT BRANCH
DSTO SALISBURY LIBRARY-REPORTS DISTRIBUTION
PO BOX 1500 SALISBURY SA 5108

Reference: R9607/7/9 Pt 1 F29
Contact: Natalie Mahlknecht
E-mail: natalie.mahlknecht@dsto.defence.gov.au

Telephone: (08) 8259 6255
Facsimile: (08) 8259 6803

28th May 1999

To All Copyholders
cc: To the Team Leader of Records & Archives

ITD-C054467

Notification of Downgrading/ Delimiting of DSTO Report

Please note that the Release Authority has authorised the downgrading/ delimiting of the report detailed here:

DSTO NUMBER	**DSTO-TR-0034**
AR NUMBER	**AR-008-549**
FILE NUMBER	**G6/4/8-4342**
REVISED CLASSIFICATION / RELEASE LIMITATION	**UNCLASSIFIED** **Public Release**

Please amend your records and make changes to your copy of the report itself to reflect the new classification/ release limitation.

Natalie Mahlknecht
Reports Distribution
DSTO Library, Salisbury